FEDERAL UNIVERSITY OF ITAJUBÁ

INSTITUTE OF ELECTRICAL SYSTEMS AND ENERGY

GRADUATE PROGRAM IN ELECTRICAL ENGINEERING

DOCTORAL DEGREE IN ELECTRICAL ENGINEERING

"Voltage control in mixed energy systems with intelligent microgrids under operating uncertainties."

Student: Vicente Tiburcio dos Santos Júnior, MSc

Supervisor: Prof. Tales Cleber Pimenta, PhD

Itajubá, July 2024

Doctoral Thesis presented by

Vicente Tiburcio dos Santos Júnior, MSc

to obtain the doctoral degree in Electrical Engineering

of

Federal University of Itajubá

"Voltage control in mixed energy systems with intelligent microgrids under operating uncertainties."

July 2024

Concentration area: Electric Power Systems

Supervisor: Prof. Tales Cleber Pimenta, PhD

Examining Board: Prof. Robson Luiz Moreno, PhD

Prof. Luiz Henrique de Carvalho, PhD

External Examiner: Prof. Alexandre Baratella Lugli, PhD (INATEL)

Prof. Paulo André Dias Jacome, PhD (UFCE)

Acknowledgements

The formulation of this thesis research work was successful with the participation of University of Kentucky (Ampere Laboratory), CAPES(UNIFEI), and honourable recognition for my family and everyone who collaborated for the execution and conclusion and deserved prominence.

Itajubá, Brazil 2024

Vicente Tiburcio dos Santos Júnior

Table of Contents

List of figures

AC – Alternative current;
ACO – Ant colony optimization;
ADS - Active Distribution System ;
AI – Artificial intelligence;
ANM - Active Network Management;
ANN – Artificial neural networks;
APSO – Accelerated particle swarm optimization;
ATP - Alternative Transient Program;
BES - Bulk Electric System;
BESS – Battery Energy Storage System;
BPSO - Binary Particle Swarm Optimization;
BSP - Bulk Supply Point;
CBs – Circuit Breakers;
CCP – Common coupling point;
CHP - Combined Heat & Power;
COPs -Constrained Optimization Problems;
CT – Current Transformer;
CVPP - Commercial Virtual Power Plant;
CWT - Continuous Wavelet Transform;
DAS – Distribution Automation System;
DC – Direct Current;
DEM – Dynamic Electric Energy Management;
DER - Distributed Energy Resources;
DFIGs – Double-fed induction generator;
DFT – Discrete Fourier Transform;
DG - Distributed Generation;
DN - Distribution Network;
DNO - Distribution Network Operators;
DOE – Department of energy;
DR - Demand Response;
DSO – Distribution System Operators;
DSOC – Dynamic stochastic optimal control;
DSTATCOM – Static compensator;
DVR - Dynamic Voltage Restorer;
DWT - Discrete Wavelet Transform ;
EAs – Evolutionary algorithms;
EP – Equilibrium point;
ESS – Energy Storage System;

EV – Electric vehicle;
FACTS – Flexible Alternating Current Transmission Systems;
FC – Fuel cells;
FES - Flywheel energy storage ;
FFR – Fast Frequency Response;
FFT - Fast Fourier Transform ;
FLC – Fuzzy logic controller;
FLD - Fault-Localized-to- Downstream;
FLU - Fault Located Upstream ;
FRT - Fault Ride Through ;
FTU - Feeder Terminal Unit;
GA – Genetic algorithm;
GOOSE - Generic Object Oriented Substation Event Message ;
GPS – Global Positioning System;
Hh - Harmonic percentage;
HMI – Human Machine Interface;
HV- High Voltage;
IBFFR – Inertia-Based FFR;
ICT - Information and Communication Technologies;
IDS - Interconnected Distribution System;
IEC - International Electrotechnical Commission;
IED -Intelligent Electronic Device;
ISE – Integral Square Error;
IVV – Intelligent VOLT-VAR;
IVVH – Intelligent VOLT-VAR with Hysteresis;
KCL - Kirchoff's Current Law;
LD - Logic Devices;
LN - Logical Nodes ;
LQR – Linear Quadratic Regulator;
LTC - Load Tap Changer;
LV - Low Voltage;
MATLAB - **Matrix Laboratory(Program);**
MES - Massive Electrical Storage;
MMC - Modular Multi-level Converter;
MMS – Maintenance Mode Switch ;
MPPT - Maximum Power Point Tracking;
MSC - Mechanically Keyed SVCs and Capacitor;
MSR - Mechanically Keyed SVCs and Reactors;
MV – Medium Voltage;
NUEP - next unstable equilibrium point ;
OLTC - Operations to Change Tap Under Load;
P2V – Power-to-Vehicle;
PCC - Point of common coupling;

PEV – Plug-in Electric Vehicles;
PFC - Power Factor Control;
PI – Proportional Integral;
PSO - Particle Swarm Optimization;
PT – Potencial Transformer;
PU – Per Unit;
PV – Photovoltaic;
PWM - Pulse-width modulation;
RER – Renewable energy resources;
RESs – Renewable energy sources;
RET – Renewable Energy Technologies;
RMS - Root Mean Square;
RSCAD – Real Time Digital Simulator Computer-Aided Design;
RTDS – Real Time Digital Simulator;
SCADA – Supervisory Control an Data Acquisition system;
SCC/LCC - Auto or online switched converter;
SEG – Self-excited induction generator;
SG -Smart Grid;
SGs - Synchronous Generators;
SLG – Single-line grid;
SMG – Smart Microgrids;
SPWM - Sinusoidal Pulse Width Modulation Method ;
SR - Saturated Reactor;;
SRGS - Switched Reluctance Generators;
STATCOM – Static Synchronous Compensator;
STFT - Short Time Fourier Transform ;
SV – Sampling Value;
SVC - Static Var Compensator;
SVIB - Single VSG connected to the Infinite Bus;
SVS - Static Var System;
TCR - Thyristor Controlled Reactor;
TCT - Thyristor Controlled Transformer;
THD - Total Harmonic Distortion;
TSC - Thyristor-Switched Capacitor;
TSO – Transmission System Operators;
TSR - Thyristor-Switched Resistor;
TVPP - Technical Virtual Power Plant;
TW - traveling waves ;
TWBFL - Traveling Wave-Based Fault Location method ;
UEP - Unstable Equilibrium Point;
UPFC - Unified Power Flow Controller;
UPS - Uninterruptible Power Supply;
VCI – Voltage collapse index;

VD – Voltage deviation;
VPA - Virtual Power Angle;
VPP - Virtual Power Plant;
VSC – Voltage Source Converter;
VSG – Virtual Synchronous Generator;
VSI – Voltage stability index;
WAMS – Wide Area Measurement System;
WAN – Wide Area Network;
WECSS - Wind Energy Conversion Systems;
WOA – Whale Optimization Algorithm;
WT - Wind Turbine.

Symbol	Description
Ac	Central cross-sectional area
B(t)	Magnetic induction time
C	Capacitance (Capacitor of the filter)
C_{bus}	Bus Capacitance
C_f	Filter capacitor
D′	Distortion
D	Equivalent damping coefficient
D_{P1}	Damping coefficient of VSG1
D_{P2}	Damping coefficient of VSG2
D_q	Q-V droop coefficient
D_p	Active damping coefficient[W/rad²]
D_q	Voltage-drooping coefficient [Var/V]
E	Amplitude of output voltage
E^*	Reference Inverter's internal voltage [V]
E_0	Initial Inverter's internal voltage [V]
f_n	Nominal Frequency
f_s	Switching frequency
$H(t)$	Magnetic field measurement of the core
Hh	Level of harmonic percentage
i	Time interval
i_{oq}	q-axis reference current [A]
i_{0d}	d-axis reference current [A]
i_{Lq}	q-axis line current [A]
i^*_{Lq}	q-axis line current [A]
I	Current
I_C	Capacitor Current
I_L	Inductor Current
I_S	Current of the Static Var System
J	Inertia value
J_1	Inertia value of VSG1
J_2	Inertia value of VSG2
J	Moment of Inertia $[kg \cdot m^2]$
δ	Virtual Power Angle [rad]
δ^s	Power angle stable EP
δ^u	Power angle UEP
δ_c	Power angle When the fault is cleared
$\varphi 1$	Impedance angle [degree]
φ	Energization angle[degree]
α	Function of t_0
K	Integral constant

K_S	Slope characteristics of the SVS
K_{s1}	Proportional coefficient of VSG1
K_{s2}	Proportional coefficient of VSG2
kω	Angular frequency
L	Inductance
L_f/L_l	Filter/line reactance
m, n and p	Constants determined for any kind of steel rolling of the core
N_1	Turns number
Pcon	Converter Power
P_S	System power
P	Active Power
P^*	Rated Active Power
P_{01}	Rated active power of VSG1
P_{02}	Rated active power of VSG2
Q	Reactive Power
Q^*	Rated Reactive Power
R_1	Resistance
R_f	Filter Resistance
R_l	Line resistence
S	Apparent Power
S_{tr}	Transformer Apparent Power
T_1	Time constant
T_e	Output torque
T^*	Rated torque
THDI	Total harmonic distortion (where I stands for current.)
THDU	Total harmonic distortion (where U stands for voltage.)
u	Opponent value in the system under attack
U_k	k represents the harmonic order of the effective value U
V	Voltage
V_{dc}	DC link rated voltage
V_{dc1}	DC link rated voltage of VSG1
V_{dc2}	DC link rated voltage of VSG2
$V_t^{(k)}$	k^{th} harmonic voltage magnitude
V_{trcon}	Transformer Converter Voltage
ω	Angular speed
ω_{01}	Reference angular speed of VSG1
ω_{02}	Reference angular speed of VSG2
ω^*	Reference angular speed
X	Reactance
X_{SL}	Slope characteristics of the SVS
X_{Tr}	Transformer Reactance
$Y^{(k,k)}$	Array containing partial derivatives of the k^{th} harmonic

	of injection currents
$\theta_t^{(k)}$	**Phase angle at the t^{th}**
θ	**Angular position of the rotor with respect to a stationary axis in (rad)**

Summary

In this research, the operation of the electrical energy system susceptible to voltage instability, covering distribution systems, such as intelligent microgrids that operate in connected and island mode, highlights the study in favor of optimizing mixed composite systems with active networks.

Specifically, the highlighted oscillations in electromagnetic transients related to the connection and synchronization of the microgrid in which the virtual synchronous generator operation is impacted by oscillations in voltage, frequency, and supply capacity, in which the first swing stability is experienced in the system in changes noticeable, with characteristics of making the system unstable or returning to a state of stability. Regarding the activation of consumer loads composed of devices that increase the possibility of oscillations due to transients, it is observed that, by connecting the load, composed of electric vehicles fast chargers in the microgrid, increase electric loads and reduce the energy system stability.

The influences of electromagnetic incompatibility of the inrush current, due to its unpredictability and intermittent condition, have complex identification studies. With the inclusion of loads composed of electric vehicle chargers, the demand increases substantially, therefore, concerns about the effects of grid integration increase proportionally.

With recent control methodologies for developed distributed generation standards and definition for intelligent inverters, development models are required for intelligent inverters that operate with more advanced functions, relating voltage control to the available assignments.

This research emphasizes the operation of microgrids that connect or disconnect to a main grid, highlighting the configurations for the analysis of systems composed by

microgrids susceptible to different effects with variation of power related to the re-synchronization phenomenon and stability, as well as proposing a system with a virtual synchronous generator based on Static var compensator by incorporating VSG//SVC as a single fast optimizer electrical system.

Keywords: Distributed Generation, Electric Power Systems, Hybrid Energy Systems, Renewable Energy Sources, Smart Microgrid, Voltage stability.

1. Introduction

The amount of distributed generation consisting of renewable sources is increasing proliferation worldwide. Thus, distribution system operators need to improve system performance by keeping it within the stability margins, even when the amount of renewable energy in its portfolio increases, contributing to the balance of generation resources. Through a range of analysis and variation functions, active network management systems provide reliable voltage regulation imposing a pattern that avoids overload situations, efficiently informing the load flow direction and providing updated values.[1]

Power inverters stand out in the most complete electricity distribution systems as one of the most requested elements, and a power supplier interconnection of a large part of distributed generation in distribution systems. Currently, these devices perform advanced control functions that provide accurate control of active / reactive power and other electrical parameters, which allows the differential to have more extra functions in electricity systems. With recent control methodologies for developed distributed generation and defining patterns for intelligent inverters, development models are required for intelligent inverters operating with more advanced functions such as: intelligent VOLT-VAR.

Currently, in relation to the grid connected to the main grid, there is a diversity of operations for control for the DG (distributed generation). In 2009 the standards, Electric Power Research Institute (EPRI) and others define inverters: the intelligent VOLT-VAR (IVV) and the Intelligent VOLT-VAR with Hysteresis (IVVH) are among the various proposals. These functions define the control of reactive power injected according to the voltage at the point of common coupling (PCC), making the generation distributed an important element for the effectiveness of the electricity

system. As these functions are linear by parts, their modeling by traditional nodes PQ and PV presents differentials in classic solutions for energy flows.[8]

The electricity system formed by a microgrid has its operational characteristic considered at a stable level if state variables demonstrate steady state values that meet restrictions on operational limits, such as acceptable current levels, voltage and frequency with local supply patterns of electricity, when an oscillation or disorder occurs in this system, which can be considered stable as soon as all state variables demonstrate recovery values (possibly new values), i.e. state values that correspond to the limits of operational restrictions, maintaining all the planned offer load and proving the effectiveness of the Energy Efficiency Microgrid project, which covers the restricted definitions necessary for intrinsic and operational control. If a load reduction in response to the demand is necessary, it must contain planning in relation to the necessary conditions for the microgrid to remain stable. In unexpected situations where the load can be completely disconnected to delimit defective elements after a disturbance, the microgrid will be considered stable if it meets the necessary conditions, even if the reduction of loads does not occur only due to problems in the system related to voltage levels outside the acceptable limit range.

Identifying the main potential threats to an electricity system provides the best initial support to the resilience of the sector or electrical system in question. Current and future threats should be evaluated as well as the possibility of these threats over time. Threats are mainly divided into: natural threats from acts of nature (bad weather, floods, earthquakes, hurricanes, and extreme temperatures), as well as wildlife iteration with the electricity system (squirrels, snakes or birds causing short circuit in the electricity distribution system), threats caused by man, resulting from an accident (line cut), or intentional actions of an opponent (cyber attacks or terror acts).

There is no priority scaling of any isolated load on the stability of the electrical system as a whole, in traditional power electrical systems, in this case the intentional

load dispatch remains acceptable to preserve the continuity of its operation, due to the high number of demanded loads and the large scale of the system.

As the loads demanded in a microgrid are relatively restricted in quantity, the operation prioritizes the connectivity of certain feeders (supply hospital, various loads) over the rest of the electricity system; If one or more critical feeders have been triggered, the microgrid will operate differently from the main planning. Thus, intentional load activation in order to establish the resulting system operation during a disturbance, in addition to the previously mentioned specific, will imply instability to the system by the previous definition. The disorders may represent any exogenous inputs and similarly correspond to changes in the load, component failures or operational mode/adjusting mode adjustments. If disturbances represent "small" changes, such as minimal load fluctuations, being called as stability to small disturbances. Otherwise, this system would be called a large stable disturbance in relation to the change in question if the microgrid has stability as previously defined. Thus, a great disturbance occurs when there is an unpretentive transition between the modes connected to the network or island.

Unlike traditional electricity systems, in which the main factors of voltage instability appear the long electricity transmission lines, limiting the flow of electricity between generation and loads, in microgrids feeders have relatively short lengths, which results in reduced voltage decay between the ends of feeder generation and loads. Thus, voltage collapse, characterized by slow and constant voltage decrease along with the load reestablishment process and reactive energy supply, in microgrids will not have the same characteristics as in conventional systems. However, with the current electricity distribution networks increasing the active generation active microgrids systems, the voltage drop could become a difficulty in simpler and older networks.

In conventional electricity systems, voltage control at the terminals of generators and loads to be compensated occurs with reactive energy variation in a specific way. However, in electrical microgrids, as soon as a noticeable level change occurs in the DERS terminals, they are automatically reflected in the spare system due to the reduced size of the feeders. The sensitivity of the electricity consumption of the load with respect to the supply voltage level represents culminating aspects in the introspection of the voltage instability. Voltage instability may occur in the form of dynamic voltage and steady state into intolerable limits. If compensation coordination does not infer the small divergences of DERS voltage magnitudes in a compatible manner, high reactive power flows will form, resulting in greater voltage fluctuations.

Microgrid voltage instability may occur in small disturbances, such as when there are incremental variations in electricity demand, highlighting systems that operate near the load limit, similarly to stability analyzes to prevent voltage collapse, or act predominantly unbalanced. Voltage instability after a large disturbance can be verified proportionally to the system response, as well as the load characteristic, with the sensitive and sudden variation of the demand and/or disconnection of RES (Renewable Energy Source), or shutdown a system generator. Voltage instabilities are characterized as short or long term phenomena. In the short term voltage instability may occur due to the precarious composition of control coordination, usually in unknown phenomena of expected scaling, or sudden and fast dynamic alteration in the incompatibility of active and/or reactive power. On the other hand, the influence of the exits of distributed energy resources defines long term instabilities, characterized by the constant elevation of the demand, for example in resistive thermoelectric charges. In general, voltage stability represents a characteristic of electricity systems with a function of reactive power variation by following a load elevation or greater disturbance as a fault. For this reason, some tools and methods are developed and proposed to deal with the calculation of the load margin and

determination of critical analysis environments, from this an important role in the study of stress stability is formed. In this sense, the inclusion of electrical microgrids inserts new concepts analyzed, as soon as the electric vehicles plug-in are incorporated into the system. Thus, recharge scheduling to avoid voltage levels beyond the established limit becomes necessary, as well as the development of new standards regarding standardization enters the research assessment topics.[11]

Raising incentives spent by governments projects massive integration of electric vehicles into electrical power systems, as well as intelligent microgrid. The evolution of energy conversion systems necessary for systems for conversion into electrical energy has imposed several specific characteristics that bring different results to electrical energy grids. The impacts related to the inclusion of compound loads with electric vehicles on intelligent microgrid need to be extremely verified with different methods of analysis and stability, even though the environmental, economic and social benefits of the implementation of electricity-powered transport systems are extremely expressive.

Loads connected to the electricity system make functions related to the characteristics determined in their specifications, with evidence in the power flow imposed by the resulting scale system in reactive and active powers along the terminals determined to supply electricity, the margin of voltage stability it is defined from this resulting system, which may vary depending on the index required to maintain the voltages provided at the terminals into accepted values and within the limits established by the defined patterns.[13]

In terms of electrical power systems, voltage stability has a critical issue since many years. The stability of the electrical power system can be defined as the property of an energy system that allows it to remain in the operational equilibrium state under normal operating conditions and to recover an acceptable balance of equilibrium after being subjected to a disorder. The voltage collapse imposes a challenge faced in the

modern energy system in larger loads in the charging buses of an electricity system. The collapse of the voltage, in turn, will affect the stability of the electricity system. In this research, a new way to mitigate the collapse of the voltage, providing reactive power in load bus, discusses and drives simulation results. The voltage collapse is a process by which the sequence of events that follow the voltage instability leads to a low unacceptable voltage profile in a significant part of the electricity system. Voltage collapse has the ability to manifest itself in many different ways. The study comes down to describing a typical voltage scenario and providing a general characterization of the phenomenon based on real collapse incidents. Voltage instability in an electricity system is attributed to several factors, especially increasing loads to be tied, such as the inclusion of power supply systems for electric vehicle batteries, distributed generation interruption, reactive reduction sources exceeding the limitations, dynamic for the recovery of linked loads, transformer switching action and line disarms. To avoid voltage instability in systems, some modifications need to be made, which directly reach the generation, transmission, and consumption of reactive energy in the electricity system. Escalonated control to solve these problems and resolve voltage collapse makes up some of the actions described: Use of derivative-connected capacitors, generation redespach, transformer switching interruption, interim overload of generator reactive power and load minimization.

Dynamic and static analyzes make up the primordial scientific foundations in voltage stability research methodologies. Static approaches to voltage stability analysis are directly related mainly to the steady state model in question, such as the linearized dynamic model or as the power flow model, both expressed by the operation in the steady state. Dynamic analysis involves the use of a model defined with non-linear algebraic expressions and differentials, composed with generation dynamics, transformer switches, with transient stability simulations.

With the increase in the satisfactory characteristics of the microgrid, the imposition of electrical systems have incorporated in recent decades the benefits linked to intelligent microgrids, whether in autonomous or isolated forms, supported by the premises of the use of electricity in remote locations and the main function of providing greater resilience through optimized management and load scheduling in different situations of programmed and better system reliability using distributed energy sources and the best results to them. Jointly, the introduction of microgrids imposes an intrinsic use of the use of electricity in parallel to conventional power systems integrated with intelligent electrical systems which attracts to its composition the distributed electricity generation resources. The implementation of electrical systems with microgrids are constantly growing worldwide, can be seen in places composed of government entities formed by higher education institutions, military bases, as well as overall dealers, which projects an express growth for expected load forecast in the coming years. As a result, the analysis and specification of reflected behavior, voltage control and stability of the electrical system linked to the intrinsic imposed management in protection, defines the best feature required for the evolution of the electric system composed of active grids. The concept of stability in microgrids have a continuous aggregation of specific aspects regarding the electrical systems of conventional powers. Functions necessary to establish stability analysis attributed to this system unlike conventional power electrical systems relate to the characteristics of linked feeders, constant use of renewable power generation sources, converter interface components, systems operation in an unbalanced way and low inertia, which imposes constant specifications of the definitions of stability, standardization, analysis tools and modeling of components in the composition of microgrids. The design of these microgrids more efficiently and widely encompasses the restricted definitions of the intelligent microgrids necessary for the efficient operational control under various existing conditions and the corresponding system analysis methodology.

Distributed generation integration happens mainly in medium and low voltage networks. DGs (distributed generators) with clean energy have significant technical advantages for the distribution system, as well as the beneficial environmental highlights of these pure DGs in the power grid, generating loss reduction in electricity systems, voltage profile improvement, elevation network reliability and quality improvement of voltage. But the volatile nature of some types of DGs, such as wind and solar generation, makes it difficult to use in autonomous systems. To solve these difficulties, the energy storage system (ESS), such as batteries, is used to maintain the equilibrium of electricity of the microgrid.[17]

Increased penetration of electric vehicle charging in the mains may lead to problems related to increased electric charge. On the other hand, Plug-in Electric Vehicles (PEV) batteries have the advantage of supporting the electricity grid on the load peaks as an auxiliary power storage device. Defining the concept of vehicle to the grid (V2G), meaning that PEVs can provide energy to the electricity distribution network. PEVs act as electricity charges in the charging step or as electricity suppliers during discharge periods. Use in charging and uncharging of the PEVs usually imply technical obstacles, such as increased voltage, missing levels and transitional stability.

1.1. Publications

- V. Tiburcio Dos Santos Junior, "Fault Location Techniques Based on Traveling Waves with Application in the Protection of Distribution Systems with Renewable Energy and Particle Swarm Optimization," In: Mohamed, A.W., Oliva, D., Suganthan, P.N. (eds) Handbook of Nature-Inspired Optimization Algorithms: The State of the Art. Studies in Systems, Decision and Control, vol 213. Springer, Cham. https://doi.org/10.1007/978-3-031-07516-2_3
- V. T. dos Santos Junior, "Verification of Inrush currents from electromagnetic transients influencing the stability of voltage in Smart Microgrids connected to systems with electric vehicles," 2022 17th International Conference on Control, Automation, Robotics and Vision (ICARCV), Singapore, Singapore, 2022, pp. 961-965, doi: 10.1109/ICARCV57592.2022.10004345.
- TIBURCIO DOS SANTOS JUNIOR, VICENTE. Autonomous Electricity Generation System in Diverse Microgrids with Static Power Converters. 2023, Brazil. Patent: Innovation Privilege. Registration number: BR1120230254485, title: "Autonomous Electricity Generation System in Diverse Microgrids with Static Power Converters", Registration institution: INPI - National Institute of Industrial Property.

2. Challenges and expected results

The integration of photovoltaic or wind systems in a mixed junction of electricity generation of a hybrid system associates development and operational procedure with various technical and non-technical challenges. Primary non-technical calculations relevant in the integration of photovoltaic systems are mainly related to system planning and design, operation and maintenance, which essentially demonstrate all localized problems and thus differ from location to location.

Technical problems appear globally, including voltage and frequency fluctuation, harmonics, voltage sparkles (flicker) and unbalance, causing the electrical power system shutdown, electromagnetic interference, unintentional island, where a protection system fault due to the configuration of generation systems in microgrid can lead to serious consequences in terms of protection, safety, voltage quality and frequency stability and reliability.

Electricity generation in remote areas using renewable and sustainable power generation sources make up situations with numerous adverse conditions, including high operating costs. Although it has adversity, the set of scheduled actions are intended to be used as coordination of renewable generation based on their systems and are linked to financially capable and viable solutions for solving potential adversities.[20]

Therefore, new hybrid and micro-generation renewable energy development system strategies are adopted to facilitate the increase of renewable resources that properly address the technical and economic challenge.

System operational strategies and component technical restrictions impact significantly on the grid's photovoltaic hosting capacity. The calculation of the downward photovoltaic hosting capacity does not only depend on the voltage, frequency and thermal limit of the associated electricity distribution lines, but also on other factors, such as the value of the system operating reserve, load profile annual, annual generator loading profile, diversity factors and fluctuation of photovoltaic systems, generator initialization and generator load capacity.

Solar photovoltaic system output variability tends to increase quality voltage problems provided in the grid. Voltage quality problems relate to voltage and frequency fluctuations, harmonics and trembling problems. As photovoltaic systems have no mechanical inertia and do not include any local governor, it is complicated for hybrid systems with high PV penetration to maintain system resilience and stability. Within networks with high and safe supply capacity, the frequency response is managed by rotary masses, for example, synchronous generators. Therefore, in a hybrid system with high shares of photovoltaic systems, renewable generation, converting control systems must be adjusted to provide the previously obtained response from directly connected rotary masses. Due to the nature of the output of photovoltaic systems, it is often called as an unconteed source of electricity generation system. As stakeholders and electricity networks are implementing more and more photovoltaic systems in the architecture of electricity generation hybrid systems, public services find numerous challenges to integrate high participation of photovoltaic generation into the grid. Hybrid systems in remote areas differ from metropolitan or urban electrical grids in relation to behavioral and operational characteristics and load demand standard so they are prone to improvement by technical challenges. Generation with fast frequency response (FFR) and other desired control features can provide needed "synthetic inertia" as a synchronous generator on the electrical grid and may act as "virtual generation" to provide frequency support. FFR batteries can offer training and network processing capacity required on a power

grid, such as batteries and flywheels can quickly adjust the active power supply or demand in response to a series of control sign types, such as also, Wind Inertia-Based FFR (IBFFR), often called synthetic inertia or emulated inertia. When detecting a frequency disorder, the wind turbine extracts kinetic energy from the drive train, providing a small explosion of additional active energy (sustained by ~ 10 seconds). A recovery period usually follows, during which turbine blades should rekindle and active energy delivery is reduced below pre-event levels (for the same wind energy).[21]

Generally, hybrid systems outside the electrical grid worldwide have a similar nature of characteristics. Whether the existing system in Asia, Africa or Australia, the philosophy of operational measures of philosophy and management represent this perception. However, technical challenges due to PV battery integration range from developed countries and developing countries due to many non-technical factors, such as socioeconomic and political conditions. The load profile also varies from community to community. Therefore, system design and planning tend to differ. Some of the main common technical obstacles faced by the electricity dealers who operate the hybrid systems are as follows:

- Reliability and supply voltage quality due to comparatively weak networks.
- Problems occur from PV output variability.
- Inadequate resource and data monitoring facilities.
- Generation scheduling during the night time, when the PV output is not available.
- Configuration of grid protection systems according to distributed renewable resources.
- Keep operational and safety standards continuously.

The implementation of RET-based hybrid systems (Renewable Energy Technologies) in remote areas becomes a challenge due to various reasons ranging from technology and application without neglecting environmental gains on business profits.[22]

Lack of technical knowledge and customer awareness regarding renewable electricity generation becomes one of the non-technical barriers to establishing hybrid systems based on renewable energy in remote communities.

Long-term energy costs are usually very low for small and medium-sized industries, where rapid and continuous generation is a significant concern.

Prominent industries in remote areas (e.g., mining, oil and gas) are more concerned with the reliability of the system than in fuel economy emissions and initiatives through the use of renewable resources for environmental preservation.

Typical displacement factors: distance from the nearest urban area, supply chain operating problems, variety of comparatively lower economic activities, quality and level of education, availability of vital and essential facilities and standard of living.

3. New and emerging technologies and applications

New and emerging technologies are generally technologies that are currently under development or expected to become available in the next five to ten years, and are generally reserved for technologies that are creating, or are expected to create, significant or innovative social or economic effects.

3.1. Mixed Multi-Energy Systems

Multi-energy systems (figure 3.1/3.2) are integrated schemes of different vectors, sectors and energy networks such as electricity, heating, cooling and transportation. Generation sources from different forms of renewable energy capture in a mixed system produce the quantity necessary to meet the requested supply through the sum of the different and volatile forms of electrical power production (figure 3.1), acting as a single resulting generation source (figure 3.2). These systems are essential to generate new types of energy flexibility as well as technical, economic and environmental opportunities for reliable operation and lower cost of future intelligent electricity networks. Renewables are the backbone of any energy transition to obtain electricity systems without carbon emissions. As the world increasingly distances itself from carbon-emitting fossil fuels, the understandable specification of the current role that renewables play in decarbonization of various sectors reflects the essential potential to ensure a soft way of zero liquid carbon emission. [26]

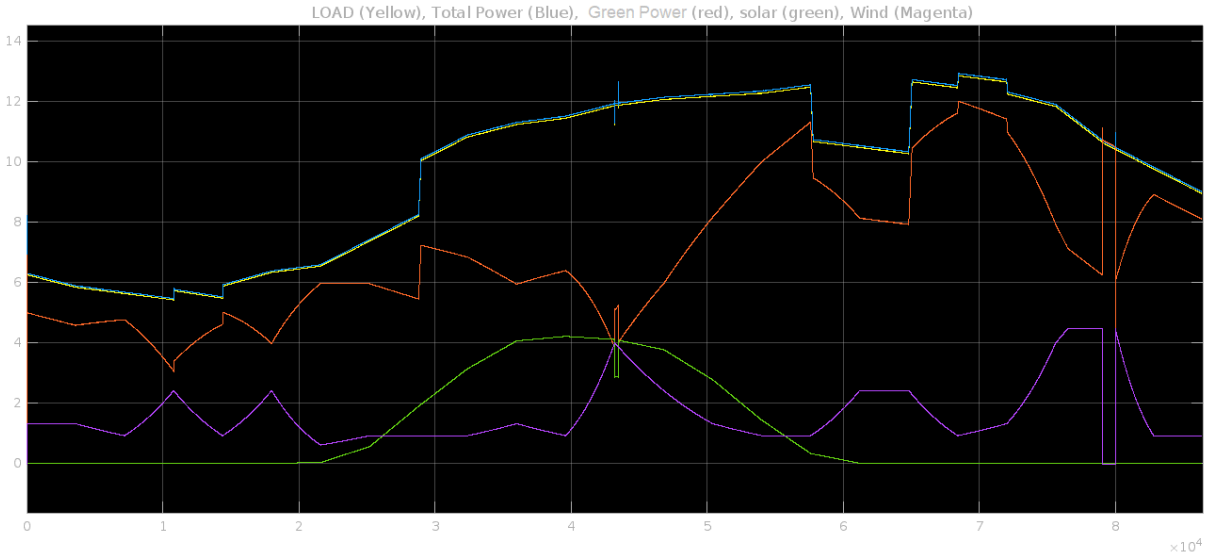

Figure 3.1 - Hybrid system electricity generation sources.

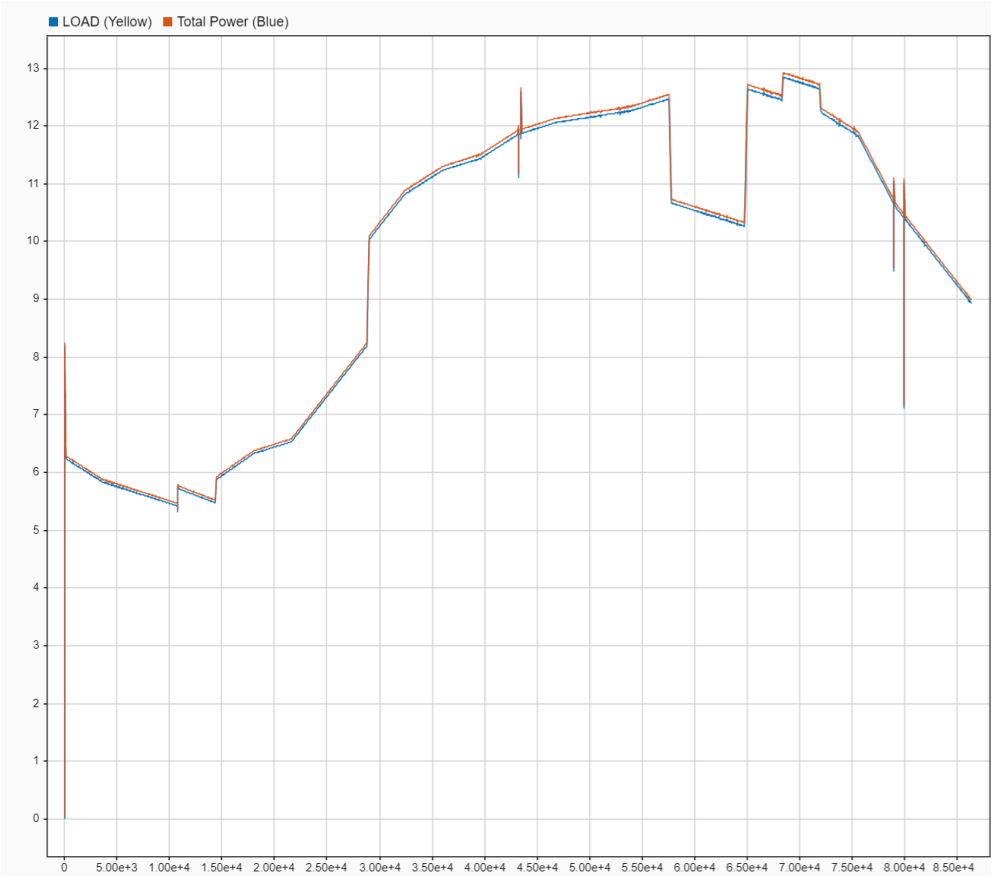

Figure 3.2 - Total power and total consumption of the hybrid system.

Among the benefits of mixed multi-energy systems, they include:

- Better energy efficiency of the total power generation and supply system;
- Expansion of the possibilities of using more renewable energy, for example, the excess energy of wind generation or PV (figure 3.3);
- Use of new forms of storage installations heating/cooling and also electricity, for example, use of the concept of vehicle to grid (V2G);
- Possibilities to neutralize fluctuations from generation sources from renewable energy (figure 3.4);
- Exploitation of possibilities to use wasted energy from industry.

When planning to enable interactions of mixed systems with various energy in electricity distribution networks, it is necessary to study and improve the configurations, impacts and perspectives of mixed systems of various energies that provide electricity of improved solutions to smart systems, energy storage and lateral management of demand in electricity networks with a growing participation of distributed electricity generation sources [27].

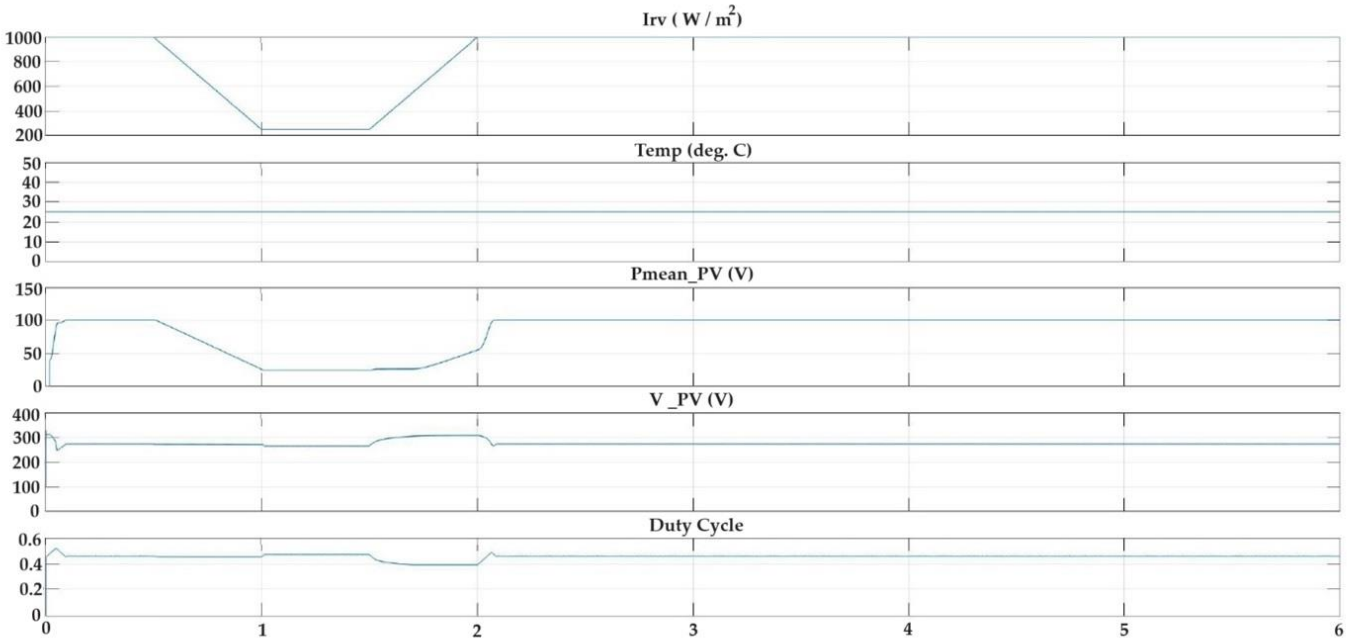

Figure 3.3 - Photovoltaic power generation system (by time in seconds)[Matlab].

There are currently a growing number of opportunities and impacts of mixed systems with future electricity systems. Thus, technologies and systems that integrate various sources of energy need to be considered and sized for harmonious integration in the sector. This includes power to grid (P2G), including electrochemistry, fuel cells, hydrogen storage; Power-to-Vehicle (P2V), including grid vehicle services (V2G); and Compressed Air and Hydro-Charities Pumped, more specifically, the electricity generation systems coming from renewable sources, which hold the necessary functions to attribute greater reliability, autonomy and resilience to electrical power systems.

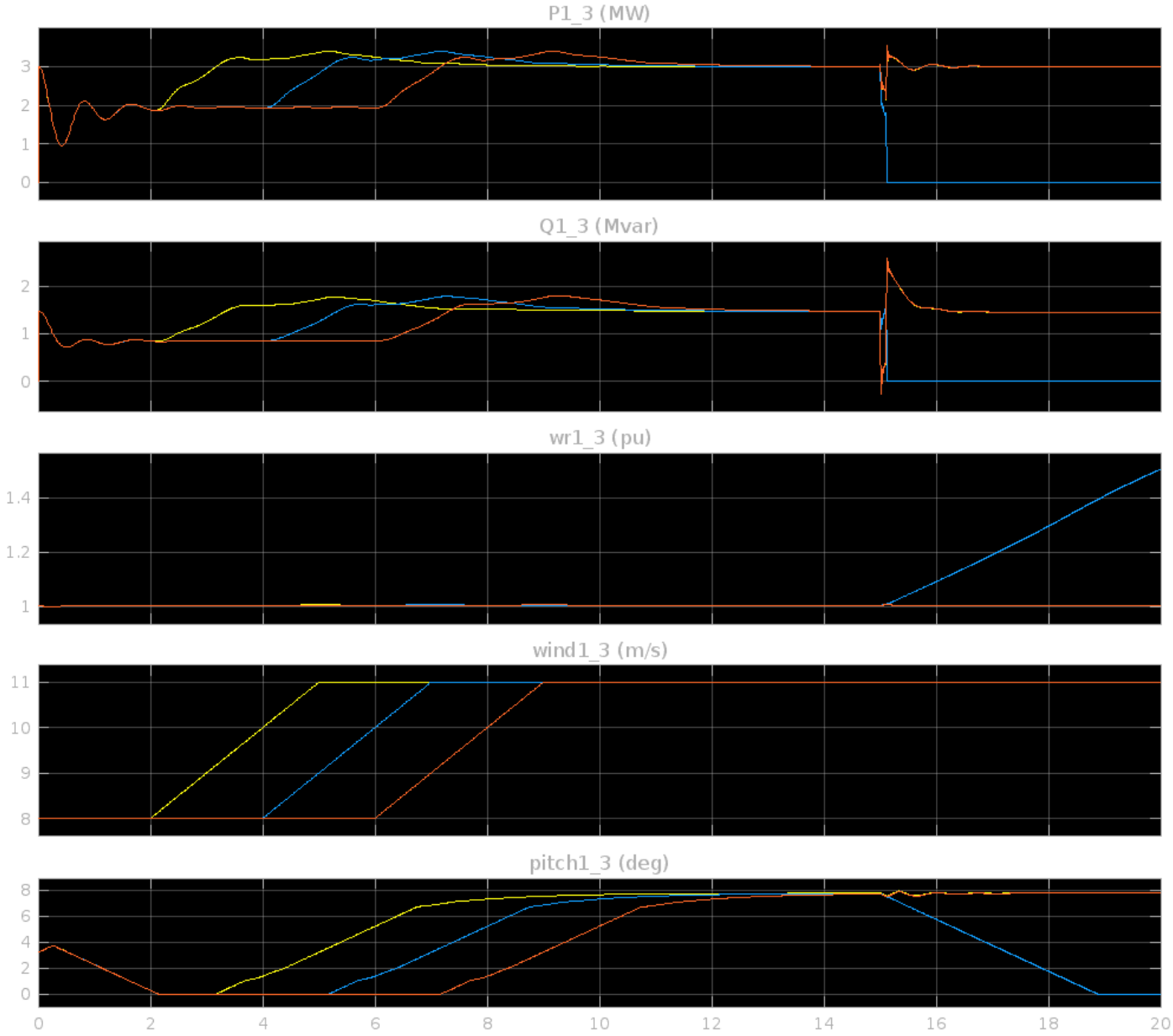

Figure 3.4 - Wind Electric Power Generation System(by time in seconds)[Matlab].

3.2. Electric Transportation System

The impact of electrical mobility on the electricity system can create local restrictions as LV (Low Voltage) and MV (Medium Voltage) infrastructure needs to meet the increased needs of electric vehicle charging systems. Increasing the supply capacity of the electricity grid may be necessary, especially when charging time

coincides with the time of load peaks or may create new peaks for double tariffs. This use of non-controlled electric vehicle charge will inevitably lead to increased capital expenses, overload can be minimized, however, applying intelligent electric vehicle charging techniques that wisely distribute loading energy over a time period. This intelligence system can soften the load curve, providing a much better use of network infrastructure. The impact of the inclusion of electric vehicles on the network (V2G) has not been widely viewed due to the reduced rate of inclusion of electric vehicle load systems, and these characteristics will become more practical to adopt when the load number included in the vehicle market, increases substantially. Currently, the high costs of purchasing electric vehicles are limiting the acceleration of the adoption of EVs for private public and commercial transport purposes.

3.3. Electric vehicle charging systems such as DER

Driven by national policies with inclusion of subsidies to fossil fuel-based transport electrification programs, the number of electric vehicles tends to increase worldwide. The most relevant aspects of the impact of the inclusion of EVs on future electricity supply systems include:

• Implementation of EV charging systems and charger technologies: smart electric vehicle chargers using smart converters, fast and slow chargers, significant connection in the electricity distribution system (slow chargers) or on dedicated feeders specific to systems with Electric cars (quick chargers).

• EVs used in order to act grouped as an electricity storage technology that can be implemented in electricity distribution systems, with the ability to act as a source of renewable electricity generation and providing electricity to the network, beyond the charging of electric vehicles.

This technology allows new raids to stipulate greater reliability and resilience to the electricity distribution system and the entire system to this connected that depends on distributed electricity generation.

• EVs acting as adaptable electricity resources. The EVs have the ability to be a component of consumer action and promotion, allowing the supply response and the performance of the demand for electricity supply.

• EVs acting as a resource and planning for smart cities: technologies for support based on EV, energy, control, and information and technology for expansion and reliability of power electrical systems.

The storage system of an electric vehicle can provide more planning options to the Distribution System Operators (DSO) when the EV is connected by the charger to the electricity distribution system, analogous to a stationary BESS. The supply of electricity through this type of distributed generation source will be directly related to some system characteristics related to this, in this system with the electric vehicle battery being used as a storage system, the Electric vehicle's battery charge state and the amount of energy available depends on how it was employed in the past and the designed use of the EV, as well as the battery-packed energy collection by performing the charging operation at the time of use of the system, such as a DER. In the charging operation, the EV battery becomes a fully controllable charge storage, potentially allowing DSO control, as needed, the loading rate. By the time it is fully charged, the EV battery is characterized as a fully controllable BESS. Similarly, to what is described, when several EV chargers are considered in connecting to the electricity distribution

system, EV charging can be controlled and coordinated to meet the requirements and restrictions of the distribution network, if the system that makes up the supply Electricity depends on the distribution grid and has no preset autonomy for its operation. What's more, when fast chargers incorporate stationary batteries for fast battery charger, demand rates can be reduced and stationary battery acts as a BESS, even in the fault of an EV connection, as this system battery-incorporated loaders depend on the power supply to these batteries, which will depend on where and how to generate batteries supply the amount of energy for their storage, varying between renewable generation, distributed generation sources and systems of energy connected to distribution networks with SmartGrid, respecting the environmental conditions of use.

As noticed, several EV charging stations settings can be obtained in supply operating, and these settings evolve as use and their aggregate development. The benefits and divergences of the various configurations in the distribution network and its potential to provide different solutions for intelligent electricity distribution systems need to be considered when a system that includes a greater load acceptance and consequently more bidirectional power flow in its planning, in part to the necessary expansion capacity and from distributed generation systems and use by storage in batteries with electric vehicles.

Some aspects of the research methodology that need to be highlighted:

(a) Impact of electric vehicle charging (and discharge) on the distribution network and the supply capacity of distribution networks for EV chargers;

(b) Charging requirements, electric vehicle charger specification standards regarding the quality of the voltage in use, charger location and slow and fast charging standards for different types of EVs: cars, buses and trucks;

(c) Magnificence of expected technology and developments, charger types (slow and fast loading), charger manufacturing technology, bidirectional resources training (vehicle-to-grid and consumer building vehicle); Different semi-fast and fast loaders with integrated storage (battery storage, other technologies), installation in residential, commercial and electricity utility configurations; Coupling of porters with renewable energy resources, standardization (existing and planned);

(d) Electric vehicle charging scheduling, including single EV charging, control and coordination of multiple chargers, demand management and response to meet network restrictions to be connected; Quick charging management and impact on the planning and operation of distribution systems;

(e) Provision of auxiliary services for electric vehicle chargers for DSO and TSOs and the associated legal regulatory issues, business models and property for expansion coordinated charger network to be installed and required compliance with power supply for proliferation supply of electrified vehicle technology, technological, socioeconomic, financial aspects and business cases for the implementation of EV loaders.

4. Smart Microgrid

Smart microgrids are designed to meet the specific energy needs of local populations, such as a single consumer customer, a university campus, offices, or a rural community.

4.1. Technologies used for Smart Microgrid

The development of intelligent microgrid technologies requires a portfolio of large research and studies for operational improvement and imposition of better resilient

characteristics. In this regard, sensor arrays optimization is still the basis for the best direction of performance resulting in reliable operation and fewer executions regarding computational processing on smart devices. Switching systems encompass the need for automated management of secure operation. The use of digital control system mechanism completes the technological structure implementing artificial intelligence in robust and effective control systems with diverse functions directly related to the expected electricity supply.

4.1.1. Microgrid Control Systems

The microgrid appears as the main premise for future electricity distribution networks. As the use of technologies for microgrid deployment expands in traditional electricity distribution networks will imply the adequacy of traditionally utilizing control systems employed. The structure of microgrid control system formation is based on control doctrines being categorized into three fundamental methods:

i. Centralized Control

Characterized as common and traditional, centralized control represents a control method for microgrid. In centralized mode there are two types of control systems for microgrids. In the first form of control, a distributed generation system controls distributed energy (DER) resources. In the second form of control, a central unit of control and decision management controls the microgrid. The centralized control system consists of all data from all instruments in the microgrid and determines the operation with databases in that data.

ii. Decentralized Control

Uncoordinated control represents another control approach. Each unit performs a task independent of other drives in this type of control. In this mean, reducing interchangeable information will reduce demand for a high-cost communication network. In addition, its characteristic is to provide plug-and-play capacity for installing additional distributed power resource units and consumers on the microgrid.

iii. Hierarchical control

As the electric power system receives improvement control system objects become less complicated at the operational point of view. The modes islanded and connected to the network in microgrid applications have always been considered by separate approaches. With this, there was a need to develop a microgrid operation system in both operating modes, connected to the network and islanded. The scalability and profitability of the microgrid became fundamental to the operation after deregulation. In this way, microgrid operations have changed completely. It is necessary to implement hierarchical control as the best option in this situation, where its control objectives are organized in three levels:

a) Primary control

Frequency adjustment and voltage amplitude are the focus of this control level which are placed as the input parameters for the internal control loops of current and voltage. Changes in supply for load supply and changes in power supply are attended with faster responses guaranteed by primary control. The provision of the operational scope of this regulation is established in milliseconds, being paramount to maintain the operational stability of the network. The continuity of the performance of energy storage systems, such as batteries, has its features assisted by the use of primary

control. The power availability and battery charge level for supply define the mode of operation for this purpose. The ideal settings for primary regulation in island mode are defined by the battery charge state.

In this respect, each inverter will have an external power loop based on a tilt control, defined as autonomous or decentralized control, whose purpose is to share active and reactive power between distributed generation units and impose the best system performance and stability, whose adjustments at the same time define the frequency and magnitude of output voltage.

b) Secondary control

The bandwidth of the secondary control has a lesser amplitude than that of the primary control, because it thus dissociates the two dynamics, and also reduces the communication speed and has sufficient time to perform all the necessary calculations. Of course, it compensates for the voltage and frequency variations obtained by the primary control and performs network synchronization. In other overhand, secondary control can also act as the Power Management System, defining energy flow and energy quality within the microgrid, defining itself as the highest level of control when the microgrid is in island mode.

c) Tertiary control

In the third hierarchical control loop, the inverter references connected to the microgrid are adjusted even to generator MPPTs so that power flows are optimized. Power references provided to secondary control can be calculated based on an economic analysis structured by market prices, weather forecasting (as sources with stochastic behavior are employed, such as panels photovoltaics) and the agreement between the customer and the network operator. When deploying this level of control, some extra features can be obtained, with island detection or harmonic reduction of harmonic network voltage by harmonic injection. The implementation of

the multilevel hierarchical approach will be related to communication infrastructure and future intelligent network codes.

4.1.2. Communication in Microgrids

With the implementation of the advanced communications system, intelligent microgrids operate under the scope of a methodological control system based on communication interfaces in secondary control and intelligent agents in tertiary control to optimize the control reference values. The hierarchical control structure for monitoring and managing microgrids based on IEC 61850 is scaled at three different levels, which are explained below [41]:

• Station level (Human Machine Interface (HMI) and SCADA systems): at this level, MG has management and operation in automatic and manned management modes. This level establishes the interface between the MG and the main network, selecting the management mode between the centralized, decentralized, island or network connection modes, and sending the generated reference values for voltage, frequency and energy cost to the lower levels.

• Bay level (protection relays and control devices): The supervision, monitoring and control of the MG takes place at this level. Lower-level measurement and monitoring data is received and sent to the station and process bus after meeting management goals. Thus, generation and consumption are regulated and adjusted, imposing the safety level of the MG electrical system, especially during operation in island mode, and measurement and monitoring for electrical energy management, based on the operating condition.

• Process level (current or potential transformers (CTs, PTs), circuit breakers (CBs) and DG / ESS output / input): This level has a direct interface with the power system and its electronic power devices (such as inverters and converters) The power output of the sources and the energy management in the ESS is based on a signal received from the compartment level. Generally, each device at this level has its own data management, measurement and conversion modules. At this level, the control of the output value of the sources of the energy system occurs, the sending and receiving of the measured value of the voltage and frequency and to collect reference values, as well as to carry out energy management (especially in the ESS section) [42].

The devices and equipment on these three levels connect to each other through the station and the process buses. In general, the communication between measurement, intelligent sensors, protection and control equipment at the process level is based on the sampling value (SV) message method used by the process bus, while the protection and control equipment operate based on in the generic object oriented substation event message (GOOSE) for the compartment level on the same bus. For the implementation of intelligent control, an additional level must be added to the hierarchical information structure when several MGs are implemented in a system. This additional level is called the master level. This “master level” is located above the other three levels and interfaces with all of them managing the system through intelligent interpellation and communicating through the servers with the MMS core. To implement a complete equipment model in a cluster of intelligent MGs, logic nodes based on IEC 61850 must be used.

In IEC 61850, IEDs consist of a variety of Logic Devices (LD) and, at the lower level; LDs consist of a group of Logical Nodes (LN). An LN in IEC 61850 can be seen in this case as data from the generator or the demand side. The data is determined based on a special class defined by IEC 61850 and covers all the characteristics necessary to describe a LD (for example, protection relay, CB, power electronics, etc.). The list of

LNs in a feeder of an inverter-based source system is synthesized in Table 6.1. According to IEC 61850-7-4, the first letter of each LD's name shows its category. For example, T stands for instrument transformer and TCTR and TVTR are current and voltage transformers, respectively; X is used for the frame section and XCBR is a circuit breaker.

4.2. Sensor Systems

With the advent of distributed electricity generation, intelligent networks have acquired the ability to incorporate micro-generation allowing the expansion of power generation and trade. The smart microgrid covers the electricity system more effectively by assimilating distributed power generation resources (DERS), enabling lower than conventional scale generation systems to connect into the mass electrical grid inserting higher demand for demand from electricity to the system as a whole. For this type of function to be established with voltage quality to be provided to the main system and peripheral loads, the provision of information from the network and additional intelligence systems provided by projected sensors and software respectively needs to quantify the disturbances caused in real time by other sources.

Data collection, coming from the effective operation, performed by the architecture of the sensor system to be passed on to a central repository, uses sensor technology capable of acquiring information from the data environment generated with the aid of communication devices, hubs and Intelligent Electronic Devices (IEDS), these use data from electricity generators and sensors. The data collected follows to an interface computational base via software, which interprets the data purchased by rejecting the necessary information for the diagnoses of the specific operation. From there the range of control actions are processed and are performed as needed, assist protection devices or regulate voltage for acceptable limits, maintaining the desired operating conditions for the best supply of electricity. The inclusion of high-performance computational

processing technology allows intelligent electronic devices (IEDs) to act in multiple monitoring, communication and optimization of safe and reliable operation. IEDs can allow active network management with the inclusion of distributed generation feature, thereby performing the incorporation of adaptive protection schemes, in this case acting according to the distributed generation volatility in operation with disturbance caused by various effects, being found in microgrid connected to smart grids. Parallel to active network management, the performance of the IEDs proceeds in the resulting operation of distributed generation failure defined in network code, including, together, the interface for DG designed to increase the generation capacity and those already existing in electricity system to integrate the medium active medium voltage network voltage control system. IEDs act as high reliability devices in performing the essential functionality required in island detection.

Smart microgrid with automated sensors and computational processing with software and renewable electricity generation intensifies in the programmed operation of real-time monitoring and may tie the functions of the dynamic stochastic optimal control (DSOC) with systems active in forecasting and data determination and determination systems of electricity generation exits. These software acts with algorithms that compute offline sets of inverse induction value functions. The optimization of decision systems is performed online computing over the time of operation, using value functions. In order acting with real-time intelligent microgrid with limited renewable generation resources in supply demand requires the dynamic stochastic optimal control system (DSOC) with forecasting and characterization system of renewable energy generation (wind and solar). Neural networks play a key role in performing these computational tasks. Adaptive critical projects use neural network-based projects for optimization over time through intrinsic concept combined reinforcement learning and approximate dynamic programming.

4.3. Advanced Measurement Infrastructure

Advanced measurement infrastructure represents any type of bidirectional communication system to collect detailed measurement information across a utility's service sector. AMI stands out because it is typically automated and allows for real-time and on-demand captures from measurement endpoints.

4.3.1. Operation and Management Algorithms

Continuous operation and supply voltage values in acceptable limits proposed by the energy system are directly related to electricity management in smart microgrids (SMG), demonstrating essential when the electrical system operates in the island mode which imposes more resulting energy efficiency in the requested planning. When implementing a dynamized control, that is to be able to re-establish the acceptable voltage limits in the event of a disturbance, along with the further automated operation in the smart microgrids (SMG) completely the best electricity management and balancing. Dynamic Energy Management (DEM) makes up the set of ingenious engineering mechanisms to act in case of electricity decline imposed mainly by the non-establishment in the planned demand for the consumption of the arranged charge, as well as the oscillation in the amount of generation required to comply with the pre-established supply in SMGs connected to the network and island. The use of electricity storage systems provides the power supply operation a greater dynamism to SMG power flood. The DEM composition system generally involves a mixed electricity storage system, which implements more than one type of electricity storage device, which encompasses SMG-charged load rate scans to electricity storage systems, those with extremely wide range in commercially specified systems.

4.4. Grid Supporting Converters for Islanded Operation of Microgrids

In the island (or autonomous) operation of a microgrid, the converters operate in the grid supporting mode, as shown in the figure 4.4.1.

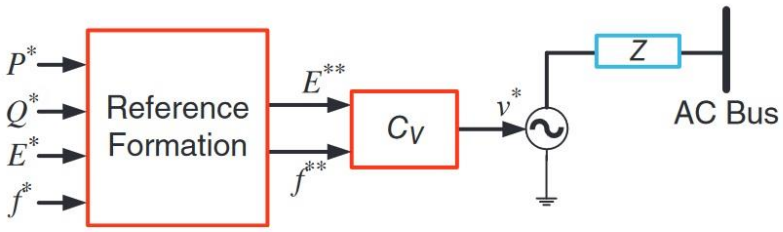

Figure 4.4.1 – Grid supporting.

The inputs of these converters are DGs (DERs) on the DC side. The converters are necessary to provide output voltages according to active and reactive power, voltage magnitude and frequency. DERs that are connected to the microgrid share power according to their classifications. In certain system configurations, energy storage works together with converters in a specific configuration to supply electrical energy in island mode, which reduces the variation in energy generation from renewable sources, such as photovoltaic sources from solar energy. A detailed approach to estimate droop gains so that accurate sharing of real/reactive power occurs is necessary. However, power sharing usually depends on the R/X ratio of feeders that connect DGs in the microgrid. The droop concept is explained when considering the behavior of a virtual synchronous generator during transients. With equations proved by [43].

A large power system is made up of several synchronous generators. They can store kinetic energy while rotating at synchronous speed. If the system load increases suddenly, generators momentarily release stored kinetic energy to meet the demanded load. Assuming that the damping of the system is negligible, the generator rotor dynamics is given by the swing equation:

$$\frac{2H}{w_s}\frac{d\delta^2}{dt^2} = P_m - P_e \tag{4.4.1}$$

where

$$H = \frac{Stored\ kinetic\ energy\ MJ}{Generator\ MVA} \tag{4.4.2}$$

Where ω_s represents the synchronous speed of the rotor in rad/s, δ represents the load angle in rad, P_m represents the mechanical power input in per unit (pu), P_e represents the electric power output in [pu].

The load angle relates to the generator Speed ω by equation 4.4.3:

$$\frac{d\delta}{dt} = \omega - \omega_s \tag{4.4.3}$$

For a three-phase synchronous generator, the mechanical input speed does not change instantly due to its large rotational inertia. As a result, when a sudden load increase occurs, the term *Pm-Pe* becomes negative. By equation (4.4.3) the generator speed ω drops below the synchronous speed ω_s, i.e. the generator slows down. The release of the stored rotational energy in which the angle does not differ occurs so that the generator maintains the balance between the mechanical and electrical power, causing the generator to lose the synchronism. This procedure is performed in a temporary process and can last only a few cycles. To supply the load increase, the generator turbine-governor action is required. This is obtained through a steady state frequency-power relation, called the droop equation.

4.4.1. Active and Reactive Over a Feeder

Consider the simple system shown in Figure 4.4.2., in which two sources are connected together through a feeder with an impedance of $R + jX$. Assuming $V_S = V_1 < \delta_1$ and $V_R = V_2 < \delta_2$, the current through the line is given equation 4.4.4:

$$I = \frac{V_1 < \delta_1 - V_2 < \delta_2}{R + jX} \tag{4.4.4}$$

Therefore, the complex power flowing from the source is given by equation:

$$P_1 + jQ_1 = V_1 \times I^* = V_1 < \delta_1 \times \frac{V_1 < -\delta_1 - V_2 < -\delta_2}{R - jX} = \frac{V_1^2 - V_1 V_2 < (\delta_1 - \delta_2)}{R - jX} \quad (4.4.5)$$

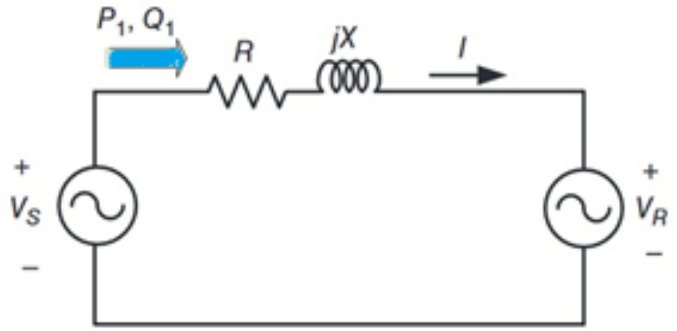

Figure 4.4.2 – Two AC source connected together through a feeder.

Defining $\delta = \delta_1 - \delta_2$ and expanding (4.4.5), the real and imaginary parts are given by equations 4.4.6 and 4.4.7.

$$P_1 = \frac{V_1}{R^2 + X^2}[R(V_1 - V_2 cos\delta) + XV_2 sin\delta] \quad (4.4.6)$$

$$Q_1 = \frac{V_1}{R^2 + X^2}[-RV_2 sin\delta + X(V_1 - V_2 cos\delta)] \quad (4.4.7)$$

4.4.2. Inductive Grid

Considering a system where the grid is formed with predominantly inductive characteristic, i.e. $X >> R$, so that it can be determined that $R \approx 0$ (i.e., the value of the resistance is considered negligible for the purpose of the calculation performed).

Moreover, it can be determined that the load angle δ is very small, such that $sin(\delta) \approx \delta$ and $cos\ (\delta) \approx 1$. Therefore, (4.4.6) and (4.4.7.) can be rewritten as by equations 4.4.8 and 4.4.9 :

$$P_1 \approx \frac{V_1 V_2}{X}\delta \Rightarrow \delta \approx \frac{X P_1}{V_1 V_2} \tag{4.4.8}$$

$$Q_1 \approx \frac{V_1^2 - V_1 V_2}{X} \Rightarrow V_1 - V_2 \approx \frac{X Q_1}{V_1} \tag{4.4.9}$$

These two relations define the direct relationship:

- Between the active power P_1 and the load angle δ;
- Between reactive power $Q_1$and voltage variation $V_1 - V_2$;

The relation in the equation (4.4.8) results in a P-δ drop. However, it is noted from equation (4.4.3) that the load angle δ derivative is proportional to the frequency difference. Therefore, the proportional relationship between frequency and active power can stabilize. Similarly, the second equation relationship, (4.4.9), results in a voltage drop that varies according to reactive power.

Suppose that a microgrid has a total number of N of DERs. Then the P-f and Q-V inclination equations for each DER are given by equation 4.4.10 and 4.4.11.

$$f_i = f^* + n_i \times (0.5P_i^* - P_i), \;\; i = 1,2, \dots, N \tag{4.4.10}$$

$$V_i = V^* + m_i \times (0.5Q_i^* - Q_i), \;\; i = 1,2, \dots, N \tag{4.4.11}$$

where f^* represents the reference frequency of the entire microgrid in Hz and V^* represents reference voltage of the microgrid in kV; P_i^* and Q_i^* represent respectively the active and reactive power rating of the ith DER and n_i and m_i represent their respective droop gains. Assuming that the frequency variation is restricted between f_{max} and f_{min}. So, according to equation (4.4.10), a DER can provide half of its nominal power when it operates in the nominal frequency f^*.

General observations:

- Constant frequency control (isochronous) means that a generating unit will regulate the frequency to a certain adjustment point, regardless of the active power output of the generator.

- Constant voltage control means that a generating unit will regulate the terminal voltage to a certain adjustment point, regardless of the reactive power output of the generator.

- For two or more generators connected to a system, isochron control and constant voltage control can lead to instability.

- With frequency drop, we directly control the active power, as there is a ratio of one to one between the frequency and the active power output to a particular generator.

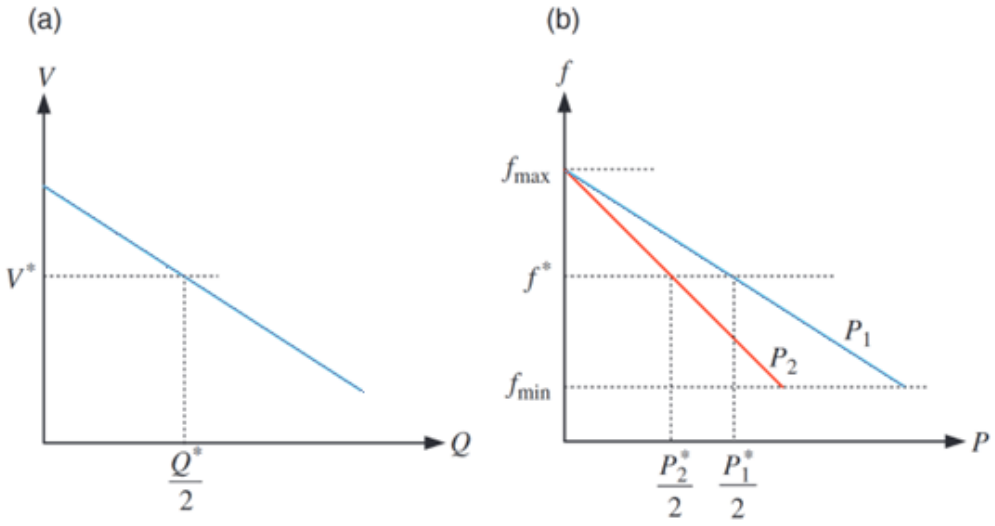

Figure 4.4.3 – Droop characteristics for inductive grid: (a) Q-V droop and (b) P-f droop.

Analysing a microgrid where only two DERs are present. At the time when DERs are operating at a nominal frequency of 50 Hz, providing half of its nominal power, when the load increases suddenly, as all generators in a grid should operate at the same frequency, on the contrary, a large amount of current will flow through the grid. Therefore, DER-1 must provide $\frac{P_1^*}{2} + \Delta P_1$ amount of energy, while DER-2 must supply $\frac{P_2^*}{2} + \Delta P_2$ such that the operating frequency of both DERs becomes $50 - \Delta f$ [Hz] (figure 4.4.4). This operation becomes the basis for a selection of fall gain. Forming a

shallower DER-1 line of DER-2. The inequality $P_1^* > P_2^*$ implies that the angle of the droop line with respect to the Y axis is higher for DERs with a higher nominal power than those with lower nominal power.

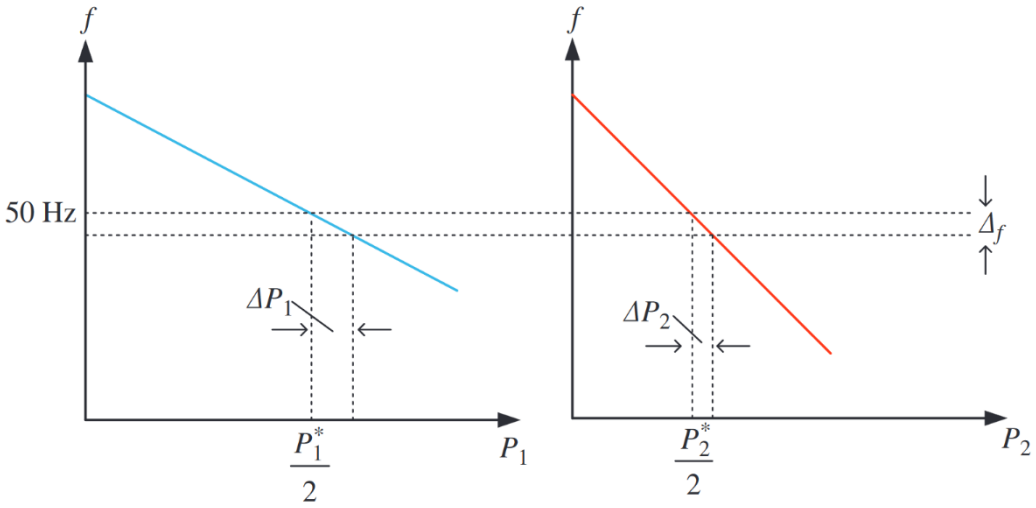

Figure 4.4.4 – P-f droop lines of a two-DG microgrid.

In general, a microgrid contains N number of DERs will follow the following expression if the frequency of all of them is restricted between $\mp\Delta f_{max}$ Hz

$$P_1 * n_1 = P_2 * n_2 = \cdots = P_N * n_N = \alpha \qquad (4.4.12)$$

Thus, fall gains for all DERs should be chosen so that α remains constant.

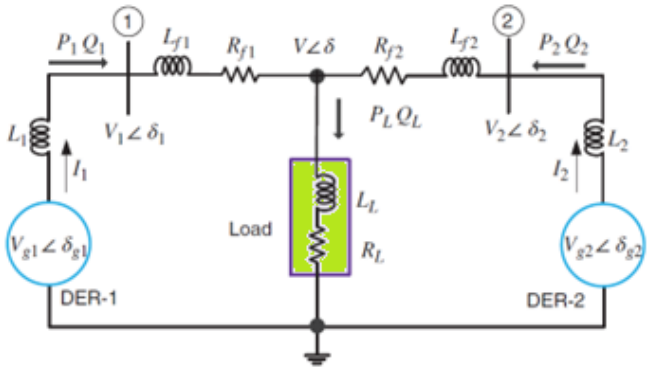

Figure 4.4.5 – A hybrid microgrid with two DERs.

As soon as the necessary voltage magnitude and frequency are obtained, the reference voltages for each DER are obtained as by equations 4.4.13:

$$\begin{cases} v_{ai}^{*} = \sqrt{2}V_i \sin(2\pi f_i t) \\ v_{bi}^{*} = \sqrt{2}V_i \sin(2\pi f_i t - 120^o) \\ v_{ci}^{*} = \sqrt{2}V_i \sin(2\pi f_i t + 120^o) \end{cases} \qquad i = 1,2,\dots,N \qquad (4.4.13)$$

Each DER is trained by a VSC, connected to the microgrid through an output LC filter. Reference voltages are then reproduced through the filter capacitor in an ABC table using a state regulator feedback controller (LQR). DERs is supposed to be fed by fixed DC sources.

4.4.3. Resistive Grid

A high X/R ratio represents the main feature of energy transmission systems. On the contrary, distribution feeders are mainly resistant and, therefore, reactance X in (4.4.6) and (4.4.7) may be neglected. These two equations are then rewritten as by equations 4.4.14 and 4.4.15.

$$P_1 = \frac{V_1}{R}(V_1 - V_2 \cos\delta) \tag{4.4.14}$$

$$Q_1 = -\frac{V_1 V_2}{R}\sin\delta \tag{4.4.15}$$

Again, assuming the load angle δ to be very small, (4.4.14) and (4.4.15) are reduced by equation 4.4.16 and 4.4.17.

$$V_1 - V_2 = \frac{RP_1}{X} \tag{4.4.16}$$

$$\delta = \frac{RQ_1}{V_1 V_2} \tag{4.4.17}$$

Therefore, in a majority resistive grid, the actual power is proportional to the magnitude of the voltage, while the reactive power varies with frequency. The P-V and Q-f cover equations for the resistive grid are given equations 4.4.18 and 4.4.19.

$$V_i = V^* + m_i \times (0.5P_i^* - P_i) \tag{4.4.18}$$

$$f_i = f^* + n_i \times (0.5Q_i^* - Q_i) \tag{4.4.19}$$

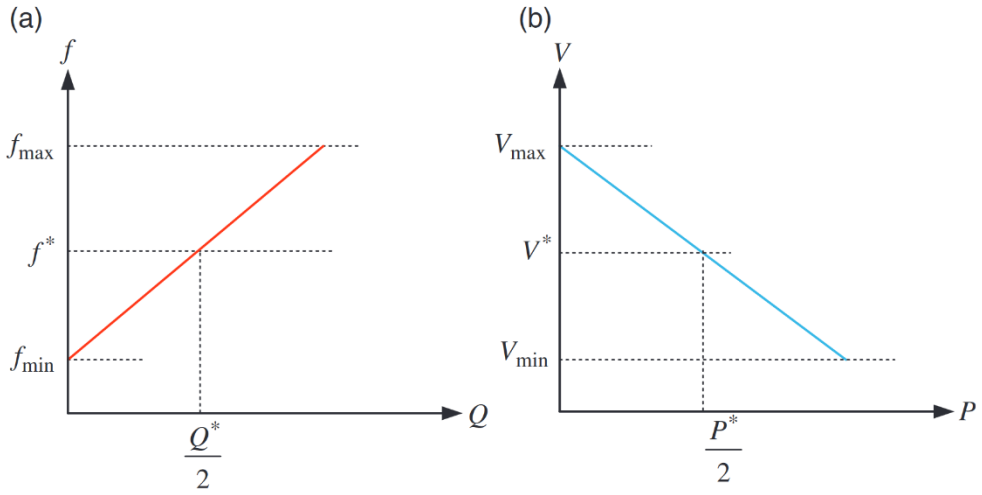

Figure 4.4.6 - Droop characteristics for resistive grid : (a) Q-f droop and (b) P-V droop.

4.4.4. Angle Droop Control

Angle droop control is suitable for a predominantly reactive grid, although it is feasible to implement it in grids with high R/X relationships using communication networks. Considering the two-DER microgrid system, it is assumed that both DERs are equipped with output LCL filters. However, DERs still operate in voltage control mode in which they control the voltage in the filter capacitors. These voltages in the capacitors are indicated by $V_{g1} \angle \delta_{g1}$ and $V_{g2} \angle \delta_{g2}$ in Figure 4.4.7. The external inductors L1 and L2 are used to control the real and reactive power flow as explained in this section. The load bar voltage is denoted by $V \angle \delta$.

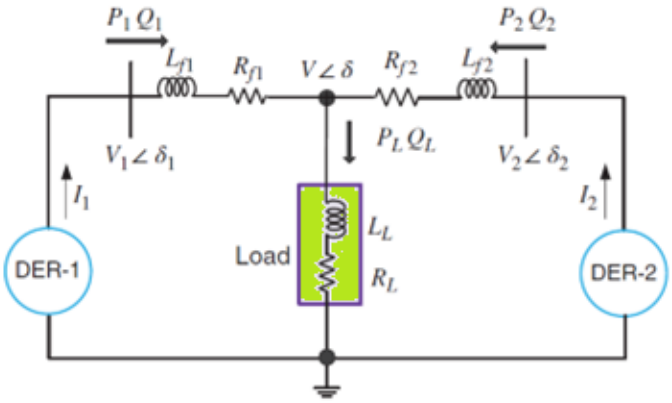

Figure 4.4.7 - Microgrid structure for angle droop control.

$$\delta_i = \delta^* + n_i \times (P_i^* - P_i), \;\; i = 1,2 \tag{4.4.20}$$

$$V_i = V^* + m_i \times (Q_i^* - Q_i), \;\; i = 1,2 \tag{4.4.21}$$

where δ^* is the reference angle and V_i and V^*define the magnitude of the bar voltage and its angle. Assuming that feeder resistances are negligible and applying a DC load flow, the equation 4.4.22 are obtained for the microgrid of the Figure 4.4.7.

$$\begin{aligned} \delta_1 - \delta &= X_1 P_1 \\ \delta_2 - \delta &= X_2 P_2 \end{aligned} \tag{4.4.22}$$

Where $X_1 = \frac{wL_{f1}}{VV_1}$ and $X_2 = \frac{wL_{f2}}{VV_2}$ represents the fundamental frequency in rad/s.

In an DC system, the power flow depends on the relative angular difference and, therefore, the reference angle δ^* can be considered as 0. However, all DERs in a microgrid should measure their angles in relation to this reference angle and

therefore, a global clock will be necessary to synchronize all units. Angle drop gains should be chosen as (4.4.12), therefore by equation 4.4.23:

$$P_1^* n_1 = P_2^* n_2 \tag{4.4.23}$$

Replacing the above equation (4.4.20), the equation 4.4.24 expression is obtained:

$$\begin{aligned} \delta_1 - \delta_2 &= n_i \times (P_1^* - P_1) - n_2 \times (P_2^* - P_2) \\ &= n_1 P_1 - n_2 \times P_2 \end{aligned} \tag{4.4.24}$$

Comparing (4.4.23) and (4.4.24), it obtains the equation 4.4.25.

$$\delta_1 - \delta_2 = X_1 P_1 - X_2 P_2 = n_1 P_1 - n_2 \times P_2 \tag{4.4.25}$$

Rearranging (4.4.25), the following power of power sharing is obtained in equation 4.4.26.

$$\frac{P_1}{P_2} = \frac{X_1 + n_1}{X_2 + n_2} \tag{4.4.26}$$

Then the power will be shared proportionally to the droop gains, i.e. $P_1 n_1 = P_2 n_2$, provided that:

$$n_1 \gg X_1 \; e \;\; n_2 \gg X_2$$

The droop EQs. (4.4.20) and (4.4.21) will produce the magnitudes of bus voltages and their angles. From these quantities, references to filter capacitors voltages need to be calculated. Consider, for example, DER-1. From figure 4.4.7, the current I_1 flowing from DER-1 to bar-1 is given by equation 4.4.27:

$$I_1 = \frac{V_{g1} < \delta_{g1} - V_1 < \delta_1}{jwL_1} \tag{4.4.27}$$

Then the complex power injected by the DER in the microgrid bus is given by equation 4.4.28:

$$\begin{aligned} P_1, + jQ_1 = V_1 < \delta_1 \left[\frac{V_{g1} < -\delta_{g1} - V_1 < -\delta_1}{-jwL_1}\right] \\ = \frac{V_{g1}V_1 < (\delta_1 - \delta_{g1}) - V_1^2}{-jwL_1} \end{aligned} \tag{4.4.28}$$

Separating the real and imaginary components, the real and reactive powers injected into Bus-1 are given by 4.4.29:

$$P_1 = \frac{V_{g1}V_1 sin(\delta_1 - \delta_{g1})}{wL_1} \tag{4.4.29}$$

$$Q_1 = \frac{V_{g1}V_1 cos(\delta_1 - \delta_{g1}) - V_1^2}{wL_1} \tag{4.4.30}$$

Equations (4.4.29) and (4.4.30) can be rewritten by equation 4.4.31 and 4.4.32:

$$sin(\delta_1 - \delta_{g1}) = \frac{wL_1P_1}{V_{g1}V_1} \tag{4.4.31}$$

$$cos(\delta_1 - \delta_{g1}) = \frac{wL_1Q_1 + V_1^2}{V_{g1}V_1} \tag{4.4.32}$$

From these expressions, the angle of the DER voltage is computed by equation 4.4.33:

$$\delta_{g1} = \delta_1 - tan^{-1}\left(\frac{wL_1P_1}{wL_1P_1 + V_1^2}\right) \tag{4.4.33}$$

In (4.4.33), the value of ωL_1 is known a priori. The voltage V1 of Bus1 and its angle δ_1 are calculated from the slope equation. Also, P_1 and Q_1 are measured.

Therefore, knowing these quantities, the angle δ_{g1} is calculated from (4.4.33). Once this is obtained, the DER reference voltages give to the three phases are decided by equation 4.4.34:

$$\begin{aligned} v_{g1a} &= V_{m1}sin(wt + \delta_{g1}) \\ v_{g1b} &= V_{m1}sin(wt + \delta g1 - 120^o) \\ v_{g1c} &= V_{m1}sin(wt + \delta_{g1} + 120^o) \end{aligned} \tag{4.4.34}$$

Where V_{m1} is computed from (4.4.29) by equation 4.4.35:

$$V_{m1} = \sqrt{2}\frac{wL_1P_1}{V_1sin(\delta_1 - \delta_{g1})} \tag{4.4.35}$$

Similarly, the voltage and the DER-2 angle can also be derived.

The island operation of microgrids receives highlight in this research, when assuming that all DERS operate in dispatches mode and all of them are interfacing with the microgrid through VSCs, the virtual synchronous generators, working as biofuels-based generators, can be easily can be easily integrated into a microgrid through a frequency drop equation. Hydrogen fuel cells and microturbines are considered sources of dispatched generation.

Solar PVs and wind turbines can also be dispatched if not operated in a maximum power point tracking mode. Dispatchable sources are those that can be controlled and

programmed to meet energy demand at any given time. In addition, they can also have this stored energy production for later use. Some examples are hydroelectric, one of the largest sources of energy in use today, and biomass. Photovoltaic energy may be considered dispatched, but it needs to meet some requirements. The main one is the modulation of generation through batteries, in at least 20% of the monthly generation capacity of the generation center [44]. In addition, renewable battery generators can also act as a dispatched generator.

For example, consider the case where a solar PV and a battery are connected to the same bus and work together. So, during sunny hours, the PV-Battery combination can provide a fixed amount of energy most of the time. If the photovoltaic generation is high, it can charge the battery as it keeps the nominal output power constant.

On the other hand, when the photovoltaic generation is low, the battery can discharge, keeping the nominal output power constant. Battery storage can also act as a dispatches source if they are fully charged, especially at night. By definition, a microgrid is composed of the integration of several distributed generation resources, electricity storage and loads in a secondary distribution system capable of operating connected to a main electricity distribution grid and also in islanded operation, controlling the electricity parameters providing conditions for recomposition actions and auto restoration of the supply of electricity. When considering these variables, microgrid planning becomes an important aspect that needs to be considered for the successful implementation and operation of a microgrid.

5. Reactive power control in mixed systems with renewable energy generation sources

The integration of renewable energy sources (RESs) in power electrical systems have become a necessary and fundamental aspect to supply in terms of electric power handling the large increase in electricity demand and reduce environmental pollution problems in which for supply the fossil fuels were used. Different types of RESs are used in electricity generation, including wind generation, photovoltaic (PV), fuel cell and biomass. Both types of generation most integrated in electrical systems are wind generation and PV in favor of their multiple most pronounced results in relation to other types of generation, which are planned due virtue evident from the marked annual RESs growth rate.[45]

Hybrid electricity systems based on Wind Energy Conversion Systems (WECSs) and photovoltaic generation systems are not able to provide the reactive energy required during floating events. Consequently, the voltage profile at the point of common coupling (PCC) between the RESs and the grid will float. These voltage fluctuations have adverse effects on the performance of the electricity system, including system stability, power factor and electricity quality provided, as a result, voltage quality. In addition, if not properly controlled, these voltage uses will vary to undesirable levels that will lead to the disconnection of these systems due to the lack of reactive power support during these absences according to some network codes or supply patterns. Network codes are technical specifications that define the parameters that any equipment connected to a public power grid needs to meet to ensure reliable, safe and adequate system operation. Installation can be a power generation plant, a photovoltaic solar generation farm or any other source connected network.

Inadequate control of voltage fluctuations results in unwanted system disconnection of the system due to lack of reactive system power support during these faults according to some network codes.

Various types of electrical generators were used in WECS, such as self-excited induction generators (SEGs), double-fed induction generators (DFIGs) and switched reluctance generators (SRGs). Despite the simple construction of the SEGs, they are sensitive to wind speed variations and cannot operate ample speed ranges. DFIGs are not sensitive to wind speed variations and can operate in large speed ranges. However, DFIGs have high defective sensitivity and need continuous maintenance due to the structure of the rotor sliding ring. Due to their advantages, SRGs are commonly used in many WECs applications. Its low cost, robustness and continuous maintenance lack are among the specific SRGs resources, despite the reactive energy support requirement [46].

Reactive energy supply for hybrid electricity systems needs some external devices during defective events using flexible alternating current transmission systems (FACTS). These devices play an essential role in improving the RESs connection in the power system, providing the reactive power required.

FACTS devices can be categorized according to your system connection, shunt and series/shunt combination.

Each connection category has its own way of use and characteristics. Serial FACTS devices are used to increase the transmission line capacity and adjust line reactance. Series compensators are used in hybrid renewable systems, the dynamic voltage restorer (DVR) is characterized as a device that can be used in distribution networks to inject three-phase voltage into series and synchronization with distribution feeding voltages, to correct fall of short voltage (so-called voltage sags). Derivation devices support voltage injecting/absorbing reactive power during, respectively. Derivation

compensators, such as VAR (SVCs) and static synchronous (Statcoms) and superconductors static compensators, are presented to control different RESs connected to the network. In addition, the compound type, which is a combination of shunt series and facts devices, such as the UNIFIED Power Flow Controller (UPFC) (Table 5.1.), has been introduced to improve the RESs connection to the network. The compound type can play the standard role and facts of derivation devices [47].

FACTS device	Applications in RESs
DVR	Enhance the performance and support the FRT capability.
	Voltage sag mitigation.
	Support low-voltage ride-through capability.
SVC	Support the reactive power.
	Hosting the capacity.
STATCOM	Improve the power quality.
	Voltage stability improvement.
	Power quality support.
UPFC	Support low-voltage ride through.
	Power enhancement.

Table 5.1. - Different applications of facts devices in RESs.

So far, classics are still used in many applications related to the electric generation field due to their simplicity and direct resources. PI control prevents the system and can also return the system to its adjustment point. Although the response time for PI control is faster than control only I, it is still up to 50% slower than the control only P.

PI controllers were used to improve the performance of hybrid energy systems, including fuel, PV and wind cells. Despite the resources of all PI controllers, their

attributed function will not perform correct or appropriate if their parameters are not properly determined.

The common structure of the hybrid electricity system contains different electronic power devices, such as converters and inverters, RESS and controllable devices, making these systems nonlinear, complex and uncertain. Adjusting PI controller parameters for non-linear, uncertain and complex systems becomes a challenge by conventional techniques such as linear programming. This challenge paves the way for modern optimization methods to adjust PI controller parameters to reach the ideal operational performance systems. The genetic algorithm (GA) has a feature that considers it a reference for the ideal adjustment of PI controller gains.

Particle swarm optimization (PSO), as well as newer optimizers based on the search for harmony and pollination of followers, were introduced to the ideal gain PI scheduling for FC (Fuel Cell) connected to electrical networks. The three optimizers are used for the almost ideal programming of PI controller gains, boosting the inverter that connects the fuel cell to the network.

The STATCOM integrates with the RES in the PCC to act as a compensator with the voltage fluctuation during the lateral disturbance of the network, exchanging the reactive power between the STATCOM and the system (Figure 5.1).

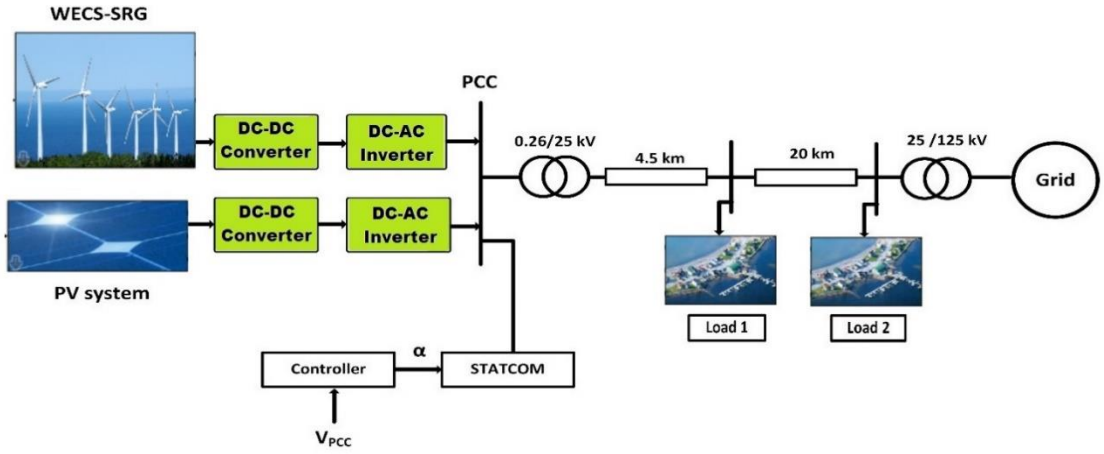

Figure 5.1 - System including a Statcom.

By regulating the PCC voltage, the system performance is maintained in an enhanced state. In addition, it complies with network codes and maintains the continuous operation of the RESS, even in fault events. The two PI controllers used to drive STATCOM are tuned using WOA. Due qualitative and qualitative comparison and unbiased analysis are introduced considering the dynamic performance of the system while controlled using near-ideal PI controllers based on PSO and WOA (Whale Optimization Algorithm).

6. Verification of Inrush currents from electromagnetic transients influencing the stability of voltage in Smart Microgrids

The importance of studying electromagnetic transients is mainly due to the effects that disturbances can have on system performance or the failures they can cause in electrical power equipment. Stresses that can damage electrical power equipment are of two types: overcurrents and overvoltages, and can also cause a reduction in the useful life of these equipment.

6.1. Re-synchronization Phenomenon of Microgrid

6.1.1. Re-synchronization phenomenon of VSG

Unlike SGs, VSGs have their own inverters characteristics and are more resistant to implement electricity sharing using electricity control loops. Due to some differentials between SGs and VSGs, the mechanism of operation of VSGs has divergent characteristics of SGs and VSGs constitute a technology more conducive to re-synchronization after the elimination of significant faults and serious anomalies in electrical systems. As a result, the VSGs re-synchronization mechanism is subject to succinct analyzes and, analogously, the influences of different parameters become relevant, referenced by [53] and equations proved by RTDS.

6.1.2. Re-synchronization mechanism

VSGs are used to replace all SGs response features. Therefore, there is also a problem of transient stability at the angle of the VSGs. With the occurrence of the degrading

effect caused by the reactive energy control loop, VSGs are succinct to be directed to the area of instability. As well as the existence of the current limiter, introduced to delimit the inverter output current, which could lead to transient instability of the angle [53].

Instability does not represent the only resource that VSGs or SGs would experience after the energy angle transpires the UEP (unstable equilibrium point). Regarding rotary SGs in the traditional electricity system, when the SG transposes UEP during the fault period, there are two results options made after the fault release: returns to a distinct state of stability, named re-synchronization or displays chaotic characteristics. In traditional SGs, the transition response of the VSGs correctly exposes the characteristics. For VSGs, it is noted that it is more likely to return to the state of stability, as a small line impedance is characterized and a larger size damping coefficient remains in the electronic power system. It is clear how and why the VSGs would return to a new state after the fault is extinguished.

Figure 6.1 appears the demystified control scheme, divided into three sections: power control loop, loop and virtual impedance of voltage stroke and current control loops. Active control of electricity in the control loop is aimed at regulating the active power of the output and assigning emulation to the dynamic response of the SGs.

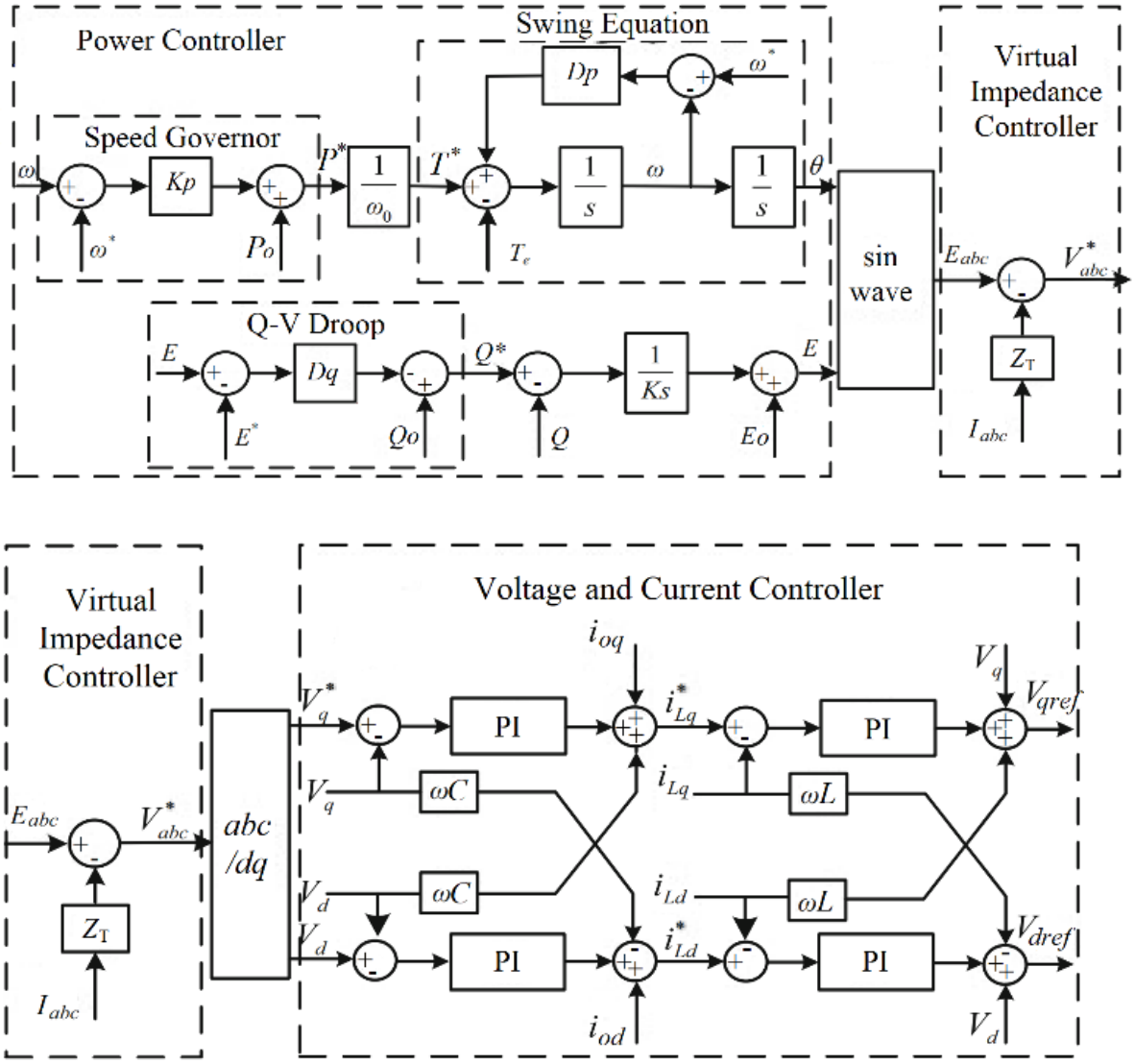

Figure 6.1 - Control block diagram of a VSG controller;

As shown in Figure 6.1, the first stage of the control loop demonstrates the voltage loop. *Vod (Vd)* and *Voq (Vq)* are the components of Vo. Obviously, there is a highlight for the arrangement of the *dq* table selected for all transformations *dq* in this system to 90 degrees, and the conversion angle ε (t) is the angle between the d-axis and Phase-A axis of the static coordinate structure, as shown in Figure 6.1. The voltage loop entrances, *Vod** and *Voq**, are obtained from the reactive power control loop output. By aligning the d-axis of the *dq* reference frame with the voltage space phasor in the filter capacitor as it rotates, the *Voq* becomes zero and the *Vod* is equal to *V** obtained from the reactive power control loop *Q-V*. The voltage loop outputs are reference values of

the *dq* components of the VSC, *ild** and *ilq** exit current, which are used as input reference current signals for the current loop.

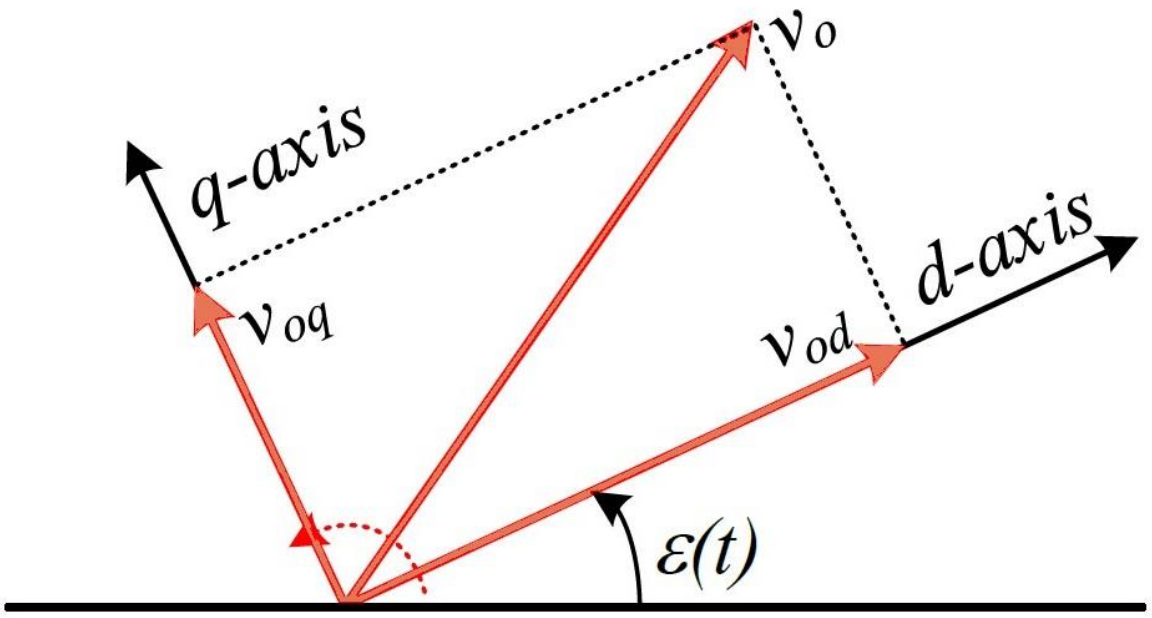

Figure 6.2 - *dq* Frame with Space Vector V_o .

The capacitor filter current, by writing the KCL (Kirchoff's Circuit Law) equation at v_o in the time domain, can be represented by equation 6.1.2.1:

$$C_f \frac{dv_0}{dt} = i_l - i_0 \qquad (6.1.2.1)$$

Applying the transformation of *dq* to the equation (6.1.2.1), it results in equation 6.1.2.2:

$$\begin{cases} i_{ld} = C_f \frac{dv_{od}}{dt} - wC_f v_{oq} + i_{od} \\ i_{lq} = C_f \frac{dv_{oq}}{dt} - wC_f v_{od} + i_{oq} \end{cases} \qquad (6.1.2.2)$$

Equation (6.1.2.2) demonstrates the differential equations of the *dq* components of the VSC output current with spatial representation of phasors.

As shown by the dashed lines of the voltage loop in Figure 6.1, *Vod* and *Voq* voltage feed feeding terms are not added, and feed current *Iod* and *Ioq*'s advancement terms are added with a *F* factor equal to 0, 75. In this way, the voltage loop PI controllers will produce the following terms in equation 6.1.2.3:

$$\begin{cases} i'_d = \left(K_{pvd} + \frac{K_{ivd}}{S}\right) \cdot \Delta v_{od} + (1 - F) i_{od} \\ i'_q = \left(K_{pvq} + \frac{K_{ivq}}{S}\right) \cdot \Delta v_{oq} + (1 - F) i_{oq} \end{cases} \quad (6.1.2.3)$$

Where K_{pvd} and K_{pvq}, K_{ivd} and K_{ivq} are the proportional and integral gains of the PI controller, respectively. Current references to the current loop are calculated by equation 6.1.2.4:

$$\begin{cases} i^*_{ld} = i'_d - wC_f v_{oq} \\ i^*_{lq} = i'_q - wC_f v_{od} \end{cases} \quad (6.1.2.4)$$

Equation (6.1.2.4) represents the voltage loop output of the control diagram shown in Figure 6.1.

The second stage of the control loop is the inner decoupled current control loop, which is the same configuration used in grid following (GFL) controls. VSG voltage output before the inductor filter, v_{inv}, can be written by equation 6.1.2.5:

$$v_{inf} = v_o + L_f \frac{d_{il}}{dt} \quad (6.1.2.5)$$

By applying *dq* transformation for equation (6.1.2.5), it has equation 6.1.2.6:

$$\begin{cases} v_{invd} = L_f \dfrac{d_{ild}}{dt} - i_{lq} w L_f + v_{od} \\ v_{invq} = L_f \dfrac{d_{iq}}{dt} - i_{ld} w L_f + v_{oq} \end{cases} \quad (6.1.2.6)$$

Equation (6.1.2.6) shows the differential equations of the *dq* components of the VSC output voltage with spatial representation of phasors.

Consulting the current control loop shown in Figure 6.1, the current loop PI controllers will produce equation 6.1.2.7:

$$\begin{cases} u'_d = \left(K_{pid} + \dfrac{K_{iid}}{S} \right) \cdot \Delta i_{ild} \\ u'_q = \left(K_{piq} + \dfrac{K_{iiq}}{S} \right) \cdot \Delta i_{ilq} \end{cases} \quad (6.1.2.7)$$

Where k_{pid} *and* k_{piq}, k_{iid} *and* k_{iiq} are the PI controller proportional and integral gains, respectively. As shown in Figure 6.1, the current loop control outputs are used as reference signals to the PWM scheme and can be represented in equation 6.1.2.8:

$$\begin{cases} v_{invd} = u'_d - w L_f i_{lq} + v_{od} \\ v_{invq} = u'_q - w L_f i_{ld} + v_{oq} \end{cases} \quad (6.1.2.8)$$

The outputs of the electric current loop and the angle θ produced by the power synchronization loop are used to produce modulation waveforms that are then translated into firing pulses to the VSC. The sinusoidal pulse width modulation method (SPWM) is adopted to generate shooting pulses in the simulation performed.

The voltage loop and the current loop are shown in Figure 6.3 and Figure 6.4, respectively.

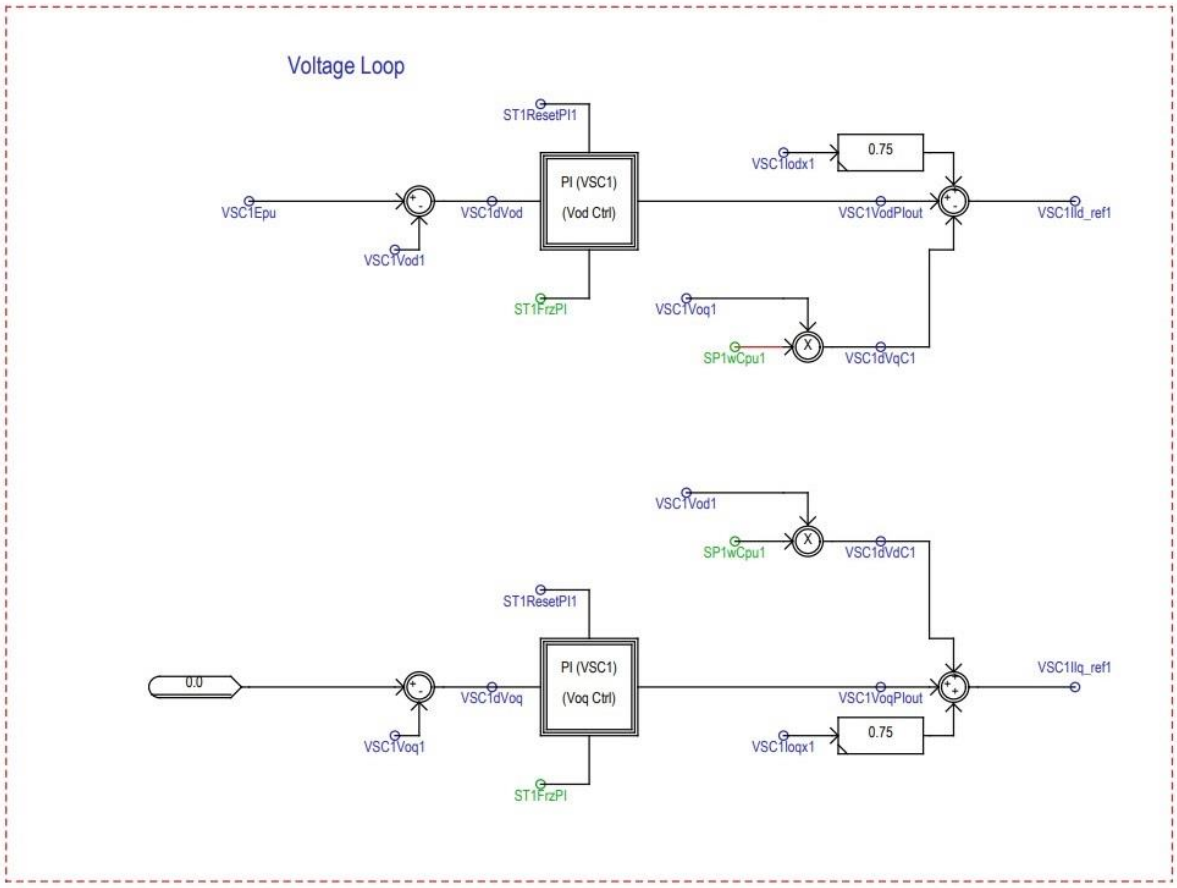

Figure 6.3 - Voltage Loop in RSCAD.

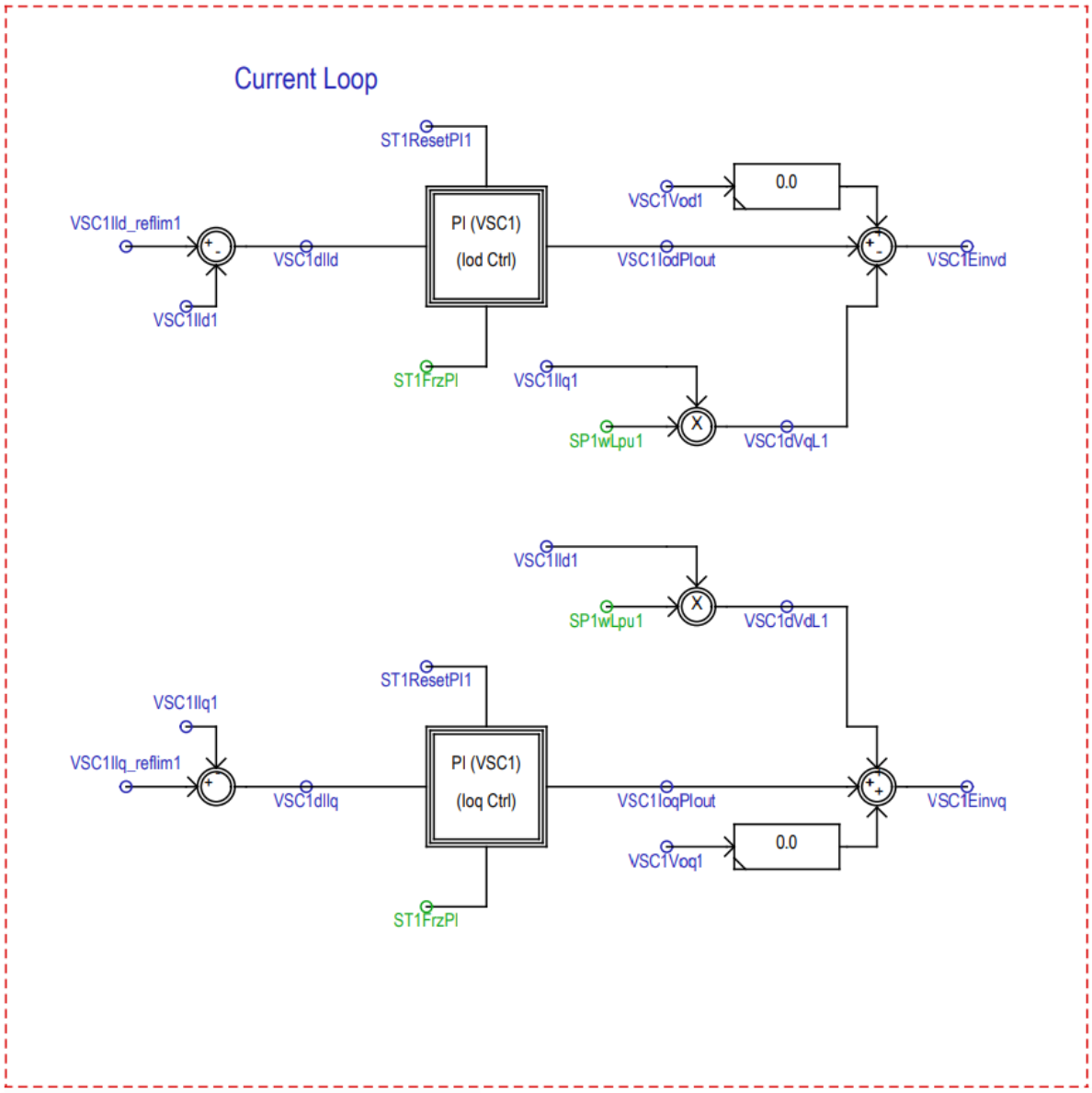

Figure 6.4 – Electric current Loop in RSCAD.

Synchronization control works only during VSG connection to the grid to maintain the phase angle and magnitude of the voltage with values within the necessary standards. Sudden oscillations can result in significant transients and pose potential risks to deteriorate the control system. In order to close the circuit breaker between the VSG and the electricity grid, synchronization criteria must be met in terms of sliding frequency, phase angle and magnitude difference. The demonstration of a typical synchronization control scheme projects as shown in Figure 6.1.

Figure 6.5 shows the synchronization control developed in RSCAD. The inputs of the two PI, "vsc1dtheta" and "vsc1dvllpu" controllers are the phase angle and the voltage magnitude differences between Vo and the 0.315 kV side of the 0.315/35 kV transformer. PI controller outputs are added to the energy synchronization loop and reactive energy control loop, respectively. The signal called "vsc1resyc" activates synchronization control and only allows synchronization control to be activated when the "BRK1" circuit breaker is open. Sync control will be deactivated after the synchronization process is completed and the circuit breaker is closed.

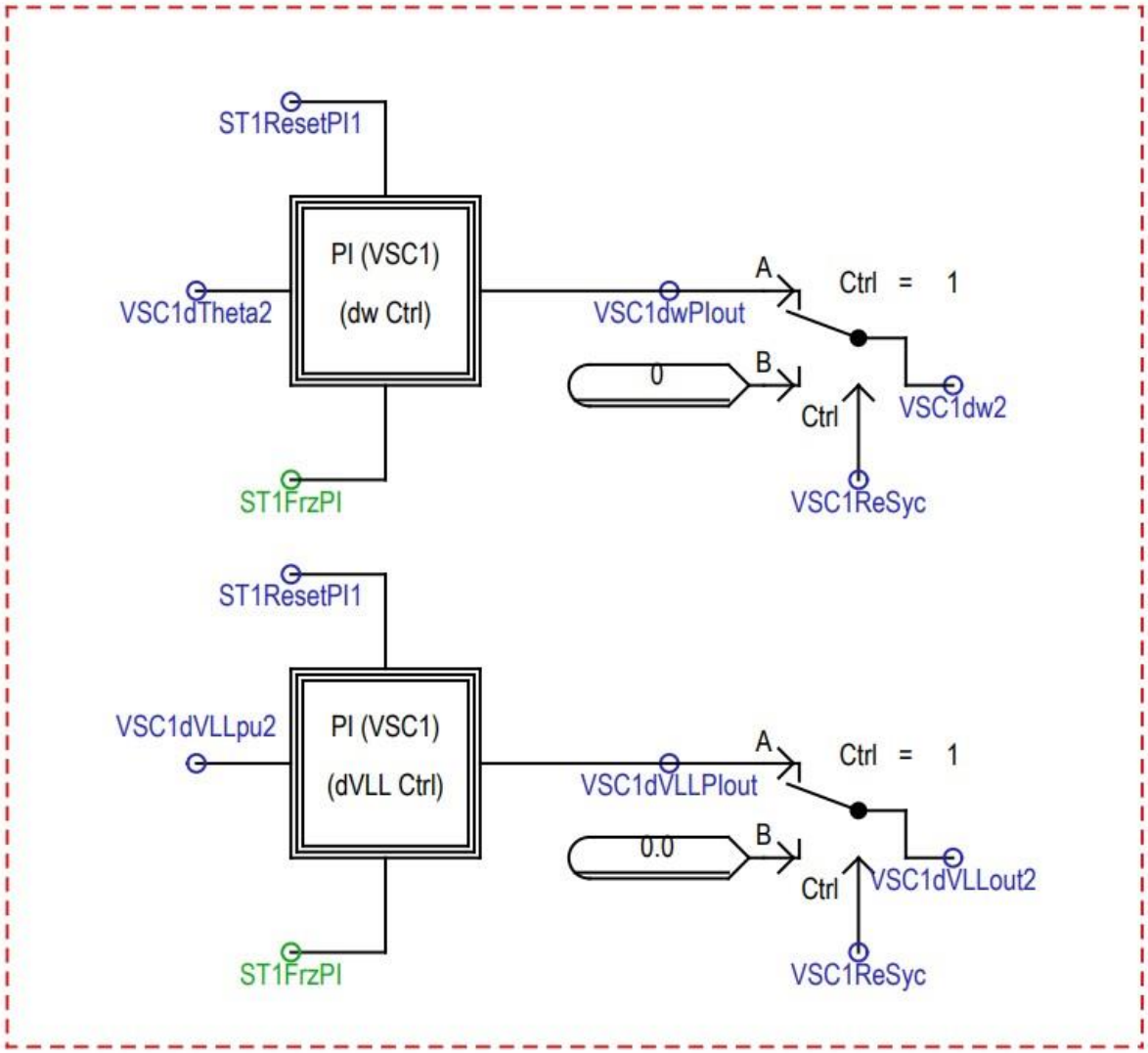

Figure 6.5 – Synchronization control in RSCAD.

The synchronization scheme will automatically verify if VSG is connected to an active bus or a dead bus (inactive) and, if an active bus is detected, synchronization control will be activated. Once synchronization criteria are met, VSG Breaker (BRK1) will close and synchronization control will be deactivated. A demonstration describing the synchronization process is provided in Figure 6.8.

- Side grid circuit breaker with synchronized verification

A synchronized check circuit breaker control is used for the "GridBRK" side circuit breaker shown in Figure 6.6. This is to ensure that the network interconnection and VSG voltage is synchronized when the side circuit breaker closes.

Figure 6.6. shows the synchronized check circuit breaker control component used in GFM models. Monitors the voltage and phase angle on both sides of the side circuit breaker of the grid, and the magnitude and phase of the circuit breaker voltage must meet the necessary synchronization criteria before allowing the circuit breaker connection to occur.

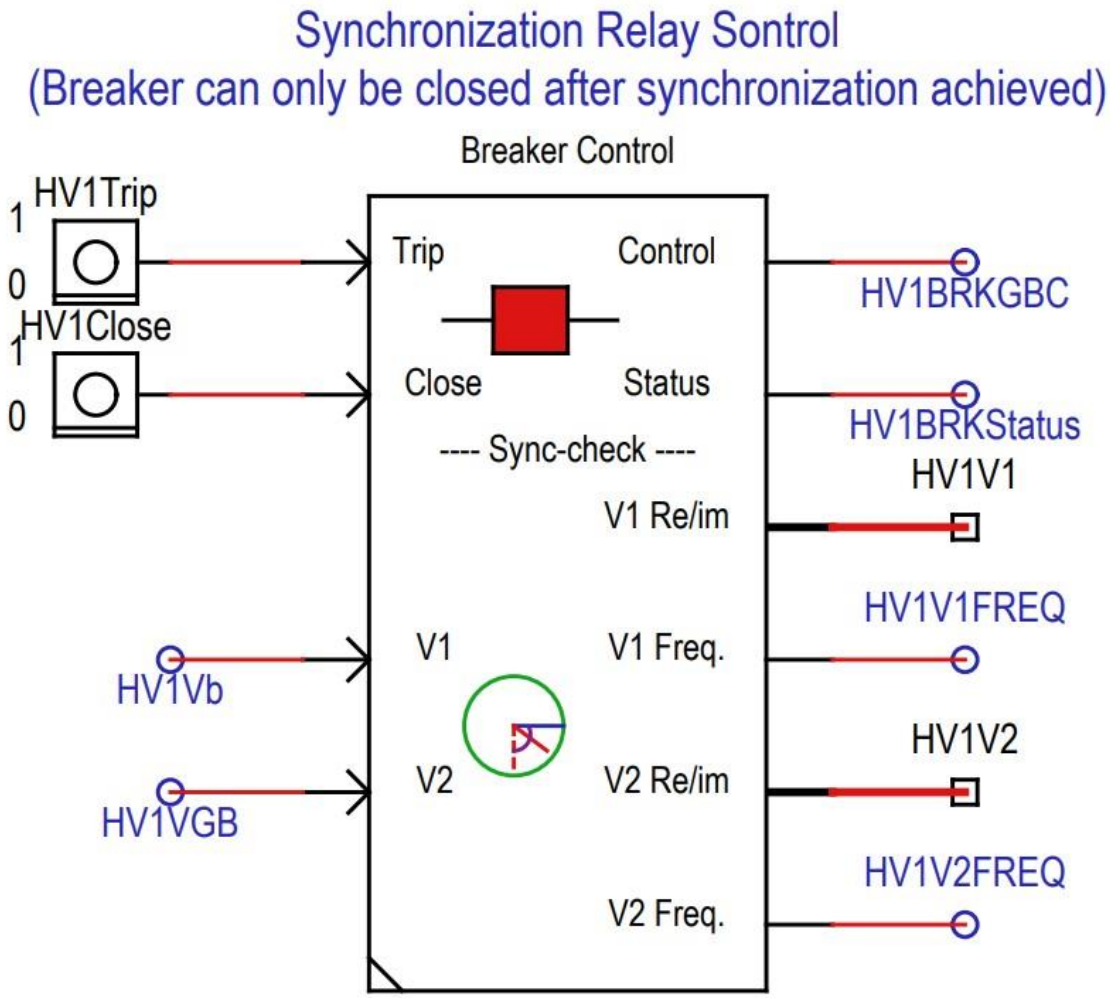

Figure 6.6 – Breaker control.

Reactive energy control has the function of performing energy sharing and output voltage regulation. There is a line impedance with resistive characteristics in the electronic power system and the virtual impedance control loop is still adopted to settle the dissociation of electricity in the energy control loop.

Voltage and current control loops aim to accelerate electric current and voltage tracking speed and optimize the output power limit of a VSG. The PWM modulation unit receives the generated signals, determining that switching devices perform the energy conversion.

The active energy control loop is expressed by equation 6.1.2.9:

$$J\frac{d^2\delta}{dt^2} = T^* - T_e - D(w - w^*) \tag{6.1.2.9}$$

where $T^* = P^*/w^*$, $T_e = P/w^*$, and $D = D_p + K_p/w^*$, D represents equivalent damping. Similarly, the reactive power control loop is expressed by equation 6.1.2.10:

$$K\frac{dE}{dt} = Q_0 - Q - D_q(E - E_0) \tag{6.1.2.10}$$

where K represents the full voltage coefficient and D_q represents the coefficient $Q - V$. E^* and Q^* represents, the voltage reference and the reactive power reference respectively. VSG output power follows as expressed by equation 6.1.2.11:

$$\begin{cases} P = E^2G - EV_gBsin\delta - EV_gGcos\delta \\ Q = -E^2B + EV_gBcos\delta - EV_gGsin\delta \end{cases} \tag{6.1.2.11}$$

Figure 6.7 demonstrates the results of a simulation, in which it seems that the fault is extinguished at 1.7 s, the VPA (Virtual power angle) does not appear on the UEP and the unfolding of the system will be poured to the original EP (equilibrium point), a fact that it can be called first-swing stability, as shown by the blue curve in Figure 6.7.

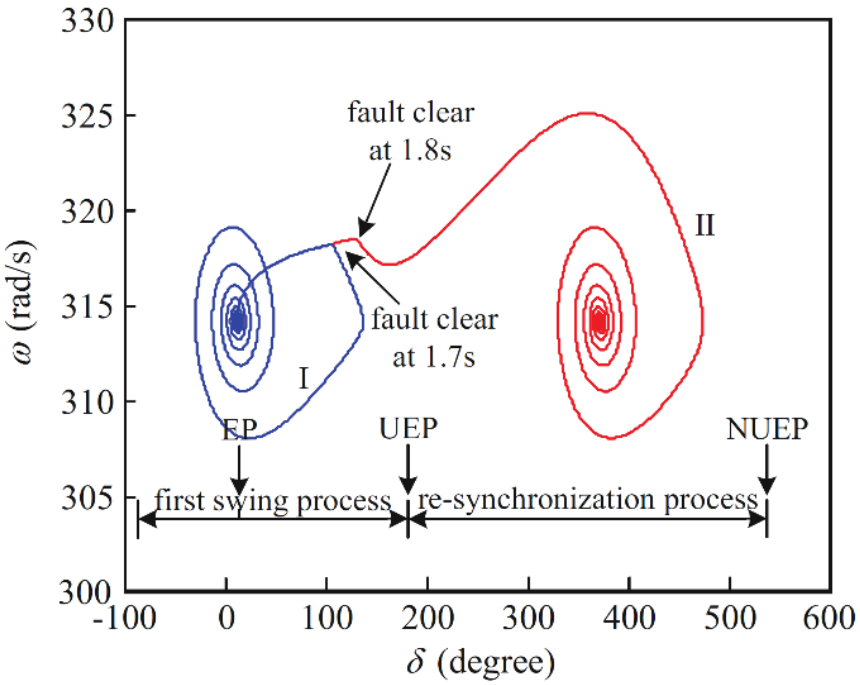

Figure 6.7 - Phase description of the transitional process of SVIB (single VSG connected to the infinite bus).

When the fault is extinguished at 1.8 s, the VPA of a VSG goes on to the UEP. From the perspective of transient stability criterion in the electrical power system, this implies that the system will move to the condition of irreversible instability and cannot be restored to the synchronous state with the network. As expressed by the results, it was found that the system has the capacity of another EP, demonstrated by the red curve in Figure 6.7. This type of phenomenon expresses that a VSG in the electronic energy system has extreme synchronism capacity, even uttering the instability of the First Swing.

Explaining, there are two resulting possibilities as soon as the system divides from stability the first time. A result has the VPA that continues to pass the next unstable equilibrium point (NUEP), which is called the transient angle instability. The next result shows that VPA tends to different EP and the system has the ability to maintain synchronism with the network, which can be called re-synchronization stability.

Figure 6.8. demonstrates the VSG synchronization process with the main grid performed experimentally by the Real Digital Time Simulator Novacor. At the moment "0", the VSG is already unlocked, but does not yet connect to the main grid. Once the command for the connection is processed, in about 0.3 seconds, the synchronization process begins, as indicated in the green box. When synchronization is reached, there is no real power or reactive energy transfer from VSG to the main grid, even after the circuit breaker closes due to the minimum voltage and phase difference between the VSG and the interconnection point. After synchronization is achieved the VSC1 circuit breaker closes, the synchronization controls are deactivated, and the VSG starts to sink/source the target Amount of power and maintain the voltage at the filter capacitor Voltage. Figure 6.8. illustrates the voltage and active power of the VSG reaching the directed values of 0.5 PU after the synchronization control deactivated. Figure 6.9 shows the status of the circuit breaker associated with synchronization indications, circuit breaker status VSG, differences in voltage magnitude and phase angle differences in the VSC1 circuit breaker.

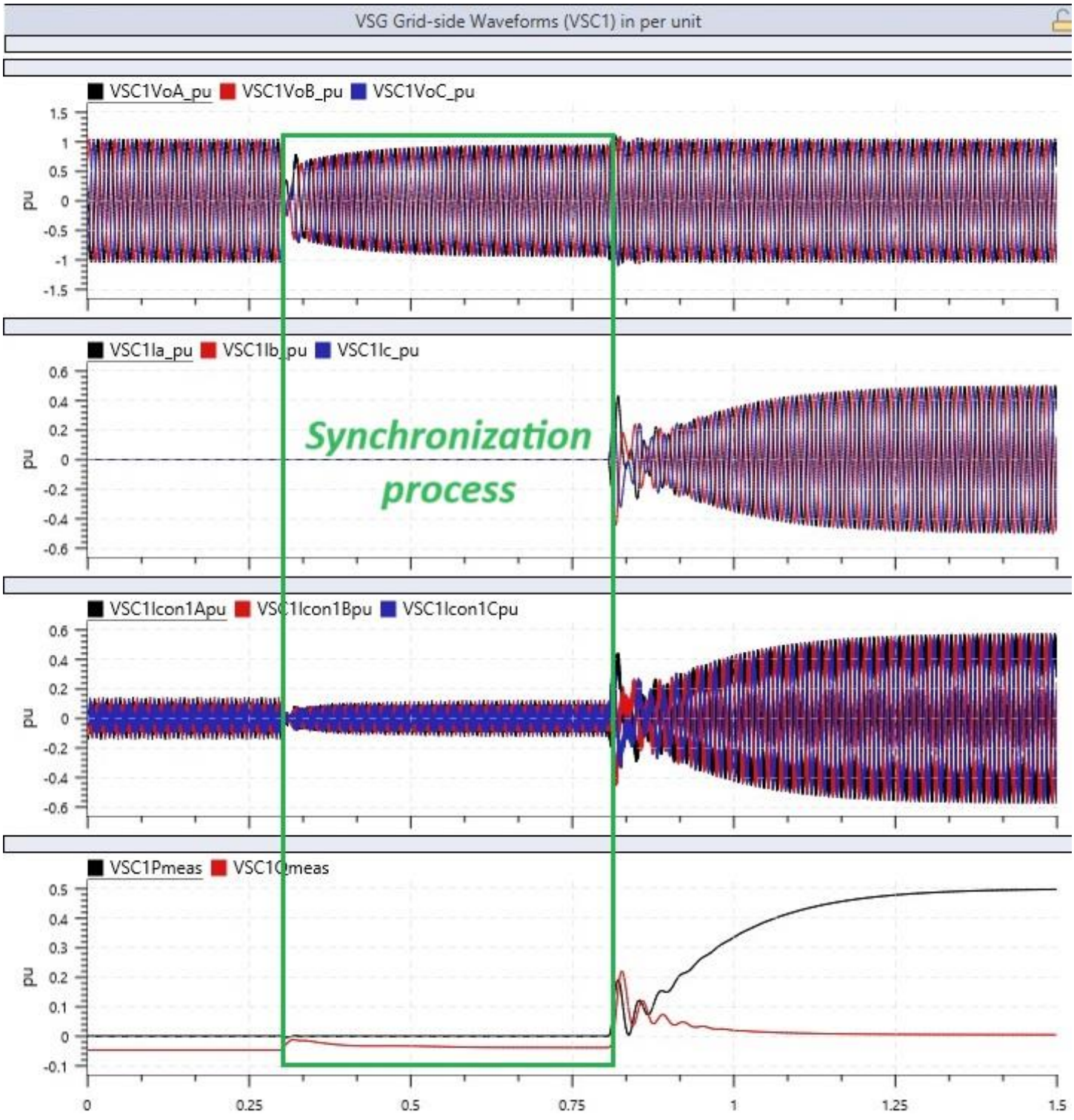

Figure 6.8 – Synchronization process of the VSG (RTDS experiment).

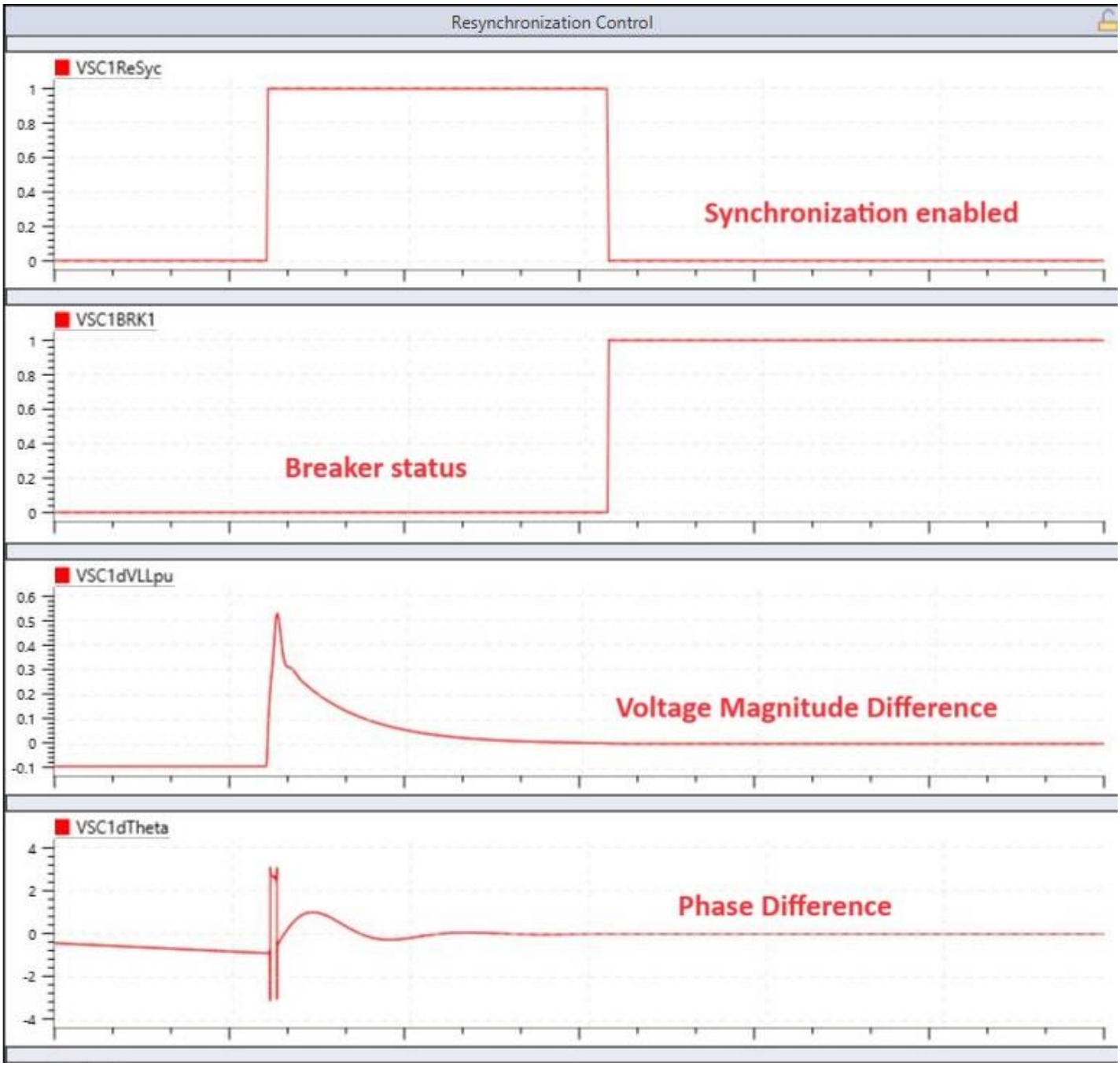

Figure 6.9 – Synchronization control and breaker status.

6.2. Stability analysis of the system

Stability analysis is extremely important in electrical power systems because it helps to ensure the reliable and safe operation of the electrical grid. Electrical power systems are dynamic systems of large or small scale and temporal variation, and maintaining their stability is crucial to maintaining operational equilibrium after disturbances and therefore, to resolve them. Stability analysis is extremely important in electrical power systems because it helps to ensure the reliable and safe operation of the electrical grid. Electrical power systems are dynamic systems of large or small scale and temporal variation, and maintaining their stability is crucial to maintaining operational equilibrium after disturbances and therefore, to resolve them.

A. Re-synchronization phenomenon of VSG

In order to analyze the stability problems of the power system in this case of Virtual Synchronous Generator, the RTDS frequency scanning tool is used. This type of tool helps to evaluate the stability of the electrical system to integrate the VSC converter in varied SCR (Short Circuit Ratio) systems. Additionally, it provides characteristic data to evaluate critical SCR specification for system specific characteristics under which VSC becomes unstable. The VSG system is shown in Figure 6.2.1. A frequency harmonic voltage source promotes the insertion of harmonic variation between the PCC bus and the AC system (Table 6.1). Once the system reaches the steady state, the harmonic voltage at both ends of the harmonic source can be measured.

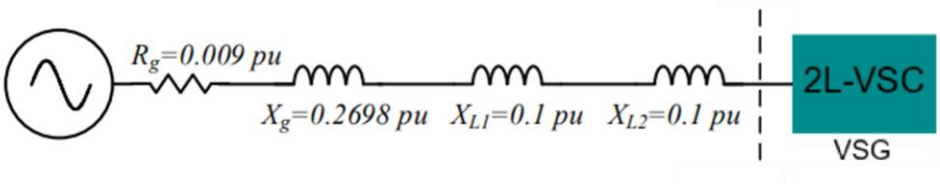

Figure 6.2.1 – Electric power system.

The results generated by the RSCAD Frequency Scanning Tool (RTDS) are shown in Figure 6.2.2. With the frequency range analysis of 0 to 100 [Hz] it is found that there is no stability problem observed for the frequency of over 18 [Hz]. Therefore, only the scan results from 0 to 35 [Hz] were listed. When verifying that the Eigenvalues (Figure 6.2.3) phase jump from +-70 degrees, it is obtained the determination of any possible system situation that may result in the instability of the VSG.

System parameters	Values
AC grid	220 [kV] (LL, rms), 50 [Hz]
Default Short Circuit Ratio	3.56 @ 1 [MVA]
Transformer 1	220 [kV]: 35 [kV], 1.0 [MVA]
Transformer 2	35 [kV]: 0.315 [kV], 1.0 [MVA]

Table 6.1: Initial system parameters.

As shown in Figure 6.2.2, the blue line crosses 70 to 18.2 [Hz] and the magnitude of the eigenvalue is 0.0047733 at this point.

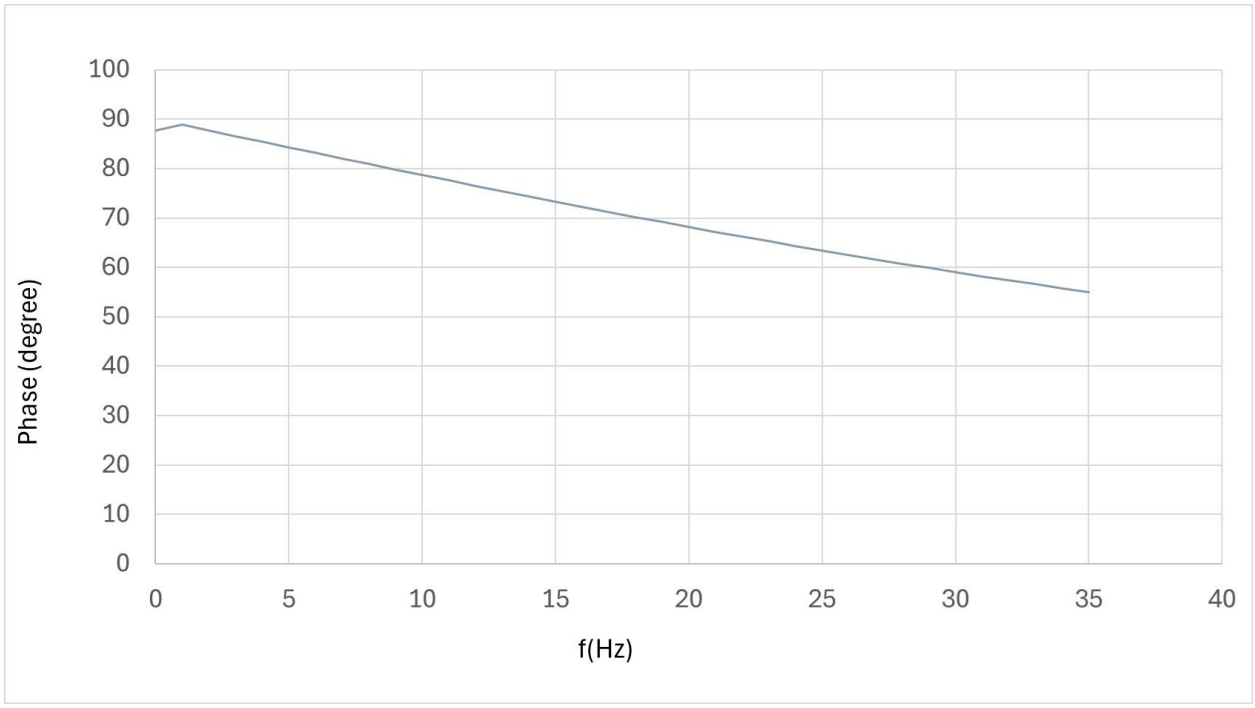

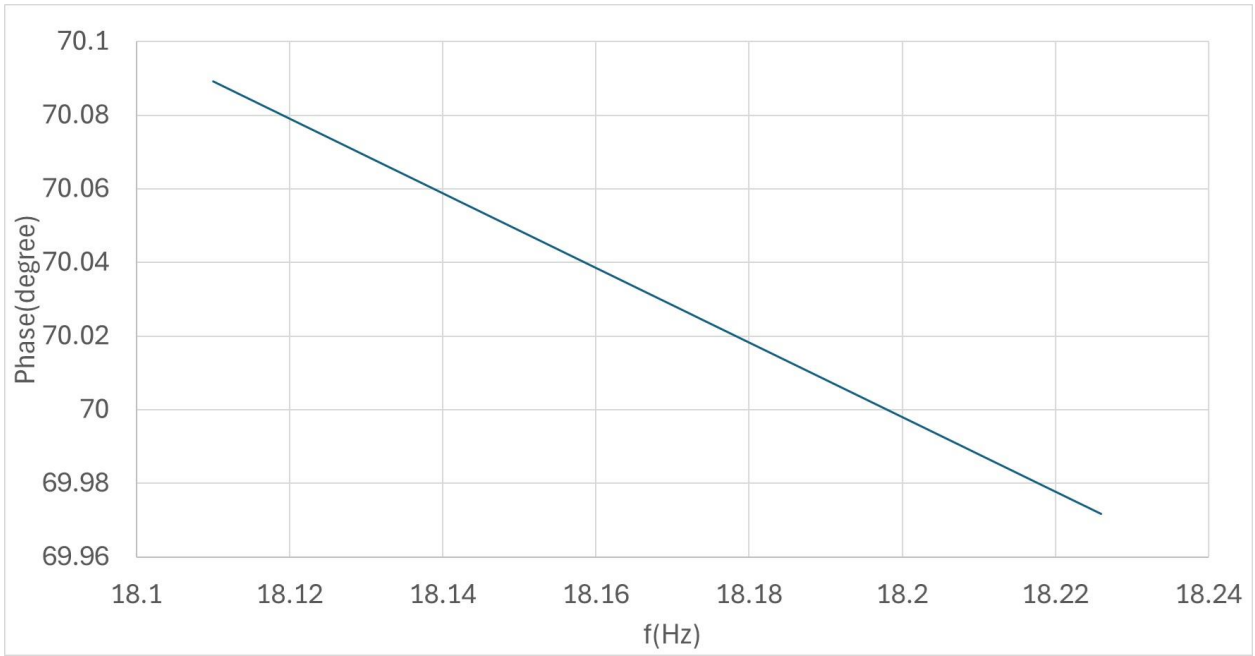

Figure 6.2.2 – Frequency scanning results.

B. Eigenvalues

Given a matrix A, it aims to find an equivalent diagonal matrix λ. The equivalence between both must be established by multiplication by a scalar $x \neq 0$, such expressed by equation 6.2.1:

$$A\,x = k$$

$$\lambda\,x = k \tag{6.2.1}$$

Therefore, a $x = \lambda\,x$. The matrix λ is called matrix of eigenvalues of A, and x is the matrix of eigenvectors. Such set of equations can be written as equation 6.2.2:

$(A\,x - \lambda\,x) = 0$

Or

$(A - \lambda\,I)\,x = 0$

(6.2.2)

where I is the matrix identity. As $x \neq 0$ The solution to the above system is given 6.2.3:

$$det\,(A - \lambda\,I) = 0 \tag{6.2.3}$$

The expression above provides the characteristic polynomial of matrix A. The zeros (or solutions) of the polynomial are the eigenvalues of A. Therefore, if all the eigenvalues are distinct, can be written as the equation 6.2.4:

$$\rho\,(y) = (-1)\,n\,(y - \lambda 1)\,(y - \lambda 2)\ldots\ldots(y - \lambda n) \tag{6.2.4}$$

Where the determinant of A is given by $\lambda_1\,\lambda_2$ .... λn.

The eigenvectors associated with each λ, i.e., each column of x, define the C^n dimension vector space, and thus any linear combination between the columns of x is situated on C^n.

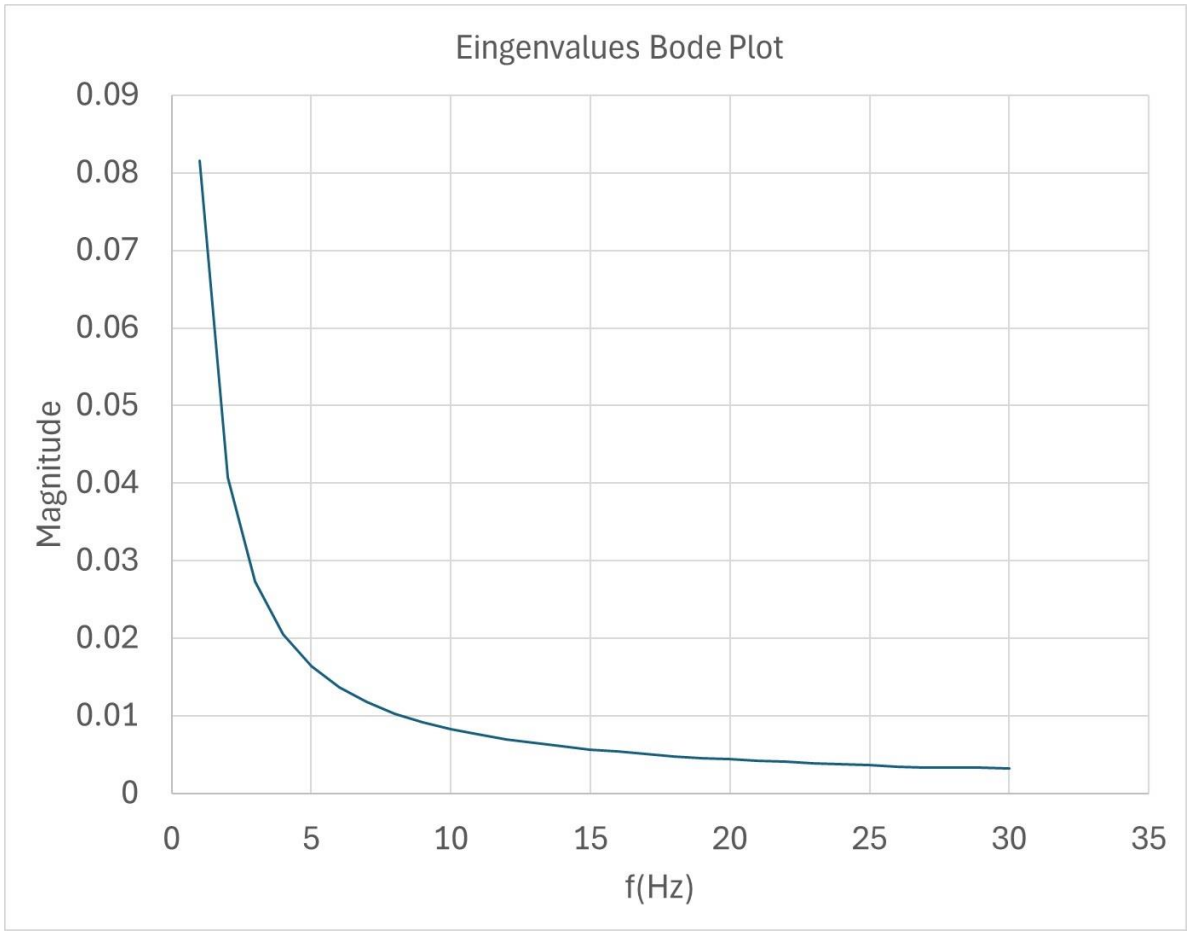

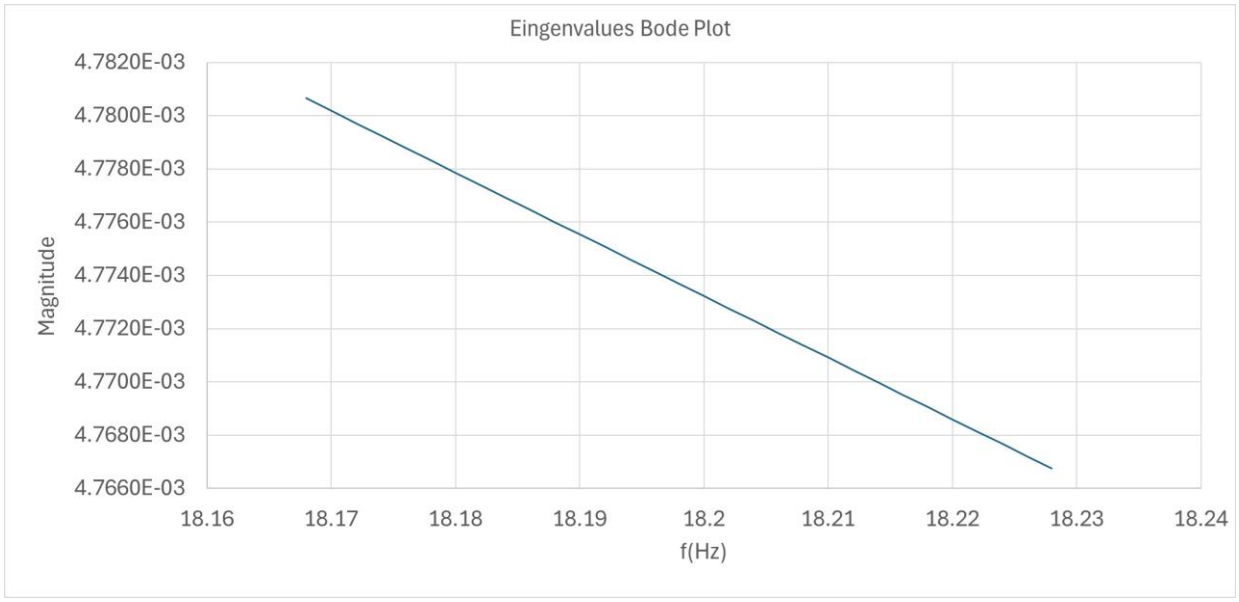

Figure 6.2.3 – Frequency scanning results.

Conceptually, the system will become unstable when the magnitude of the eigenvalue is 0.015. This means that if the SCR system drops 0.015/0.0047733 = 3.142 times, the system should become unstable and with an oscillation frequency of 18.2 Hz. By multiplying a factor of 0.0047733 to all the impedance shown in Figure 6.2.4, the SCR system will be increased to 3.142 times and equal to 6.689, which is a stronger considerable system. The system gradually becomes unstable, as shown in Figure 6.2.4, and the oscillation observed in the RSCAD simulation is 18.2 Hz, which agrees with the results of the RSCAD frequency scanning tool. In addition to verifying if the 6.689 SCR is the Critical SCR for the VSG, an additional sensitivity test was performed on a SCR of 6.0, and it is aimed that VSG is stable under this system condition. After changing the SCR system to 6.0, as shown in Figure 6.2.5, the oscillation with a frequency of 18.2 Hz still exists but decreases after a few seconds.

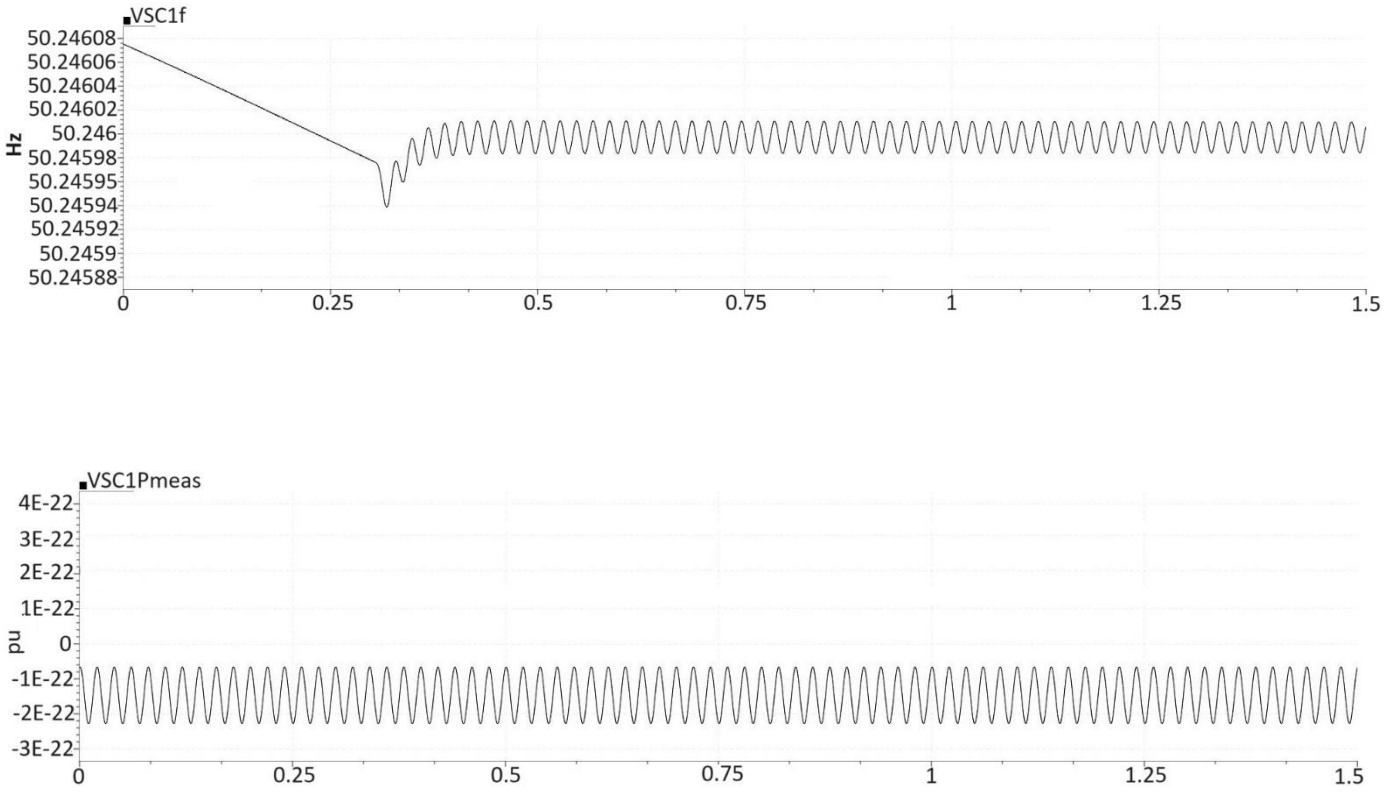

Figure 6.2.4 - Runtime Signals after Changing the SCR to 6.689 (x t[s]).

Thus, it is noted that the VGS can operate under a stricter condition of the network, occasion of the results of the stability analysis obtained using the RSCAD frequency scanning tool (RTDS).

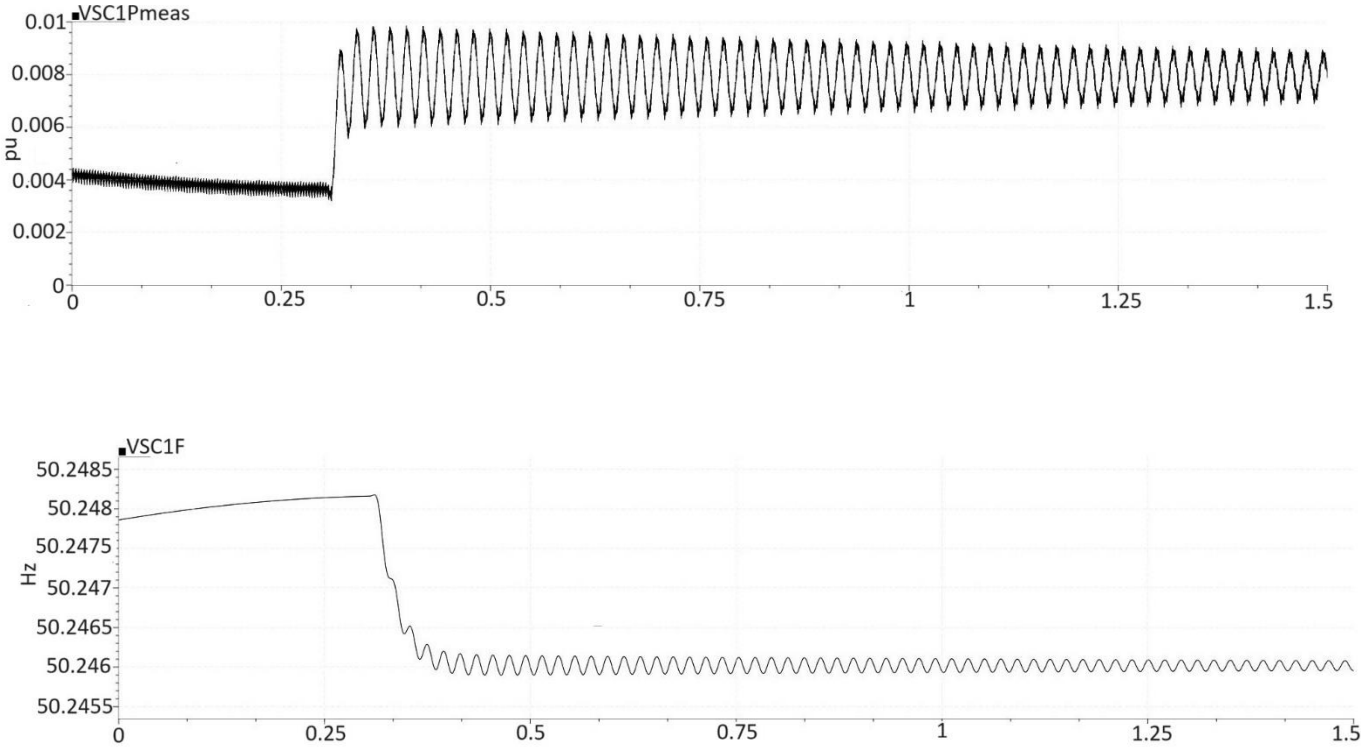

Figure 6.2.5 - Runtime Signals after Changing the SCR to 6.689 (x t[s]).

6.3. Influence of different parameters on re-synchronization

Combining Equations (6.1.1) and (6.1.3), it results in equation 6.3.1:

$$J\frac{d^2\delta}{dt^2} = T' - \frac{EV_g}{|Z|w^*}sin\delta^t - D(w - w^*) \qquad (6.3.1)$$

Where $T' = T^* - E^2\,G/w^*$ and $\delta^t = \delta - \varphi$, Z and φ means the representation of the impedance of the equivalent line and the residual angle of the impedance angle, respectively. As shown in Figure 6.3.1, point *a* and point *e* represent EP and UEP in this order. And point g represents NUEP (Next Unstable Equilibrium Point). Curve I

displays the relationship between P and δ of the pre-fault and post-fault systems, while curve II represents the curve $P - \delta$ of the system under a fault. There are two EPs indicated by δ^s and δ^u where the power balance can be achieved. δ^srepresents stable EP and δ^urepresents the UEP. δ_c represents VPA of a VSG at the time of extinction of the fault.

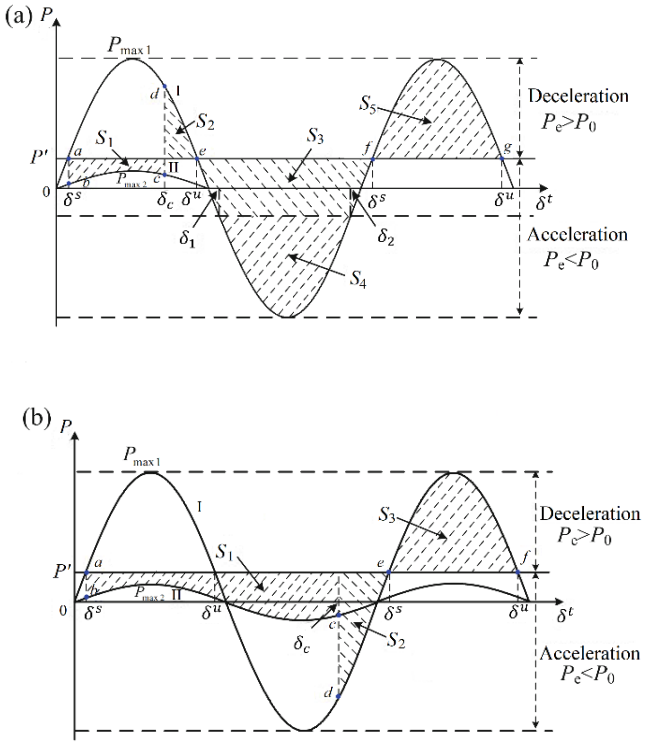

Figure 6.3.1 - Re-synchronization mechanism of a VSG. (a) Case I, (b) Case II.[53]

6.4. Simulation with $\delta_c > \delta^u$.

When $\delta_c > \delta^u$at the time of extinction of the fault, the curve is represented in Figure 6.3.1.b. Meaning that the system operating trajectory happens from point *a* to point *f*. S_1 and S_2 represents the acceleration area but S_3 represents the deceleration area. Similarly, the re-synchronization stability criterion in this case can be determined by equation 6.4.1:

$$S_1 + S_2 \leq S_3 + E_{loss} \tag{6.4.1}$$

Where E_{loss} represents the loss of energy by damping.

Combining Equations (6.1.2.10) and (6.3.1), it results in equation 6.4.2:

$$J\frac{d^2\delta}{dt^2} = T' - \frac{V_g}{2|Z|w^*}\left(\sqrt{\left(V_g cos\delta - A\right)^2 + B} + V_g cos\delta - A\right) sin\delta^t - D_p(w - w^*). \tag{6.4.2}$$

where $A = D_q X$ and $B = 4\left(Q_0 + D_q E_0\right)X$.

Re-synchronization equations proved by [53] and [83].

Thus, the $P - \delta$ curve of a VSG describes more as an ideal sine wave when the reactive power control loop becomes considered. The $P - \delta$ curve along the D_q variation is represented in Figure 6.3.2.

The value of D_q for curve I, II and II denotes at 40, 400 and 4000, respectively. It is observed that UEP δ^udecreases along with the decrease in D_q. Therefore, it becomes simpler than a VSG is conducted in the area of First-Swing Instability and therefore the system exerts a re-synchronization process. In addition, the operation of the systems becomes lower as the D_q decreases, reducing the power loss of the E_{loss} system. Therefore, S3 in case I does not change with the variation of D_q, while S3 in case II will decreases.

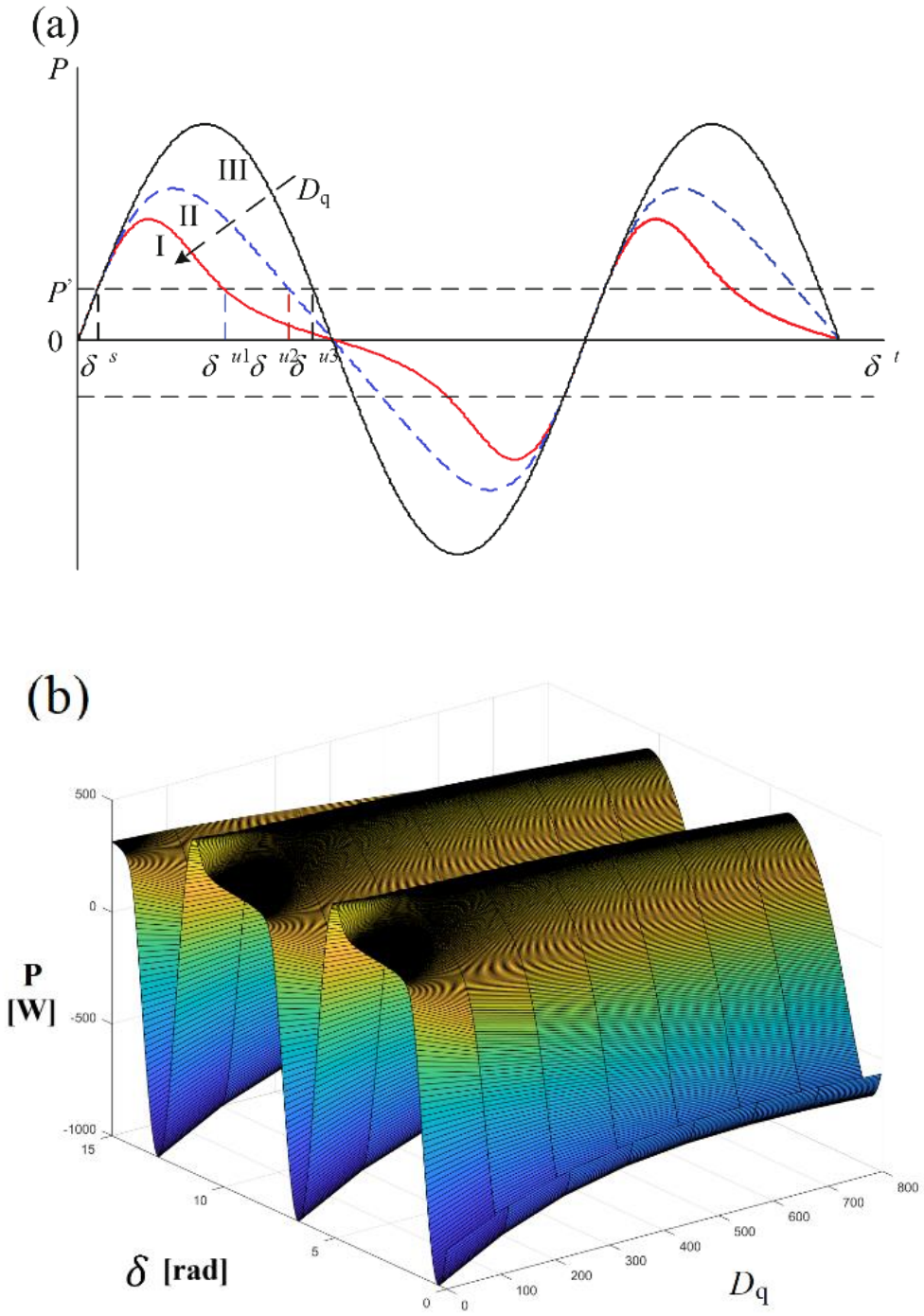

Figure 6.3.2 - P[W]-δ[rad] curve along with the variation of D_q.

As shown in Figure 6.3.3, the energization of a fast charger for electric vehicles, in this case using a power charger of 0.1 [MW], has electromagnetic transitional presented in

the figure as a maximum point of active power. In this type of energization performed in a simulation by RTDS, the microgrid fed by a virtual synchronous generator operates in isolation from the main grid, for the purpose of calculating stability limit, the energization can be performed by Figure 6.3.4, the capacity of the virtual synchronous generator to act in a reliable way by resynchronization and keeping the electrical system at a stable equilibrium point.

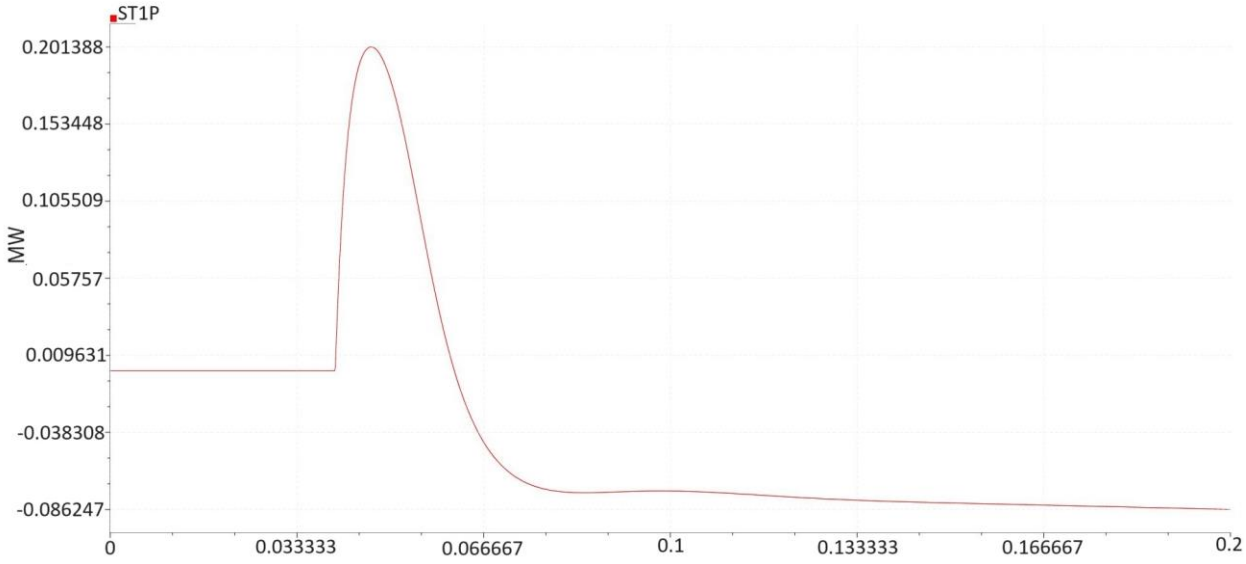

Figure 6.3.3 - Active power of fast charger energization (P[MW]x t[s]).

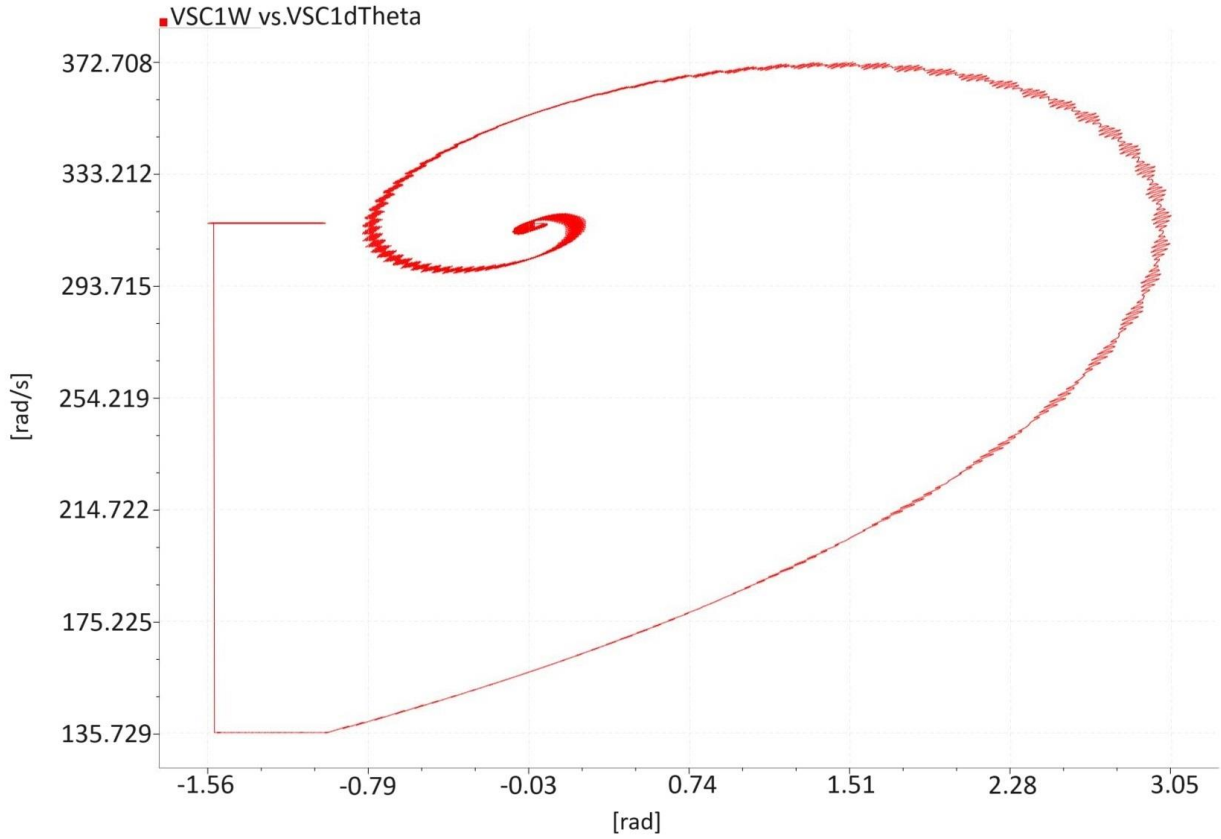

Figure 6.3.4 - Phase description of the transitional process of SVIB (RTDS simulation of single VSG connected to the infinite bus) (w[rad/s] x δ[rad]).

As shown in Figure 6.3.5, the RTDS (Real Time Digital Simulator) was able to perform the study case simulation where the VSG-composed system operates in a situation similar to the one presented in Figure 6.7, in which, when entering an instability situation, it can, as the results showed, achieve another equilibrium point, this proves that VSG can achieve synchronism, even experiencing First Swing Instability.

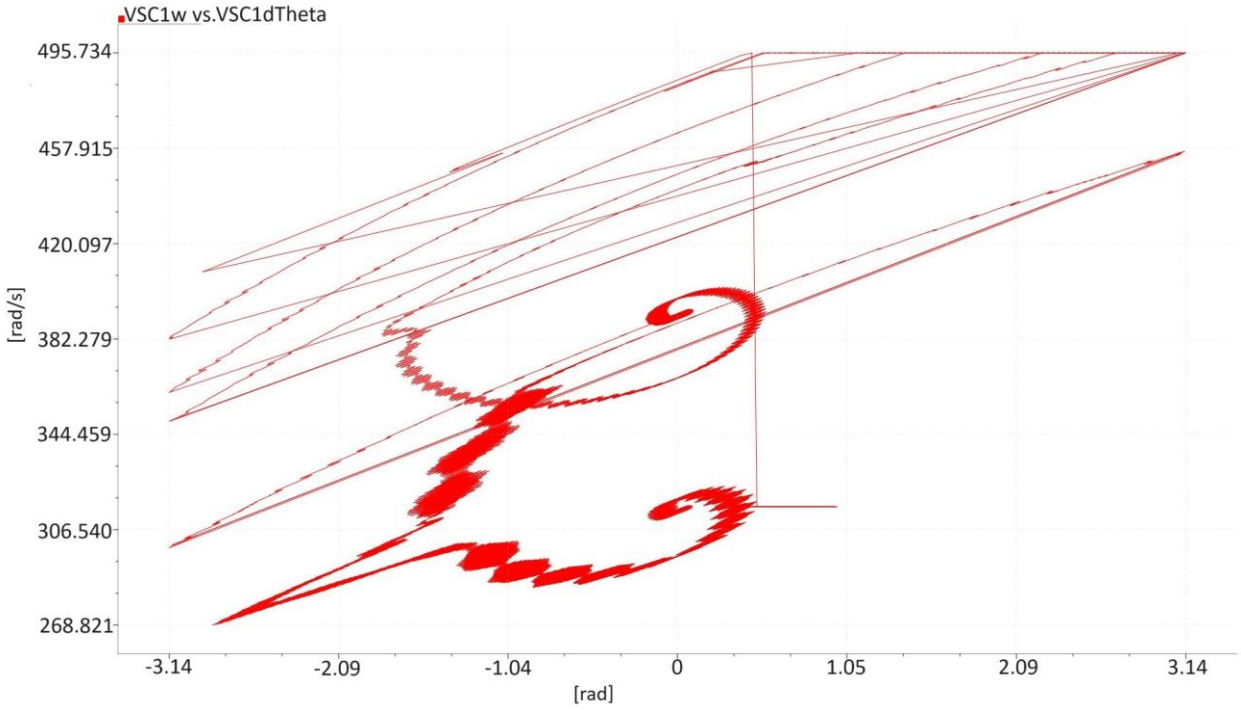

Figure 6.3.5 - Phase description of the transitional process of SVIB (RTDS simulation of single VSG connected to the infinite bus) (w[rad/s] x δ[rad]).

6.4.1. Islanded operation and damping validation of the VSG

In the event of loss or disconnection from the main grid, VSG still produces the necessary voltage of 1 [PU]. As shown in Figure 6.3.6, as the main BRKGrid is open to 0.3 seconds. Since the load connected to the 35 kV bus is 1.2 MW, VSG will produce 1.2 MW instead of the real power adjustment point of 0.5 [MW]. This change in active power results in a corresponding change in the frequency. Since the Dp damping factor is 100 and the change in the actual power of -0.7 [PU], the new frequency of stationary state is:

$$w = 1 + \frac{-0.7}{100 \times 1} = 0.993$$

This corresponds to a frequency of 49.65 [Hz], which matches the simulation result shown in Figure 6.3.6.

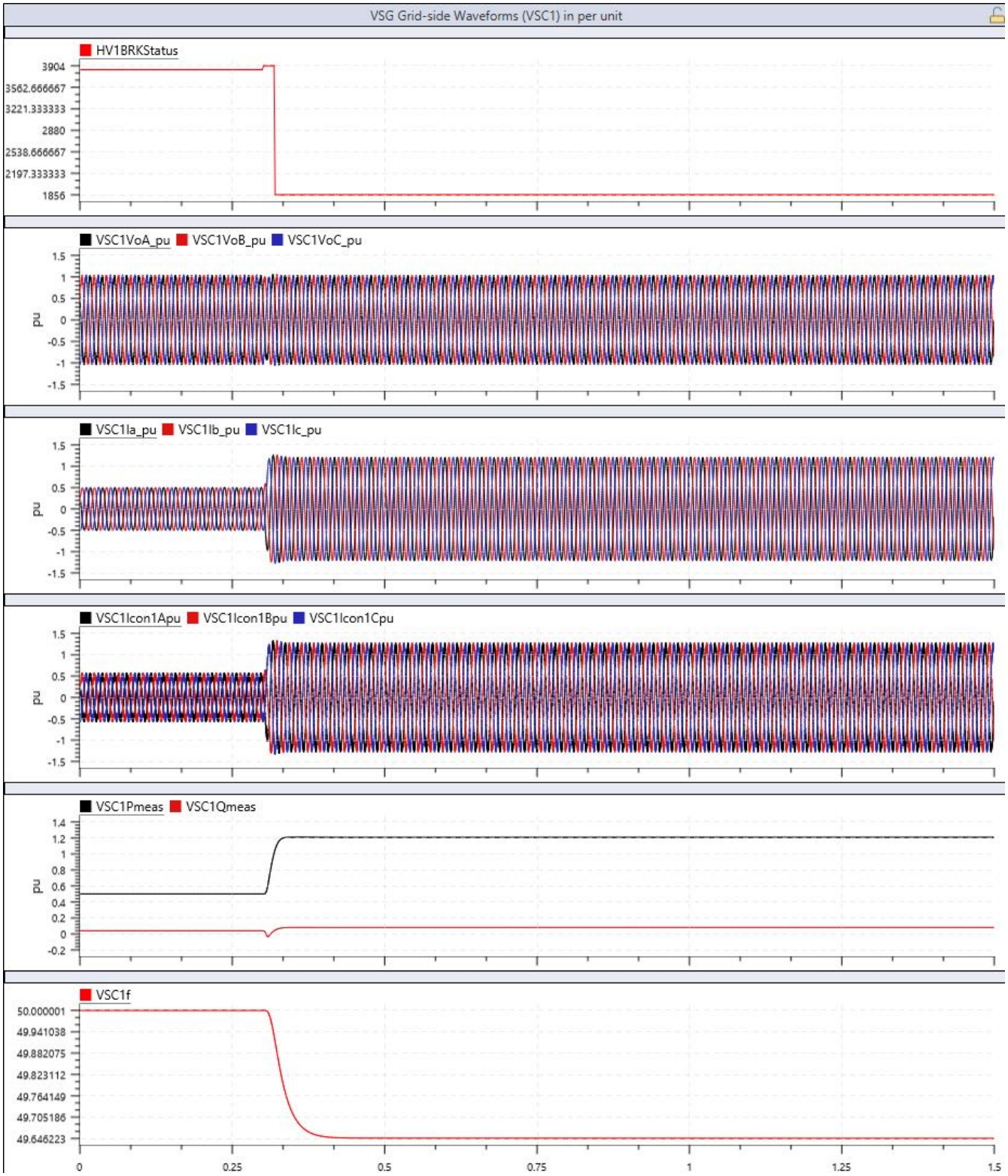

Figure 6.3.6 – Islanded operation of the VSG.

In order to verify the characteristic of the fall of reactive power and the magnitude of the voltage during the island operation, the actual power of the dynamic load is defined as 0.8 [MW], equal to the actual power and initially remains the reactive power of 0 [MVAR]. After that, the reactive power of the dynamic load to 0.5 [MVAR] increases. Figure 6.3.6 shows the simulation results when the reactive power of the dynamic load is increased from 0 to 0.5 [PU]. The cover coefficient Q-V 1/kQ is 0.05. This means that every 1 [PU] of reactive energy load increased will decrease the voltage by 0.05 [PU]. When reactive energy demand increases by 0.4 [PU], the voltage should theoretically fall to 0.02 [PU]. Figure 6.3.6 shows the magnitude of voltage that decreases from 1 [PU] to about 0.98 [PU], which proves with the theoretical value.

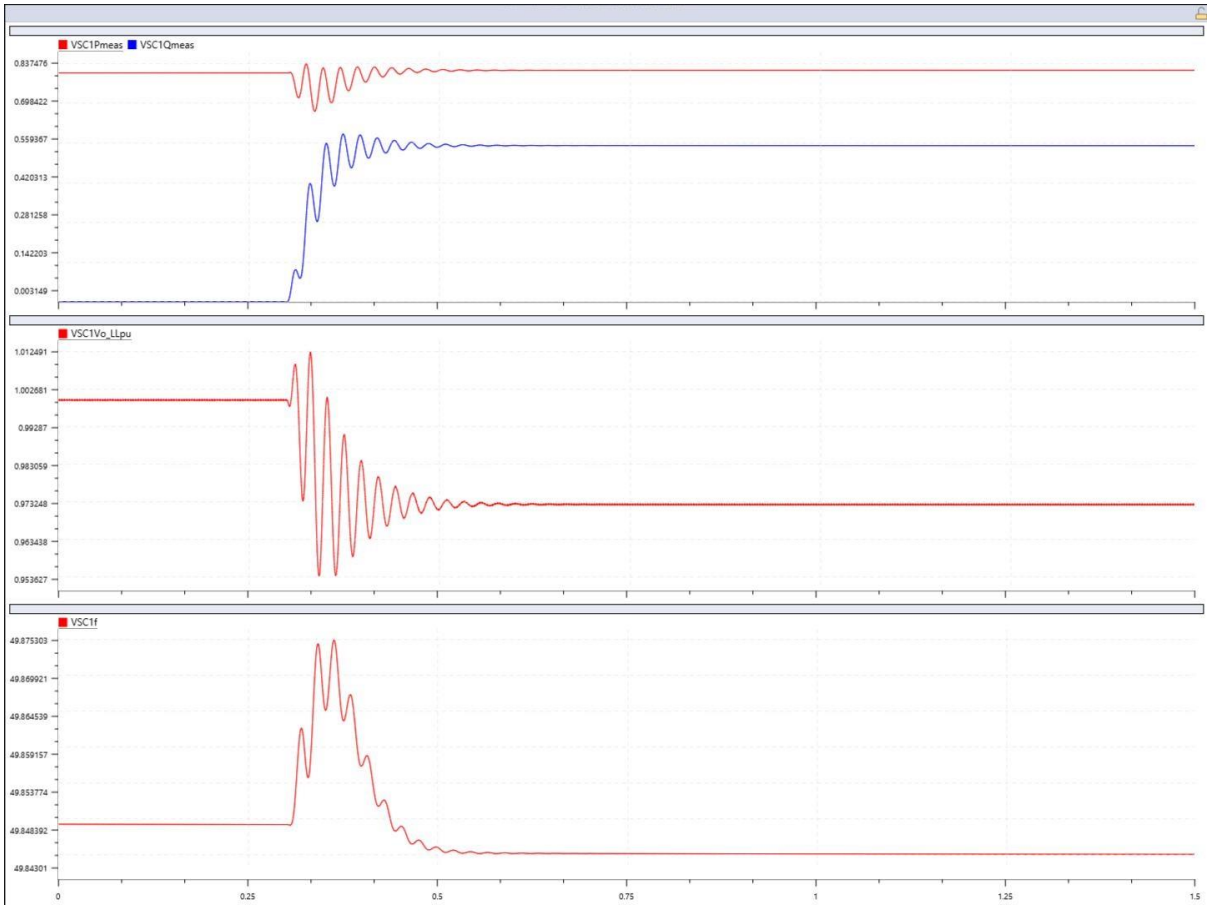

Figure 6.3.7 – Reactive Power load Change in Islanded Operation.

6.5. Fast charger inrush current calculation of electric vehicles

With the increase in the electricity classification of fast electric vehicle chargers, the specifications for the integration of the grid is required; Transient voltage and current during the initialization of these fast chargers have a negative impact on the performance of conversion and distribution systems[53].

The equation that results in the amplitude of the inrush current as a time function can be expressed as equation 6.5.1:

$$i(t) = \frac{\sqrt{2}V_m}{Z_t} * K_w * K_s * \left(sin(wt - \varphi) - e^{\frac{-(t-t_0)}{\tau}} \cdot sin\alpha\right) \quad (6.5.1)$$

Equation (6.5.1) proved by [83].

where V_m – maximum applied voltage; Z_t – total impedance under inrush, including system; φ– energization angle; t – time; t_0 – point at which core saturates; τ– time constant of transformer winding under inrush conditions; α – function of t_0; K_w – accounts for 3 phase winding connection; K_s – accounts for short-circuit power of network.

Figure 6.4.1 shows the simulation of equation (6.5.1), shown above, with the objective of determining the inrush current of fast electric vehicle chargers in a microgrid with resynchronization.

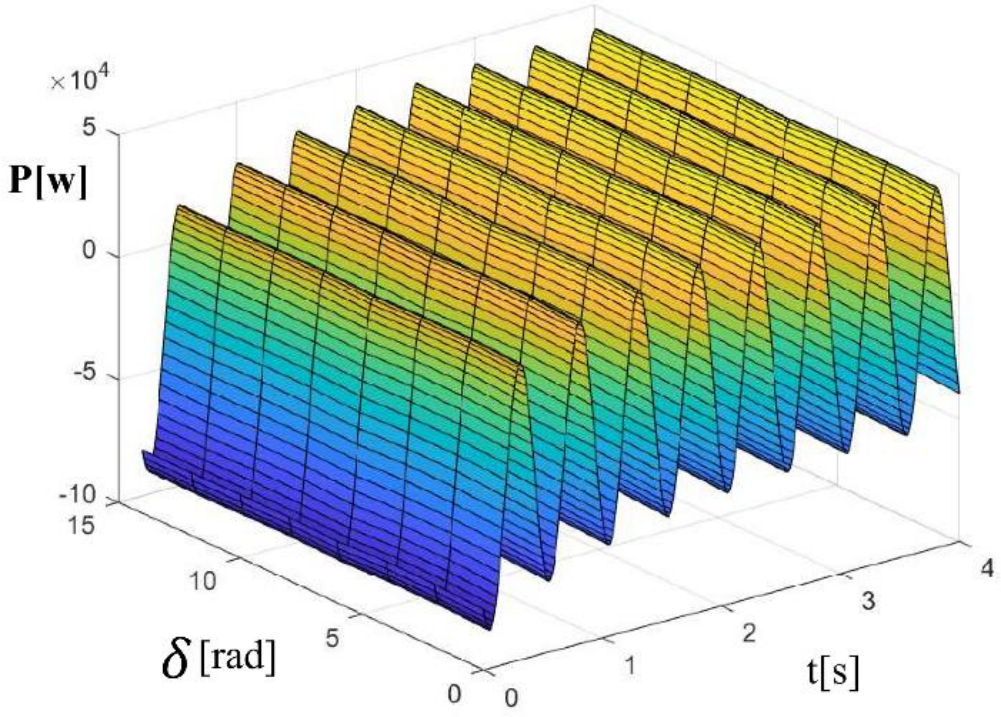

Figure 6.4.1 - Effect of inrush current at power.

In viewing the chart in Figure 6.4.1 which shows the variation of the power value in relation to the transitional relative to the current of inrush it can be noted that there is a variation over time in a certain delta angle value verified in the simulation with the value of $D_q = 0$, meaning that for each δ value in resynchronization a value will be added to the power proportional to the inrush current variation of the fast electric charger initialization for electric vehicles. Taking with the value of the random angle and $D_q = 0$ the chart in Figure 6.4.2 demonstrates the added inrush current represented by the power to the VSG system with fast electric charger initialization for electric vehicles.

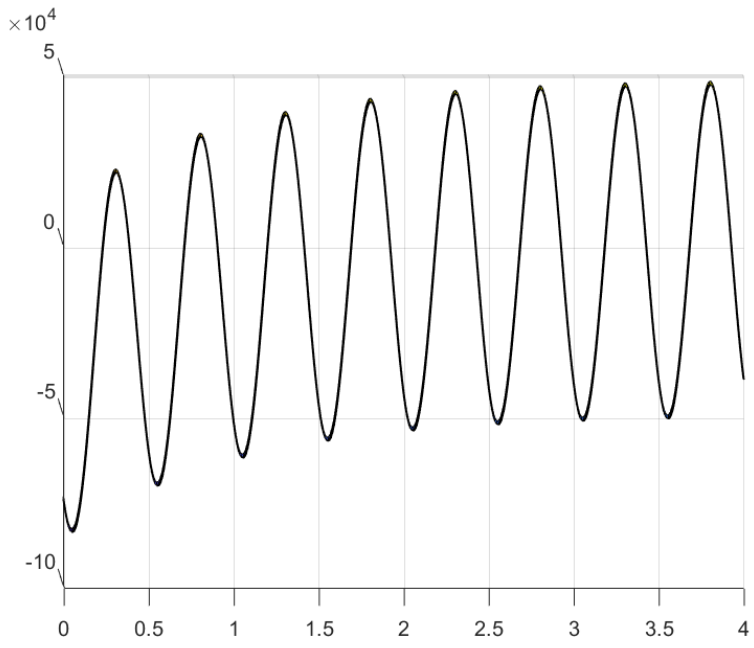

Figure 6.4.2 - Effect of inrush current at power (Pxt).

7. Objectives and applications.

The amount of distributed generation consisting of renewable sources is increasing proliferation worldwide. Thus, distribution systems operators need to improve system performance by keeping it within stability margins, even when the amount of

renewable energy in its portfolio increases, contributing to the balance of generation resources. Through a range of analysis and variation functions, active network management systems provide reliable voltage regulation imposing a standard that avoids overload situations, efficiently informing the load flow direction and providing updated values.

Power inverters stand out in the most complete electricity distribution systems as one of the most requested elements, and a power supplier interconnection of a large part of distributed generation in distribution systems. Currently, these devices perform advanced control functions that provide accurate control of active / reactive power and other electrical parameters, which allows the differential to have more extra functions in electricity systems. With the recent control methodologies for developed distributed generation and the definition of patterns for intelligent inverters, development models are required for intelligent inverters operating with more advanced functions such as: intelligent volt-var.

An inverter has a wide list of smart features. There are a wide range of use cases for intelligent inverters and each may have variants that are adjusted for each specific use case. However, sometimes necessary and often overly complex. The best approach is to create the lowest set of functions that still allow current use cases to be performed. Each change is evaluated and those considered architecturally significant - adding unavailable features using other functions - should be considered. This approach requires regular review of these functions, adding and updating the list as the sectoral system learns from field deployments and new use cases.

Understanding the intelligent functionality of the inverter requires basic knowledge of the technologies behind them. Smart inverters include any inverter-based generation where DC is covered in AC and supplied to the grid. This includes solar energy, energy storage, wind and electric vehicles. This research focuses on the system consisting of downed and microgrid generation, but many of the functions

apply to other inverter-based technologies. Each technology can have its own set of functions - such as the power storage or power storage function for power storage systems - or specific attributes that should be considered for a technology - such as storage and electric vehicles can load and discharge. As some of the functions are focused only on solar and storage, it is possible that there are gaps or ambiguities for other technologies, which paves the way for improving the optimization of systems that make up the functions of intelligent inverters and their applications.

7.1. Smart distribution grid sharing and reactive power optimization.

Increasing renewable energy integration into power systems requires more flexibility to deal with the fluctuation issues caused by renewable energy and volatility. Advanced communication and metering technologies allow power grids to move closer to smart grids, which have more solutions for the high penetration of renewable energy.

7.1.1. Basic concepts and formulation of optimization problems

The main function of the optimal reactive power flow (ORPF) boils down to ensuring that bus voltage magnitudes remain within operational limits. This is still necessary in distribution networks with high photovoltaic energy penetration, where cloud coverage can obscure specific grid areas, making traditional controls of control with an inadequate grid effect. The communication infrastructure of the intelligent grid paradigm allowed the inclusion of photovoltaic inverters as reactive energy control devices: adjusting the power factor of a photovoltaic inverter, allowing an almost real time of reactive power at the common coupling point, resulting in an

increase in versatility control. In order to formulate the problem of voltage diversion minimization to a smart Distribution Grid formed of photovoltaic generation with controllable inverters describes by equation 7.1.1.1 and 7.1.1.2.

$$\min_{u} f(u)$$

$$s.t. \begin{cases} P_{G_i} - P_{D_i} = V_i \sum_{j=1}^{N_{bus}} V_j \left(G_{ij}\, cos\theta_{ij} + B_{ij}\, sin\theta_{ij}\right) \\ Q_{G_i} - Q_{D_i} = V_i \sum_{j=1}^{N_{bus}} V_j \left(G_{ij}\, sin\theta_{ij} + B_{ij}\, cos\theta_{ij}\right) \\ V_{lower} \leq V_i \leq V_{upper} \\ APC_k \leq 0.8 \\ -90^{\circ} \leq \phi_{PV_\kappa} \leq 90^{\circ} \\ Q_{k,\,min} \leq Q_k \leq Q_{k,\,max} \end{cases}$$

(7.1.1.1)

where:

$$P_{G_i} = \begin{cases} P_{PV_k}\, APC_k, & i \in K \\ 0, & i \notin K \end{cases}$$

$$Q_{G_i} = \begin{cases} Q_k, & i \in K \\ 0, & i \notin K \end{cases}$$

$$Q_{k,\,min} = -\sqrt{S_k^2 - \left(P_{PV_k}\, APC_k\right)^2}$$

$$Q_{k,\,max} = \sqrt{S_k^2 - \left(P_{PV_k}\, APC_k\right)^2}$$

(7.1.1.2)

where N_{bus} represents the number of bars in a grid and P_{Gi}, Q_{Gi}, P_{Di}, Q_{Di}, represent the generation and demand for active and reactive power in each bar i, respectively, B_{ij} and Gij represent the susceptance and conductance of the branch that connects the nodes i and j, respectively, while Vi e Vj represent their corresponding voltage magnitudes ; APC_k , ϕPV_k e S_k represent the percentage of APC(active power curtailment), the power factor angle, and the nominal power value of the kth inverter, respectively; P_{PVk} represents the active power generated of the kth PV , where Qk represents the reactive power generated of the kth inverter. Finally, K represents the set of bar numbers where PV panels are located, and have the length of N_{PV}. The objective function f (u) of the optimization problem, in case of voltage deviation minimization (VDM), represented by equation 7.1.1.3:

$$f(u) = \sum_{i=1}^{N_{bus}} |1 - V_i|$$

(7.1.1.3)

where the goal is boil down to minimize the sum of the absolute magnitude of the Vi bars, the nominal value of 1 [p.u.], to the whole bar i. In the case of minimization of real power losses (RPLM), represented by equation 7.1.1.4:

$$f(u) = \sum_{k=1}^{N_{lines}} |I_k|^2 R_k$$

(7.1.1.4)

where *Ik* represents the magnitude of the electric current through the *Rk* resistance of the *k* line. The *u* design variable vector contains the injected APC and reactive power in each PV panel installed, represented by equation 7.1.1.5:

$$u = \left[Q_1,\ APC_1,\ Q_2,\ APC_2, \ldots\ Q_{N_{PV}},\ APC_{N_{PV}}\right] \tag{7.1.1.5}$$

7.1.2. Microgrid with multiple generation sources

Example illustrates (Figure 7.1.1) the operation of an inverter-based microgrid disconnected from the main grid (islanded mode), using the droop control technique. By definition, a microgrid can be used as a local energy grid with control capability, which means it can disconnect from the traditional grid and operate autonomously.

With the droop control technique, PLL are not required to achieve system-wide synchronization because all inverters reach the same frequency. In addition, power sharing among each inverter can be achieved since each inverter gives power in proportion to its capacity.

The microgrid consists of three parallel inverters subsystems, with power ratings of 500 [kW], 300 [kW] and 200 [kW] respectively, connected to the PCC (Point-of-Common-Coupling) bus. A dynamic load model is used to dynamically change the microgrid total load. The Microgrid Supervisory Control system, when enabled, modifies the inverters P/F and Q/V droop set points in order to bring back the microgrid frequency and voltage at their nominal values (60 Hz and 600 Volts respectively.

Each inverter subsystem contains a three-phase two-level power converter, an LC filter, a 480/600V transformer as well as an ideal DC source to represent the DC link of a typical renewable energy generation system (such as PV array, wind turbine, battery energy storage system). Each subsystem also includes a control system and a PWM generator feeding the inverter.

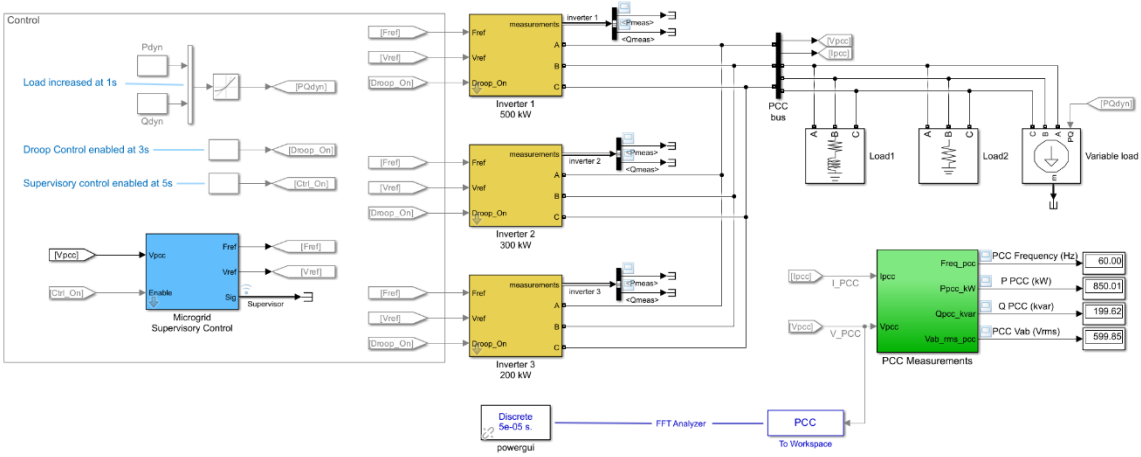

Figure 7.1.1 – Islanded inverter-based Microgrid (IEEE).

At 1[s] (Figure 7.2.1), the total microgrid load is increased from 450[kW]/100[kvar] to 850[kW]/200[kvar]. At 3 [s], droop control is enabled on all inverters. We can see that the microgrid load is now shared equally among the three inverters. At 5 [s], the supervisory control is enabled. The frequency is then being slowly increased to 60[Hz] and the line voltage to 600[V].

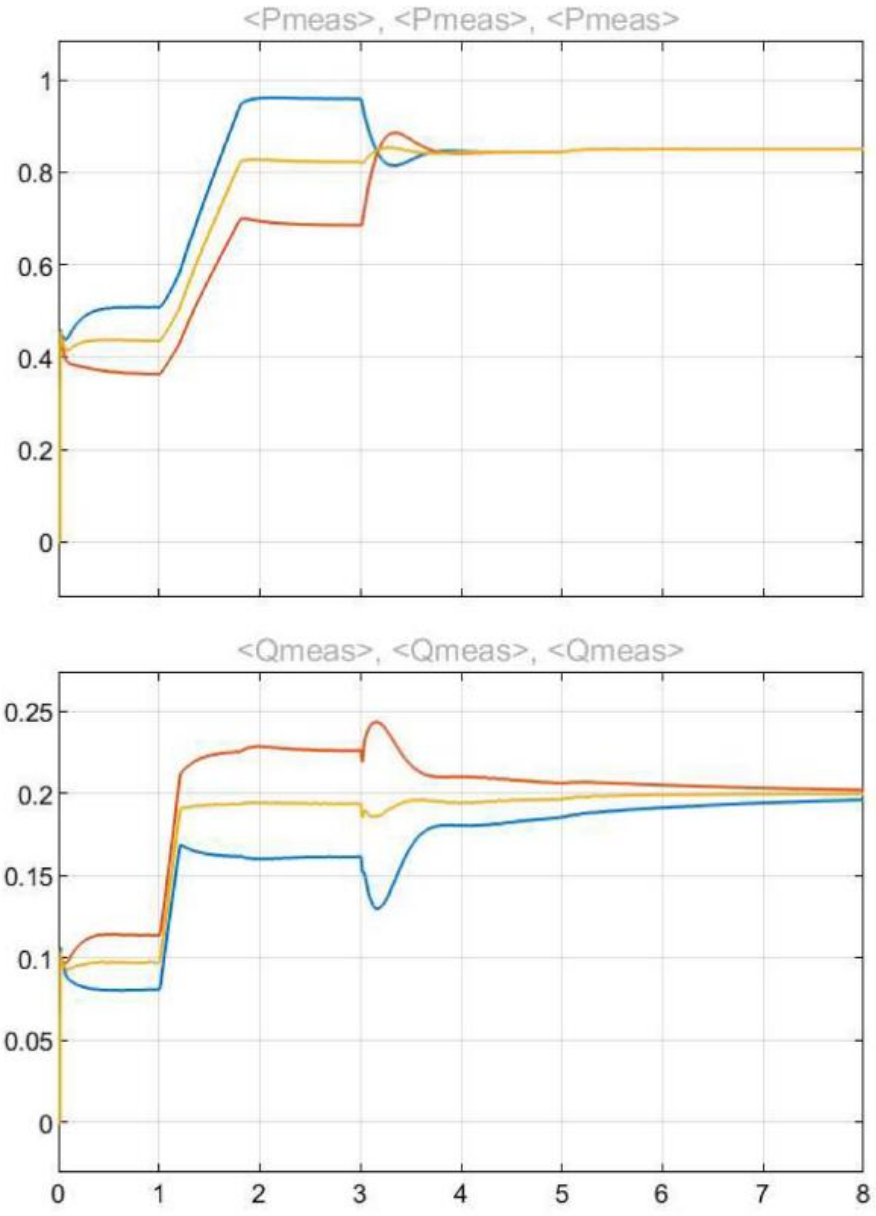
<Pmeas>, <Pmeas>, <Pmeas>
1
0.8
0.6
0.4
0.2
0
<Qmeas>, <Qmeas>, <Qmeas>
0.25
0.2
0.15
0.1
0.05
0
0
1
2
3
4
5
6
7
8

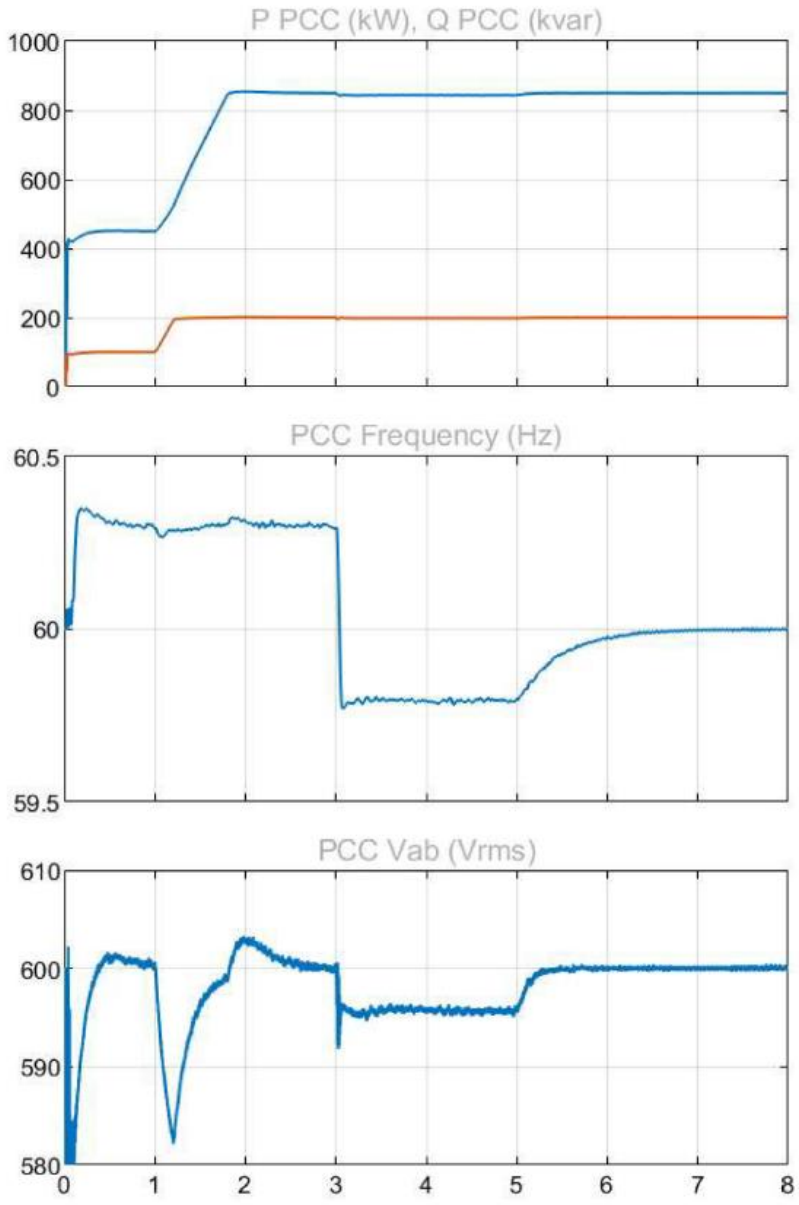

Figure 7.2.1- Measurements of microgrid output variables (by time in seconds) [MATLAB].

The integration of photovoltaic or wind systems into a mixed junction of electricity generation of a hybrid system associates the development and operating procedure with various technical and non -technical challenges. Non-technical calculations relevant to the integration of photovoltaic systems are mainly related to system

planning and design, operation and maintenance, which essentially demonstrate all localized problems and therefore differ from location to location.

Due to the conception of electricity generation through renewable sources, the continuity of supply becomes restricted to the type of generation conditioning that makes up the system in question and the type of renewable generation to which it is used, which can vary technically regarding the electrical energy converting systems to which it was planned for supply, whether or not dispatched sources.

8. Application and case study

The IEEE 13 bus feeder is contained in a smaller system used to test distribution systems. Operating and voltage 4.16[kV], has one source, a regulator, several non-balanced lines, and derivation capacitors. Figure 8.1 shows the diagram of a line of the test system. To complete the virtual synchronous generator application feature, an SVC (Static Var Compensator) was used, shown in Figure 8.2 The data belonging to the system is provided in the following tables (Tables 8.1 to 8.6). The results of the IEEE 13 document test feeder and RSCAD steady state results are compared in the following section [84].

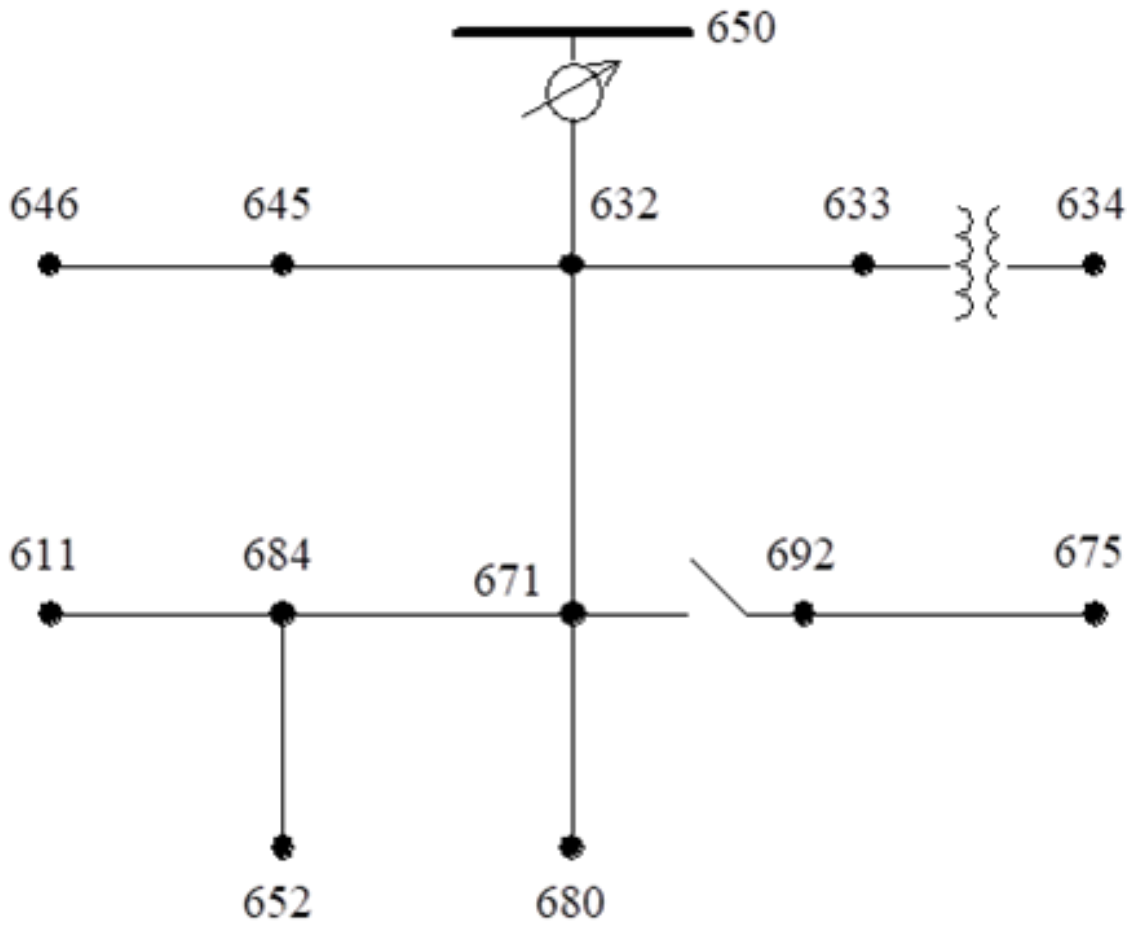

Figure 8.1 - IEEE 13 Node Test Feeder.[84]

	kVA	kV-high	kV-low	R - %	X - %
Substation:	5,000	115 - D	4.16 Gr. Y	1	8
XFM -1	500	4.16 – Gr.W	0.48 – Gr.W	1.1	2

Table 8.1 – Transformer Data.

Node	Ph-A	Ph-B	Ph-C
	kVAr	kVAr	kVAr
675	200	200	200
611			100
Total	200	200	300

Table 8.2 – Capacitor Data.

Node	Load	Ph-1	Ph-1	Ph-2	Ph-2	Ph-3	Ph-3
	Model	kW	kVAr	kW	kVAr	kW	kVAr
634	Y-PQ	160	110	120	90	120	90
645	Y-PQ	0	0	170	125	0	0
646	D-Z	0	0	230	132	0	0
652	Y-Z	128	86	0	0	0	0
671	D-PQ	385	220	385	220	385	220
675	Y-PQ	485	190	68	60	290	212
692	D-I	0	0	0	0	170	151
611	Y-I	0	0	0	0	170	80
	TOTAL	1158	606	973	627	1135	753

Table 8.3 – Spot Load Data.

Node A	Node B	Load	Ph-1	Ph-1	Ph-2	Ph-2	Ph-3	Ph-3
		Model	kW	kVAr	kW	kVAr	kW	kVAr
632	671	Y-PQ	17	10	66	38	117	68

Table 8.4 – Distributed Load Data.

Config.	Phasing	Phase	Neutral	Spacing
		ACSR	ACSR	ID
601	B A C N	556,500 26/7	4/0 6/1	500
602	C A B N	4/0 6/1	4/0 6/1	500
603	C B N	1/0	1/0	505
604	A C N	1/0	1/0	505
605	C N	1/0	1/0	510

.

Table 8.5 - Overhead Line Configuration Data.

Config.	Phasing	Cable	Neutral	Space ID
606	A B C N	250,000 AA, CN	None	515
607	A N	1/0 AA, TS	1/0 Cu	520

Table 8.6 - Underground Line Configuration Data.

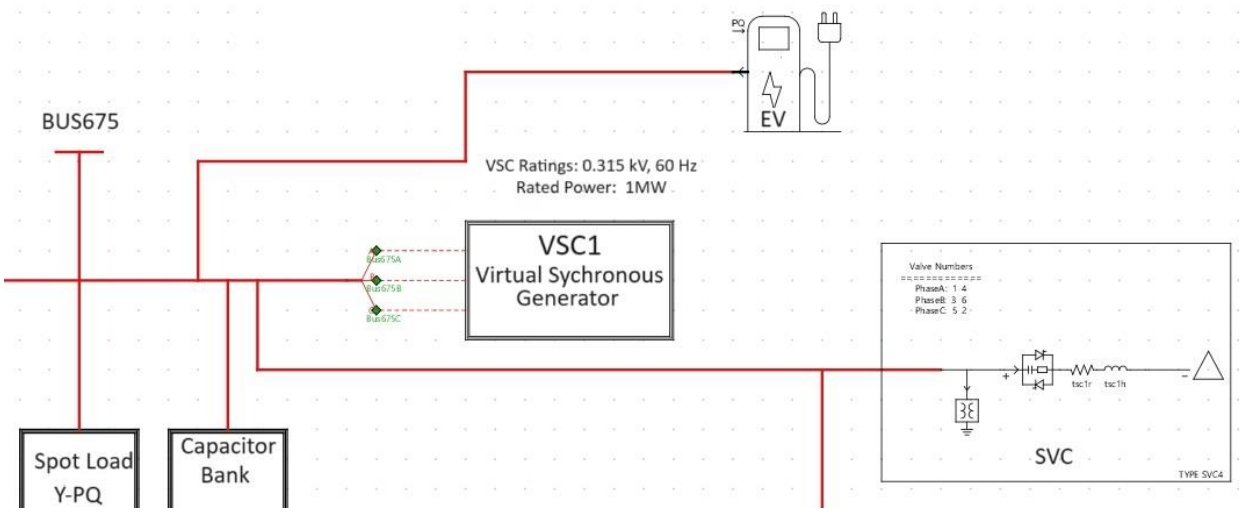

Figure 8.2 – VSG//SVC connection in the feeder bus 675.

The SVC (Table 8.7), joining the VSG, has a regulatory feature based on the reactive current output of the SVC in the load voltage. The characteristic of regulation is created by the action of a thyristor-controlled reactor (TCR) and 2 (two) thyristor-

switched capacitors (TSCs). TCR provides the inductive output of the SVC and can be controlled by the phased firing of its series of the series, from the complete inductor with the fully triggered thyristors, to no indicator with blocked thyristors, in a smooth continuous way.

Parameter	Values
f_0	**60 [Hz]**
P_s	**1.0 [MW]**
P_{con}	**1.0 [MW]**
V_{dc}	**0.8 [kV]**
V_{trCon}	**0.315 [kV]**
S_{tr}	**1.0 [MVA]**
X_{trpu}	**0.1 [pu]**
L_f	**0.063 [mH]**
C_f	**1500.0 [µF]**
R_f	**0.051[Ω]**
C_{bus}	**64000[µF]**
Switching Frequency f_s	**2000 [Hz]**

Table 8.7 - Converter Parameters.

As shown in Figure 8.3.a., fast charger energizing for electric vehicles without proper correction, and Figure 8.3.b. the same energization in a corrected manner. In the case (a), causing an increase in the energization that causes electromagnetic transients that change the voltage and current level and may be able to cause high distortions on the power grid and compromise equipment life to it connected.

The oscillation in the energization of a fast charger for electric vehicles, which as shown in Figure 8.3.a. increases the amount of power by 20%, in this case an 0.2 [MW] power charger, has an electromagnetic transient shown in the figure as a maximum point of active power measured in the bus 675 of the feeder default IEEE 13 node, which compromises the voltage level. In this type of energization performed on a RTDS simulation, the feeder has a connected VSG (virtual synchronous generator)

and can act as a microgrid, with control and adaptive protection, disconnecting from the feeder and operating in an island mode, in isolation from the main grid.

As shown in Figure 8.3.b, the energization of the same fast charger for electric vehicles, in this case in the same node but with SVC acting together with VSG and operating efficiently to maintain the voltage of the distribution system at an acceptable level even with the action of the electromagnetic transition of energization, as shown in the previous figure, surpassed the supply capacity of the feeder, which in the optimized system works normally maintaining the demand of the planned load.

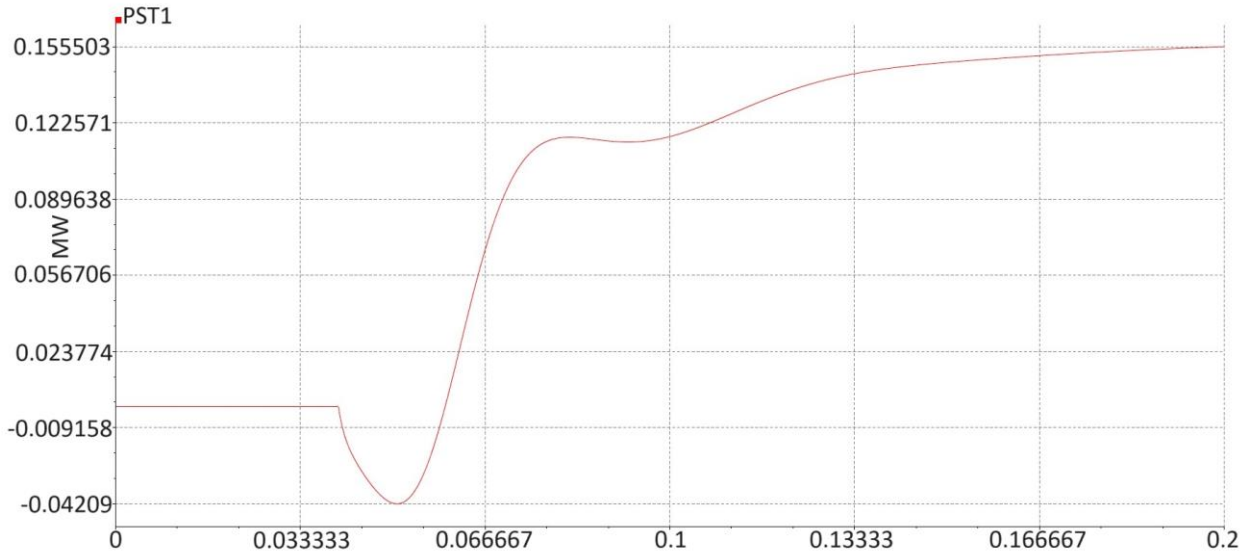

Figure 8.3.a – Energization without correction (P[MW] x t[s]).

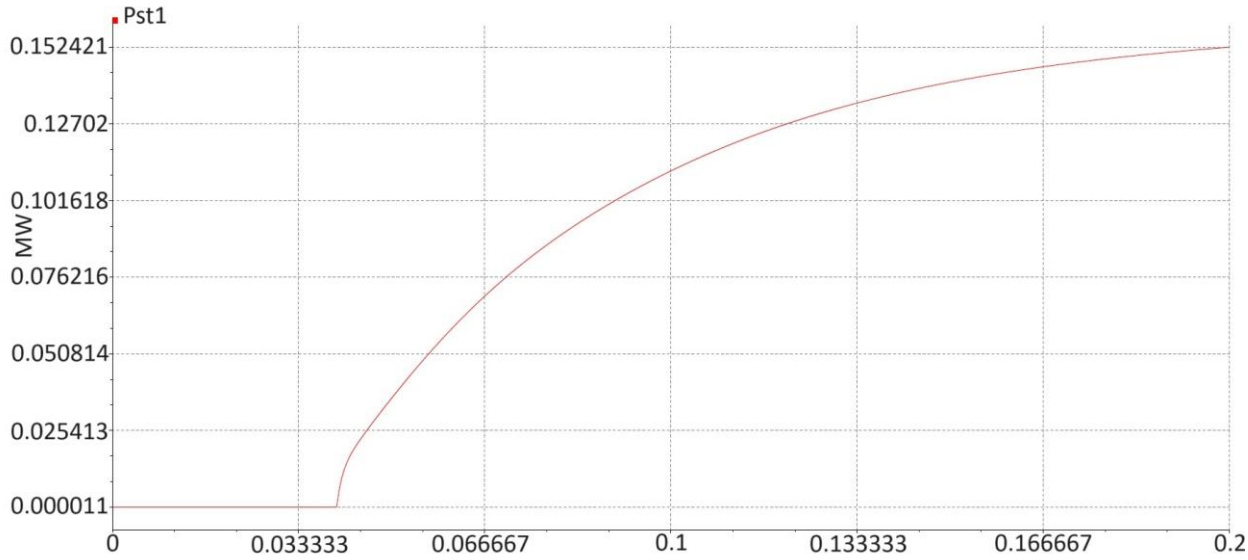

Figure 8.3.b – Correct energization (P[MW] x t[s]).

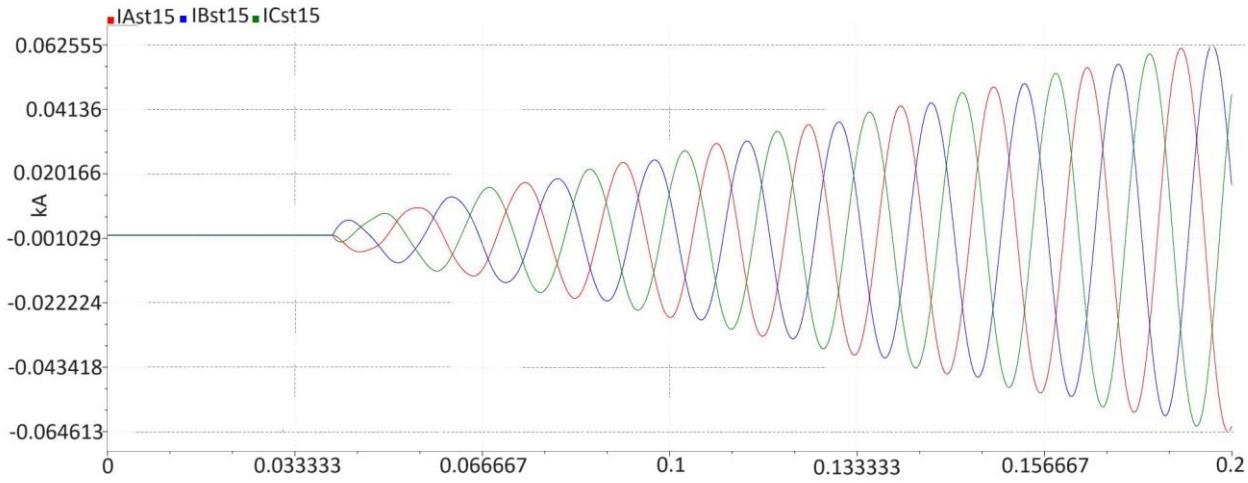

Figure 8.4 – Electric Current of fast charger energization with the VSG//SVC (I[kA] x t[s]).

Figure 8.5. shows an energization situation in which the energized fast charger causes a visible voltage drop in the system, which can cause several problems in the power grid and energized equipment.

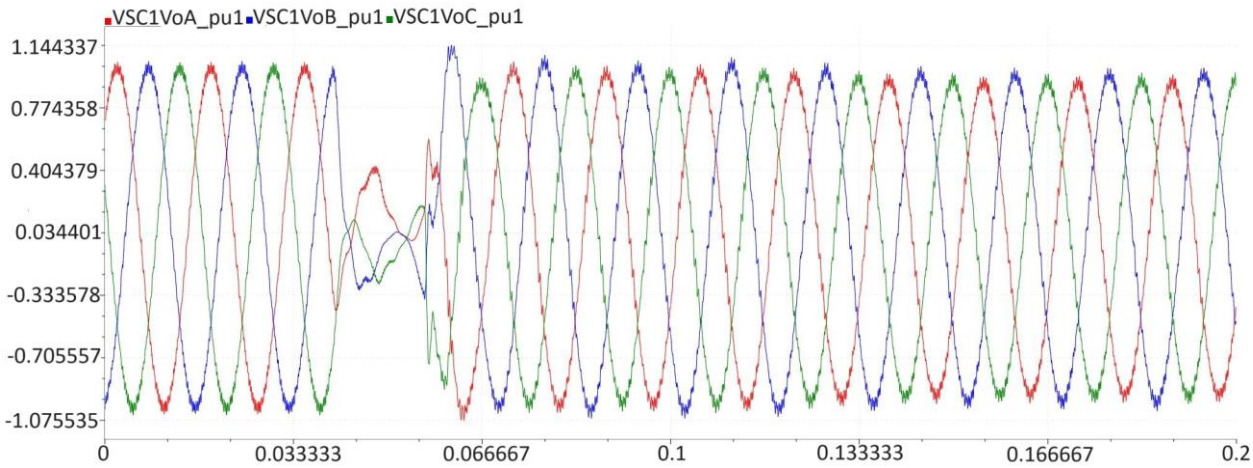

Figure 8.5 – Voltage measurement of fast charger energization without the VSG//SVC (V[pu] x t[s]).

As shown in Figure 8.6., the energization of the same fast charger for electric vehicles, in this case in the same node, but with SVC acting together with VSG and operating efficiently to maintain the voltage of the distribution system at an acceptable level even with the action of the electromagnetic transient of the energization, being visualized a very acceptable transition to the supply level, as shown in the figure there is a soft transition, which minimizes the loss by current and voltage oscillations, keeping the system more reliable.

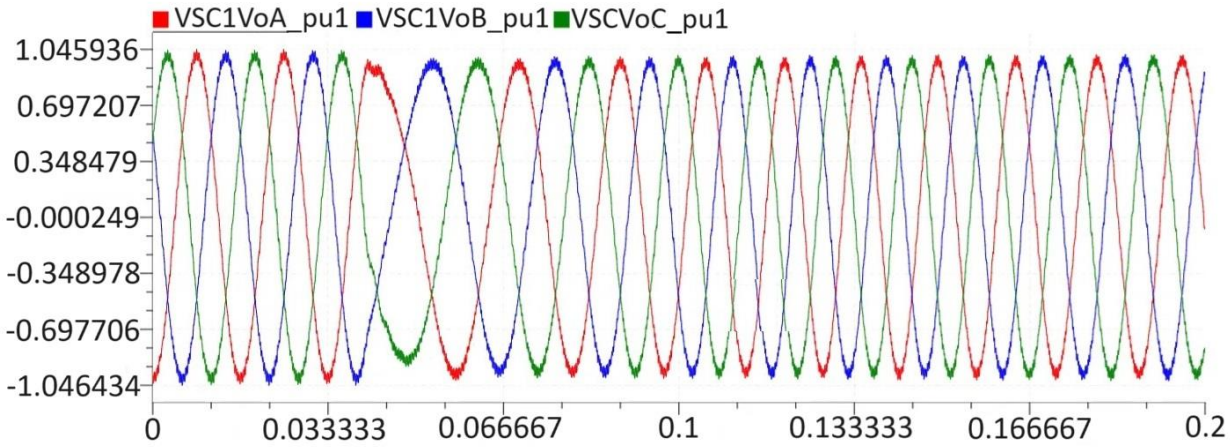

Figure 8.6 – Voltage measurement of fast charger energization with the VSG//SVC (V[pu] x t[s]).

In this way of energizing in a simulation by RTDS, the IEEE 13 Nodes network fueled by a virtual synchronous generator and SVC promotes the energization that can be viewed by Figure 8.7., which demonstrates the capacity of the synchronous virtual generator along with SVC to act reliably by resynchronization and keeping the electrical system at a stable equilibrium point.

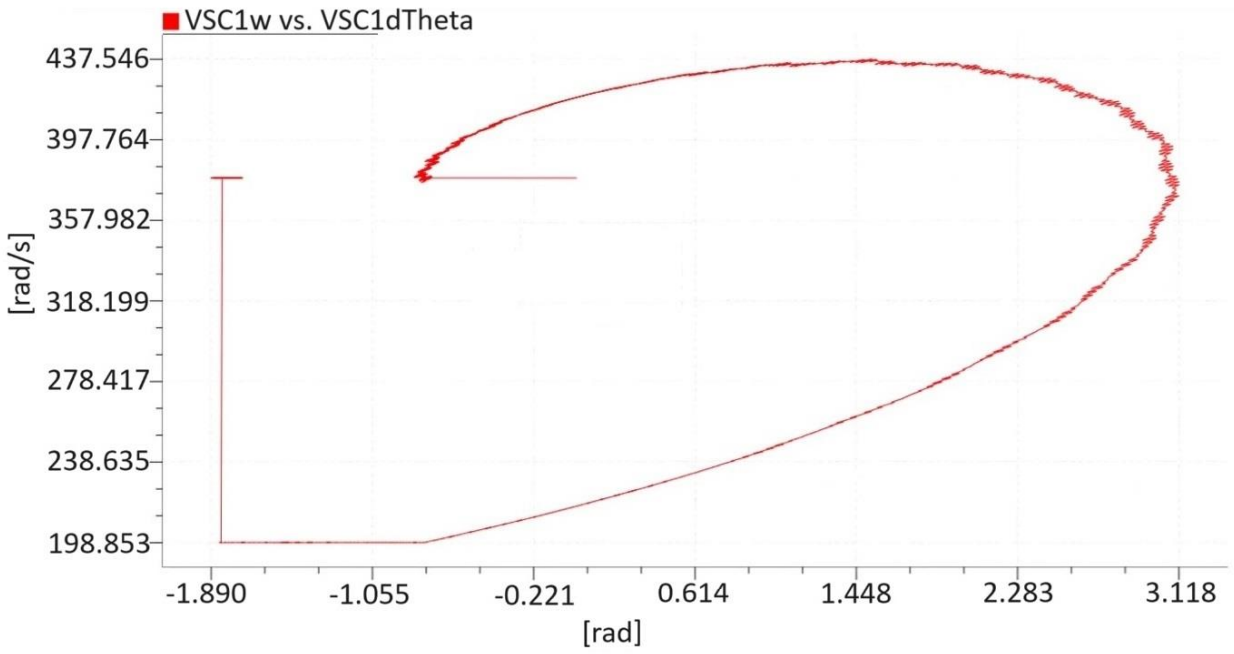

Figure 8.7 - Phase description of the transitional process of SVIB (RTDS simulation of single VSG//SVC connected to the IEEE 13 nodes) (w[rad/s] x δ [rad]).

The island operation mode, in the same specification as a microgrid, was implemented in this case study by opening the circuit section at node 692, in which the circuit formed by nodes 675 and 692 supplied by the VSC//SVC can operate independently of the rest of the circuit, with the adaptive protection system and specific control, acting as a microgrid with voltage limits (Figures 8.8, 8.9 and 8.10) within the power supply standards, as well as the energization current of the fast charger (Figure 8.3a), related to an active and reactive power balance provided by the VSG//SVC (Figure 8.3b).

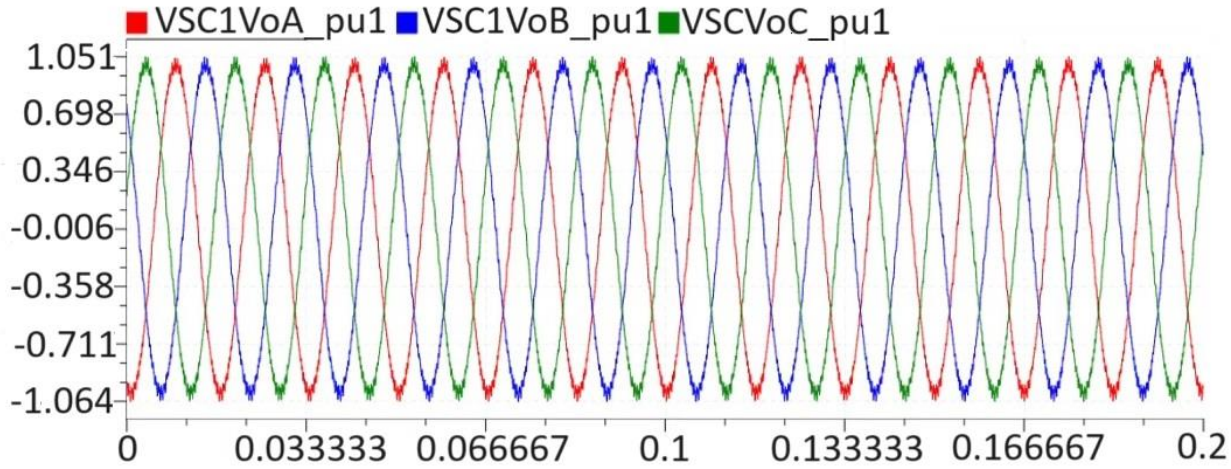

Figure 8.8 – Voltage measurement in the islanded mode (V[pu] x t[s]).

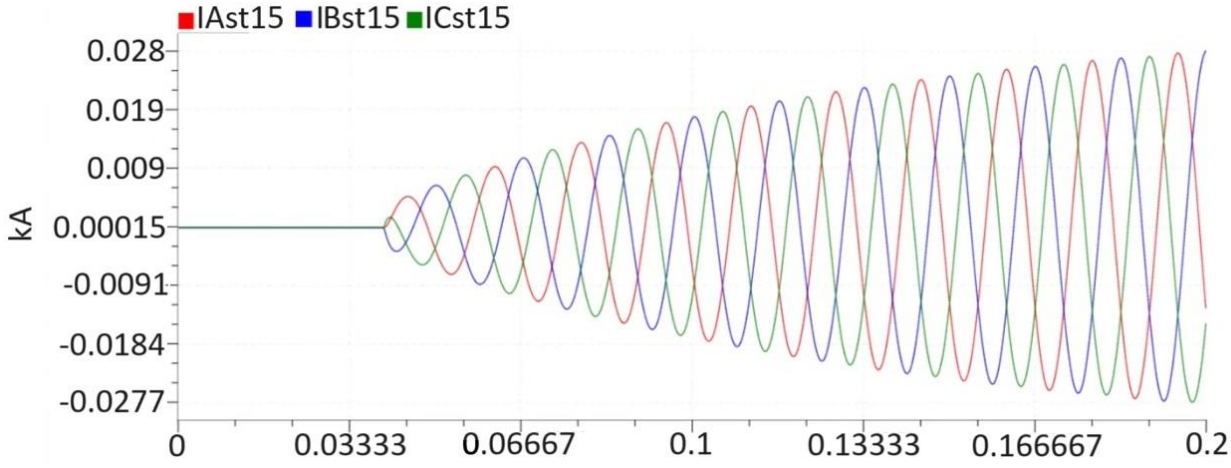

Figure 8.9 – Electric current measurement in the initialization of the fast charger(I[kA] x t[s]).

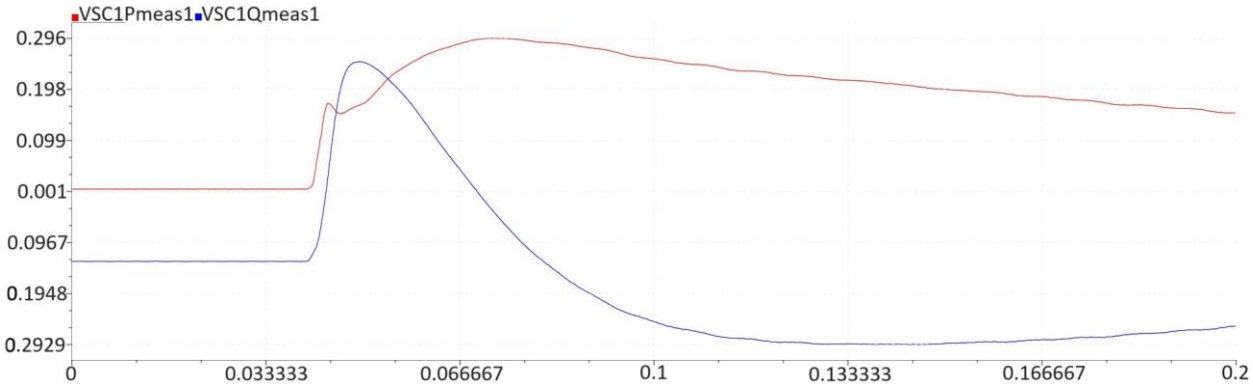

Figure 8.10 – Active and reactive power measurement P[MW], Q[MVAR], t[s].

9. Conclusions

According to the intermittent supply with a volatile characteristic of the electric power generation sources of renewable origin, the hybridization of different sources of alternative power generation completes, as far as possible, the inefficiency of the renewable generation set and to obtain greater efficiency total energy than that could be obtained from a single renewable source. The implementation of adequate control in multisource electricity systems, provides great potential for the supply of higher quality electricity and could assign more reliability to the supply to customers than a system based on a single source.

With the implementation of electricity generation hybrid systems in remote areas, more relevant solutions were presented when compared to systems connected to the network in remote areas. Energy planning of electricity systems for supply in remote areas increasingly includes hybrid electricity systems due to their characteristics compared to grid-connected feeders, reducing losses along the long lines, as well as the vulnerability related to greater exposure to weather which compromises system reliability.

The use of hybrid systems has been incorporated into distributed and micro-generation electrical systems in order to improve reliability and use a better supply capacity system. With the improvement of renewable energy systems, there is greater results in relation to the effectiveness and reduction of costs with the advancement of electronic electricity converters and automatic control that improves the operation of hybrid energy systems and reduces maintenance requirements, making it practical and economic hybrid systems.

The study of the case of the VSG re-synchronization phenomenon in microgrid can verify in the results with the simulation the stability limits where, in addition, the system enters the instability the first time, originated by significant serious faults and causing anomalies in electrical systems. The transient stability criterion studied in this

research allows engineers to determine whether the system can return to the stable state after a fault extinction. Thus, the re-synchronization mechanism of VSGs is subject to succinct analyzes and, analogously, the influences of different parameters become relevant, which was verified by studying the quick charger of electric vehicle charger in microgrid with VSG in the Synchronization process after an anomaly in the system. The inrush current of the electric charger can have a negative impact, according to the study, even in a resynchronization system, affecting the performance in conversion and distribution systems.

The generation of electricity distributed throughout the distribution system through renewable sources imposes significantly different parameters from the conventional generation used in electricity grids. As a result, the multidirectional energy flow originated in active electricity distribution networks.

To recognize the consideration of these variables along the power electrical systems with renewable mixed generation and under the influence of transitory initialization and distinctive demanded load, microgrid planning becomes an important aspect that needs to be considered for the successful implementation and operation of an intelligent microgrid.

The VSG//SVC can improve the performance of the power system distribution network in a variety of ways, as well as the active microgrids operating in islanded mode. Configuring a VSG//SVC at one or more appropriate points in the grid can increase the transfer capacity and reduce losses, maintaining a smooth voltage profile under different grid conditions, and promoting the capacity for a microgrid with diverse forms of renewable generation. Thus, proving a greater contribution of scientific and technological research, operating a virtual synchronous generator with greater capacity for stabilization and resilience to electric network oscillations through the optimization promoted by VSG//SVC.

With the applications and simulations carried out by the RTDS and MATLAB systems, the next generations of voltage source converters will be able to incorporate the compensating characteristics of the static var compensator inserted in the

converter itself in order to increase the dynamic response capacity in various oscillations in the electrical network, imposing an effective and expressive advantage over traditional electrical systems.

10. References

[1] R.J. Bravo, S.A. Robles, T. Bialek, "VAr support from solar PV inverters," 2014 IEEE 40th Photovolt. Spec. Conf., pp. 2672-2676,20.1109/PVSC.20146925479, IEEE Denver, CO (2014).

[2] IEEE," IEEE 13 Node Test Feeder Document," Resources – IEEE PES Test Feeder.

[3] B. Seal, "Common Functions for Smart Inverters," EPRI Project manager. 4th edition, technical Update, December 2016.

[4] J. E. Sarmiento, E. M. Carreno, A. C. Zambroni, "Modeling inverter with volt-var functions in grid-connected mode and droop control method in islanded mode," Electric Power Systems Research 155, 265–273 (2018).

[5] G. Alvarenga, M. S. C. Santos, R. S. Moura, "Effects of different generator reactive power limits representation on load margins," © 2019 John Wiley & Sons, Ltd. July 2019.

[6] S. Chowdhury, S. P. Chowdhury, P. Crossley, "Microgrids and Active Distribution Networks," Published by The Institution of Engineering and Technology, London, United Kingdom. © 2009.

[7] A. C. Z. de Souza, M. Santos, M. Castilla, J. Miret, L. G. Vicuña, D. Marujo, "Voltage security in AC microgrids: a power flow-based approach considering Droop-controlled inverters," Renew. Power Gener. IET 9, 954–960, (2015).

[8] J. Mitra, N. C. Cai, M. Chow, S. Kamalasadan, W. Liu, W. Qiao, S. N. Singh, A. K. Srivastava, K. S. Srivastava, G. K. Venayagamoorthy, Z. Zhang, "Intelligent Methods for Smart Microgrids; Task Force on Intelligent Control Systems for Microgrids," which is part of the Intelligent Control Systems (ICS) Working Group of the Intelligent Systems Subcommittee, under the Power Systems Analysis, Computing and Economics Committee of the IEEE Power & Energy Society, ©2011 IEEE.

[9] S. A. Roosa, "Fundamentals of Microgrids Development and Implementation," First edition published 2021 by CRC Press 6000 Broken Sound Parkway NW, Suite 300, Boca Raton, FL 33487-2742; and by CRC Press 2 Park Square, Milton Park, Abingdon, Oxon, OX14 4RN; © 2021 Taylor & Francis Group, LLC; CRC Press is an imprint of Taylor & Francis Group, LLC.

[10] H. Laaksonen, "IED Functionalities Fulfilling Future Smart Grid Requirements," Distribution Automation ABB Oy Medium Voltage Products Muottitie 2 A, 65320 Vaasa, Finland, Smart Grids and Energy Market (SGEM) research program of CLEEN Ltd.

[11] S. Bahrami, A. Mohammadi, "Smart Microgrids From Design to Laboratory-Scale Implementation," © Springer Nature Switzerland AG 2019.

[12] S. K. Kottayil, "Smart Microgrids," © 2021 Taylor & Francis Group, LLC.

[13] H. Farhangi, "SMART MICROGRIDS," © 2017 by Taylor & Francis Group, LLC.

[14] A. Chakrabortty, M. D. Ilić, "Control and Optimization Methods for Electric Smart Grids," © Springer Science Business Media, LLC 2012.

[15] G. Fusco, M. Russo, “Adaptive Voltage Control in Power Systems, Modeling, Design and Applications,” © Springer-Verlag London Limited 2007.
[16] L. Fan, “Control and Dynamics in Power Systems and Microgrids,” © 2017 by Taylor & Francis Group, LLC.
[17] M. S. Alam, M. Krishnamurthy,”Electric Vehicle Integration in a Smart Microgrid Environment,” © 2021 selection and editorial matter, Mohammad Saad Alam and Mahesh Krishnamurthy individual chapters, the contributors, CRC Press is an imprint of Taylor & Francis Group, LLC.
[18] ABNT NBR 6024, “Information and documentation – Progressive numbering of the sections of a document.”
[19] ABNT NBR 6023, “Information and documentation – References – Preparation.”
[20] E. Kabalci, “Hybrid Renewable Energy Systems and Microgrids,” Copyright © 2021 Elsevier Inc. All rights reserved.
[21] H. Xin, D. Gan, N. Li, H. Li, C. Dai, “Virtual power plant-based distributed control strategy for multiple distributed generators,” IET Control Theory Appl. 7 (2013) 90_98.
[22] J.M. Morales, A.J. Conejo, H. Madsen, P. Pinson, M. Zugno, “Virtual power plants, Integrating Renewables in Electricity Markets,” International Series in Operations Research & Management Science, 205, Springer, Boston, MA, 2014, pp. 243_287. ISBN 978-1-4614_9410-2.
[23] E. Baldwin, V. Rountree, J. Jock, “Distributed resources and distributed governance: Stakeholder participation in demand side management governance,” Energy Res. Soc. Sci. 39 (2018).
[24] R. Batchu, N.M. Pindoriya, “Residential demand response algorithms: state-of-the-art, key issues and challenges,” In: P. Pillai et al. (Eds.), Wireless and Satellite Systems, Lecture Notes of the Institute for Computer Sciences, Social Informatics and Telecommunications Engineering, Vol. 154, Springer International Publishing, 2015.
[25] U.S. Department of Energy (DOE), “Benefits of Demand Response in Electricity Markets and Recommendations for Achieving Them: A Report to the United States Demand-side management 489 Congress Pursuant to Section 1252 of the Energy Policy Act of 2005, “U.S. DOE, Washington, DC, 2006.
[26] N. Hatziargyriou, I. P. Siqueira, “Electricity Supply Systems of the Future,” © Springer Nature Switzerland AG 2020, https://doi.org/10.1007/978-3-030-44484-6.
[27] CIGRE: Technical Brochure TB 635, “Microgrids 1 Engineering, Economics, & Experience(2015).”
[28] H. Farhangi, “Smart Microgrids,” © 2017 by Taylor & Francis Group, LLC CRC Press is an imprint of Taylor & Francis Group, an Informa business.
[29] K.T.M.U. Hemapala, M.K. Perera, “Smart Microgrid Systems,” © 2022, Published August 5, 2022 by CRC Press.
[30] M. M. Samy, M. I. Mosaad, S. Barakat, “Optimal economic study of hybrid PV-wind-fuel cell system integrated to unreliable electric utility using hybrid search

optimization technique," *Int. J. Hydrogen Energy*, Sep. 2020, doi: 10.1016/j.ijhydene.2020.07.258.
[31] M. I. Mosaad, "Direct power control of SRG-based WECSs using optimized fractional-order PI controller," *IET Electric Power Appl.*, vol. 14, no. 3, pp. 409_417, Mar. 2020.
[32] M. I. Mosaad *et al.*, "Optimal PI controller of DVR to enhance the performance of hybrid power system feeding a remote area in Egypt," *Sustain. Cities Soc.*, vol. 47, pp. 101469_101483, 2019.
[33] Y. M. Alharbi, A. M. S. Yunus, and A. A. Siada, "Application of UPFC to improve the LVRT capability of wind turbine generator," in *Proc. 22nd Austral. Universities Power Eng. Conf. (AUPEC)*, 2012, pp. 1_4.
[34] M. A. E. Zaki *et al.*, "Power quality improvement of WEGCS using STATCOM based EC techniques," *Int. J. Ind. Electron. Drives*, vol. 3, no. 4, pp. 229_237, 2017.
[35] H. Kuang, L. Zheng, S. Li, and X. Ding, "Voltage stability improvement of wind power grid-connected system using TCSC-STATCOM control," *IET Renew. Power Gener.*, vol. 13, no. 2, pp. 215_219, Feb. 2019, doi: 10.1049/iet-rpg.2018.5492.
[36] M. I. Mosaad, "Model reference adaptive control of STATCOM for grid integration of wind energy systems," *IET Electr. Power Appl.*, vol. 12, no. 5, pp. 605_613, May 2018.
[37] T. Sato, D. M. Kammen, B. Duan, M. Macuha, Z. Zhou, et al, "Smart Grid Standards: Specifications, Requirements, and Technologies". John Wiley & Sons, Incorporated, 2015.
[38] O. Palizban, K. Kauhaniemi and J. M. Guerrero, "Evaluation of the hierarchical control of distributed Energy Storage Systems in islanded Microgrids based on Std IEC/ISO 62264," 2016 IEEE Power and Energy Society General Meeting (PESGM), Boston, MA, 2016, pp. 1-5, doi: 10.1109/PESGM.2016.7741411.
[39] A. Colet-Subirachs, A. Ruiz-Alvarez, O. Gomis-Bellmunt, F. Alvarez-Cuevas-Figuerola and A. Sudria-Andreu, "Centralized and Distributed Active and Reactive Power Control of a Utility Connected Microgrid Using IEC61850," in IEEE Systems Journal, vol. 6, no. 1, pp. 58-67, March 2012, doi: 10.1109/JSYST.2011.2162924.
[40] S. Chowdhry, S.P. Chowdhury, P. Crossley, "Microgrids and Active Distribution Networks," © 2009 The Institution of engineering and Technology.
[41] B. Yoo, S. Yang, H. Yang, W. Kim, Y. Jeong, B. Han, K. Jang, "Communication Architecture of the IEC 61850-based Micro Grid System," Journal of Electrical Engineering & Technology, Vol. 6, No. 5, pp. 605~612, 2011.
[42] O. Palizban, K. Kauhaniemi, "Principles of power management in a smart microgrid based on Std. IEC 61850," 2017 IEEE PES Innovative Smart Grid Technologies Conference Europe (ISGT-Europe), Torino, 2017, pp. 1-5, doi: 10.1109/ISGTEurope.2017.8260131.
[43] F. Zare, A. Ghsh, "Control of Power Electronic Converters with Microgrid Applications.", Copyright © 2023 by The Institute of Electrical and Electronics Engineers, Inc. Published by John Wiley & Sons, Inc., Hoboken, New Jersey. Published simultaneously in Canada.

[44] ANEEL BRAZIL, “REGULATORY RESOLUTION No. 1,059, OF FEBRUARY 7, 202.”

[45] M. I. Mosaad, H. S. M. Ramadan, M. Aljohani, M. F. El-Naggar and S. S. M. Ghoneim, "Near-Optimal PI Controllers of STATCOM for Efficient Hybrid Renewable Power System," in IEEE Access, vol. 9, pp. 34119-34130, 2021, doi: 10.1109/ACCESS.2021.3058081.

[46] S. Liaquat, M. S. Fakhar, S. A. R. Kashif, A. Rasool, O. Saleem, and S. Padmanaban, ``Performance analysis of APSO and _re_y algorithm for short term optimal scheduling of multi-generation hybrid energy system,”*IEEE Access*, vol. 8, pp. 177549_177569, 2020.

[47] M. I. Mosaad, F. Salem, “Adaptive voltage regulation of self excited induction generator using FACTS controllers,” *Int. J. Ind. Electron. Drives*, vol. 1, no. 4, p. 219, 2014.

[48] W. Deng, W. Pei, Z. Shen, Z. Zhao, H. Qu, “Adaptive Micro-grid Operation based on IEC 61850,” Energies 2015, 8, 4455-4475; doi:10.3390/en8054455.

[49] S. Mohagheghi, J. Stoupis, Z. Wang, “Communication protocols and networks for power systems-current status and future trends,” 2009 IEEE/PES Power Systems Conference and Exposition, Seattle, WA, 2009, pp. 1-9, doi: 10.1109/PSCE.2009.4840174.

[50] N. Hatziargyriou, “Microgrids, Architectures and Control,” © 2014 John Wiley and Sons Ltd.

[51] I. lima, C. Pinheiro, F. Monteiro, “Inteligência Artificial,” © 2014, Elsevier Editora Ltda.

[52] IEC International Standard, “IEC 61850-8-1:2004(E),” First edition 2004-05.

[53] Z. Shuai,” Transient Characteristics, modelling and Stability Analysis of Microgrid,” © Springer Nature Singapore Pte Ltd. 2021.

[54] H. Xin, L. Huang, L. Zhang, Z. Wang, J. Hu,”Synchronous instability mechanism of P-f droop-controlled voltage source converter caused by current saturation.,” IEEE Trans. Power Syst. 31, 5206–5207 (2016).

[55] I. S. Jacobs and C. P. Bean, “Fine particles, thin films and exchange anisotropy,” in Magnetism, vol. III, G. T. Rado and H. Suhl, Eds. New York: Academic, 1963, pp. 271–350.

[56] M. Jamali, M. Mirzaie, S. Asghar Gholamian,” Calculation and Analysis of Transformer Inrush Current Based on Parameters of Transformer and Operating Conditions,” Electronics and Electrical Engineering. – Kaunas: Technologija, 2011. – No. 3(109). – P. 17–20.

[57] C. Shen et al., “Re-synchronization capability analysis of virtual synchronous generators in microgrids,” 2019 IEEE Energy Conversion Congress and Exposition (ECCE), Baltimore, MD, USA, 2896–2901 (2019).

[58] P. Kundur, “Power System Stability and Control,” (McGraw-Hill Education, New York, 1994).

[59] N. Tashakor, B. Arabsalmanabadi, T. Ghanbar, E. Farjah, S. Götz, "Start-up circuit for an electric vehicle fast charger using SSICL technique and a slow estimator," IET Gener. Transm. Distrib., 2020, Vol. 14 Iss. 12, pp. 2247-2255 © The Institution of Engineering and Technology 2020.
[60] Z. Shuai, C. Shen, X. Liu, Z. Li, Z. J. Shen, "Transient angle stability of virtual synchronous generators using Lyapunov's direct method," IEEE Trans. Smart Grid 10(4), 4648–4661 (2019).
[61] H. Farhangi, "SMART MICROGRIDS-Lessons from Campus Microgrid Design and Implementation," © 2017 by Taylor & Francis Group, LLC.
[62] A. Greenwood, "Electrical Transients in Power Systems, " © 1991 by John Wiley & Sons, Inc.
[63] H. Bevrani, B. Francois, T. Ise, "Microgrid Dynamics and Control, "© 2017 by John Wiley & Sons, Inc.
[64] N. Mahdavi Tabatabaei, E. Kabalci, N. Bizon,"Microgrid Architectures, Control and Protection Methods," © Springer Nature Switzerland AG 2020.
[65] N. Watson, J. Arrillaga," Power Systems Electromagnetic Transients Simulation 2nd Edition," © The Institution of Engineering and Technology 2019.
[66] S. K. Kottayil, "Smart Microgrids, "© 2021 Taylor & Francis Group, LLC.
[67] S. A. Roosa, "Fundamentals of Microgrids," © 2021 Taylor & Francis Group, LLC.
[68] S. M. Muyeen, S. M. Islam, F. Blaabjerg, "Variability, Scalability and Stability of Microgrids, © The Institution of Engineering and Technology 2019.
[69] R. Wang, P. Wang, G. Xiao, " Microgrid Management and EV Control Under Uncertainties in Smart Grid, "© Springer Nature Singapore Pte Ltd. 2018.
[70] V. Tiburcio Dos Santos Junior, B. D. Bonatto, C. Ferreira and A. C. Zambroni de Souza, "Impact of Harmonic Distortion on the Energization of Energy Distribution Transformers Integrated in Virtual Power Plants," 2018 15th International Conference on Control, Automation, Robotics and Vision (ICARCV), 2018, pp. 1252-1256, doi: 10.1109/ICARCV.2018.8581063.
[71] S. S. Gururajapathy, H. Mokhlis, H. A. Illias, "Fault location and detection techniques in power distribution systems with distributed generation: a review," Renew Sustain Energy Rev Jul. 2017;74:949–58.
[72] S. Hasheminejad, S. G. Seifossadat, M. Razaz, M. Joorabian, "Ultra-high-speed protection of transmission lines using traveling wave theory," Electric Power Systems Res 2016;132:94–103.
[73] Y. Baghzouz, "General rules for distributed generation - feeder interaction," 2006 IEEE Power Engineering Society General Meeting. 2006. p. 4.
[74] J. Kennedy and R. Eberhart, "Particle swarm optimization," Proceedings of ICNN'95 - International Conference on Neural Networks, Perth, WA, Australia, 1995, pp. 1942-1948 vol.4, doi: 10.1109/ICNN.1995.488968.
[75] B. K. Panigrahi, A. Abraham, S. Das, "Computational Intelligence in Power Engineering," © 2010 Springer-Verlag Berlin Heidelberg.

[76] R. Eberhart and J. Kennedy, "A new optimizer using particle swarm theory," MHS'95. Proceedings of the Sixth International Symposium on Micro Machine and Human Science, Nagoya, Japan, 1995, pp. 39-43, doi: 10.1109/MHS.1995.494215.
[77] H. Yoshida, Y. Fukuyama, S. Takayama and Y. Nakanishi, "A particle swarm optimization for reactive power and voltage control in electric power systems considering voltage security assessment," IEEE SMC'99 Conference Proceedings. 1999 IEEE International Conference on Systems, Man, and Cybernetics (Cat. No.99CH37028), Tokyo, Japan, 1999, pp. 497-502 vol.6, doi: 10.1109/ICSMC.1999.816602.
[78] Y. Jia, J. Du, W. Zhang, "Proceedings of 2018 Chinese Intelligent Systems Conference Volume I," © Springer Nature Singapore Pte Ltd. 2019.
[79] X. Dong, J. Wang, S. Shi, B. Wang, B. Dominik, M.les Redefern," Traveling Wave Based Single-Phase-to-Ground Protection Method for Power Distribution System," CSEE JOURNAL OF POWER AND ENERGY SYSTEMS, VOL. 1, NO. 2, JUNE 2015.
[80] Y. Liu, L. Tong, W.-X. Zhu, Y. Tian, B. Gao. IMPEDANCE MEASUREMENTS OF NONUNIFORM TRANSMISSION LINES IN TIME DOMAIN USING AN IMPROVED RECURSIVE MULTIPLE REFLECTION COMPUTATION METHOD. Progress In Electromagnetics Research, Vol. 117, 149–164, 2011.
[81] R. Xu, J. Ma," Modeling of Traveling Wave Protection Functions Based on IEC 61850 Standard," 5th international conference on Electric Utility Deregulation and Restructuring and Power Technologies Changsha, China. 2015. p. 173–7.
[82] T. S. Ustun, C. Ozansoy, A. Ustun, "Fault current coefficient and time delay assignment for microgrid protection system with central protection unit," IEEE Trans Power Systems 2013;28(2):598–606.
[83] V. T. dos Santos Junior, "Verification of Inrush currents from electromagnetic transients influencing the stability of voltage in Smart Microgrids connected to systems with electric vehicles," 2022 17th International Conference on Control, Automation, Robotics and Vision (ICARCV), Singapore, Singapore, 2022, pp. 961-965, doi: 10.1109/ICARCV57592.2022.10004345.
[84] H. Lee, K. Yoon, J. Shin, J. Kim, S. Cho, "Optimal Parameters of Volt–Var Function in Smart Inverters for Improving System Performance," Energies. Received: 17 February 2020; Accepted: 29 April 2020; Published: 6 May 2020.
[85] V. Tiburcio Dos Santos Junior, "Fault Location Techniques Based on Traveling Waves with Application in the Protection of Distribution Systems with Renewable Energy and Particle Swarm Optimization," In: Mohamed, A.W., Oliva, D., Suganthan, P.N. (eds) Handbook of Nature-Inspired Optimization Algorithms: The State of the Art. Studies in Systems, Decision and Control, vol 213. Springer, Cham. https://doi.org/10.1007/978-3-031-07516-2_3

11. Appendix

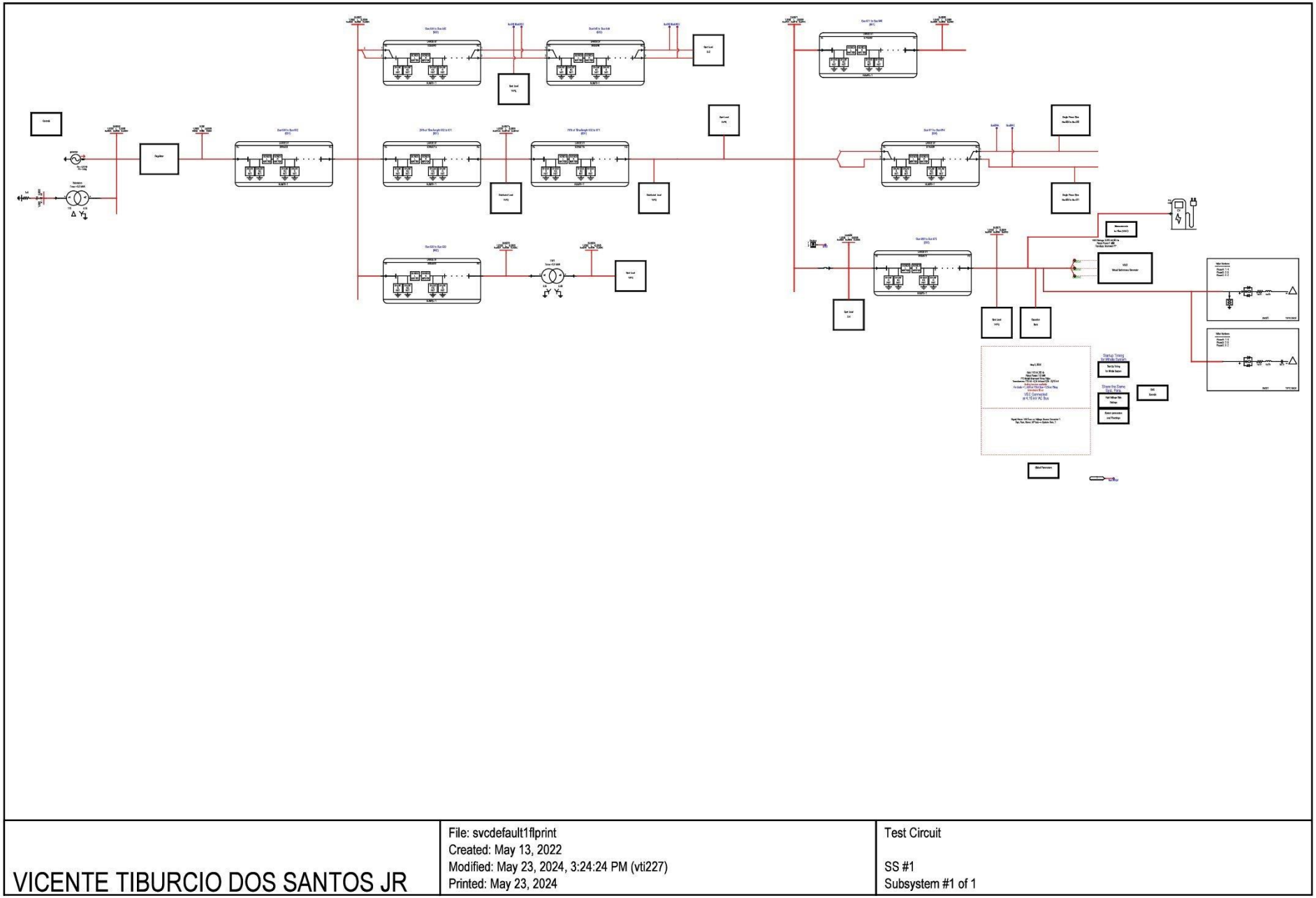

VICENTE TIBURCIO DOS SANTOS JR	File: svcdefault1flprint Created: May 13, 2022 Modified: May 23, 2024, 3:24:24 PM (vti227) Printed: May 23, 2024	Test Circuit SS #1 Subsystem #1 of 1

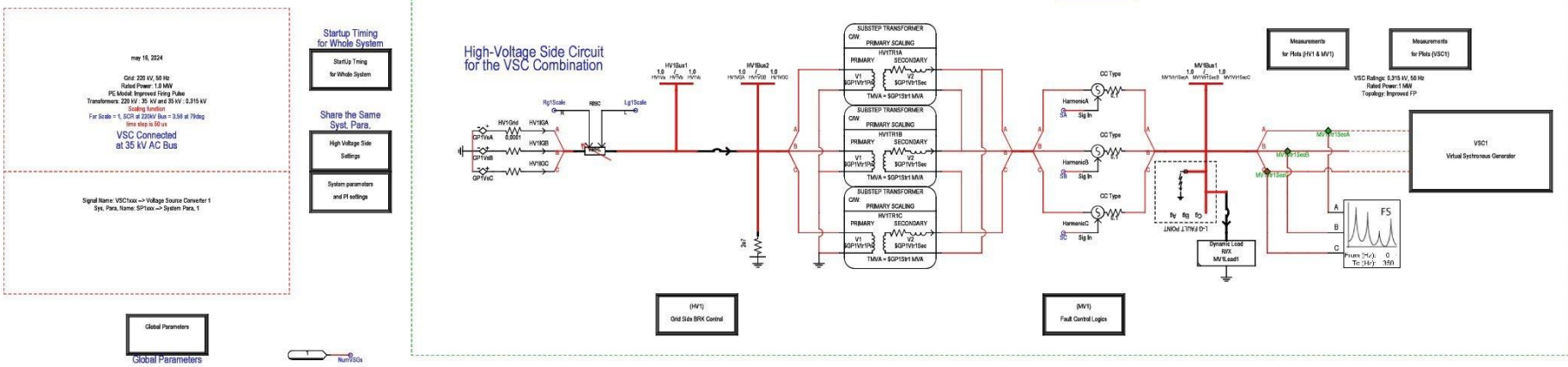

VICENTE TIBURCIO DOS SANTOS JR	File: vsg4print Created: Mar 28, 2023 Modified: May 23, 2024, 3:29:52 PM (vti227) Printed: May 23, 2024	Test Circuit SS #1 Subsystem #1 of 1

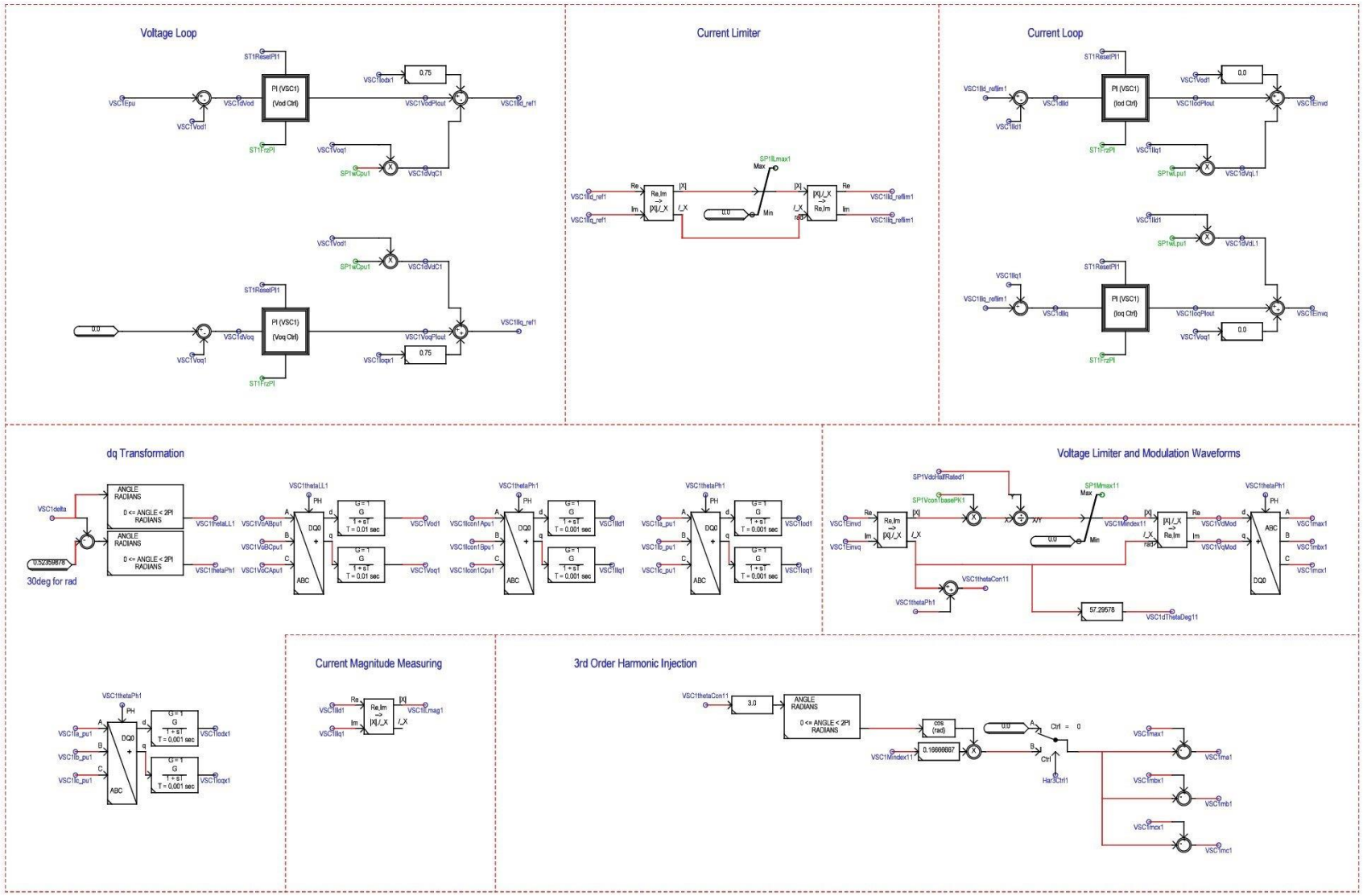

VICENTE TIBURCIO DOS SANTOS JR	File: svcdefault1flprintB Created: May 13, 2022 Modified: May 22, 2024, 9:01:12 AM (vti227) Printed: May 22, 2024	Test Circuit VSC1 V/I Loop SS #1 Subsystem #1 of 1

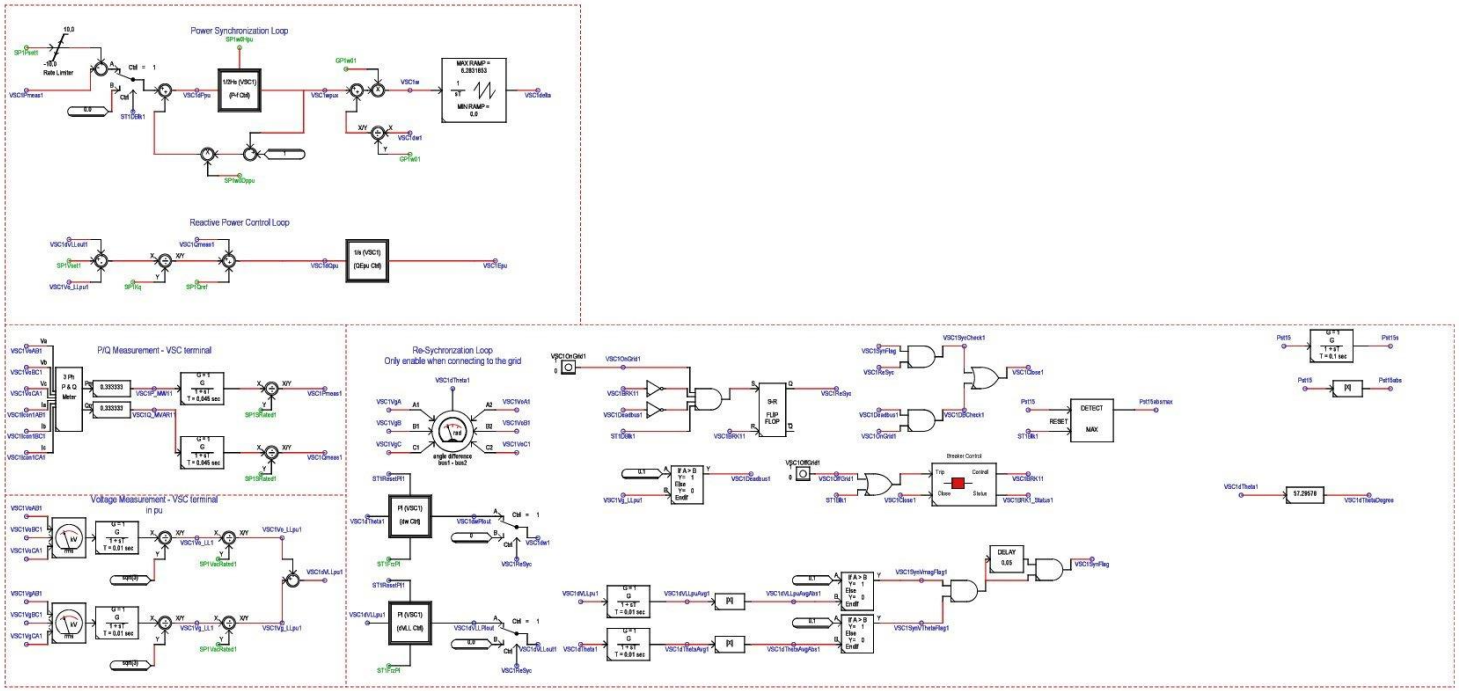

VICENTE TIBURCIO DOS SANTOS JR	File: svcdefault1flprintB Created: May 13, 2022 Modified: May 22, 2024, 9:01:12 AM (vti227) Printed: May 22, 2024	Test Circuit VSC1 VSG Control SS #1 Subsystem #1 of 1